Dissertation
submitted to the
Combined Faculties for the Natural Sciences and for Mathematics
of the Ruperto-Carola University of Heidelberg, Germany
for the degree of
Doctor of Natural Sciences

presented by

M.Sc. Biotechnologist Matthias Hagner
born in Heilbronn-Neckargartach
Oral Examination: 7th November, 2017

Relationship between impaired mucociliary clearance and airway inflammation in chronic airway diseases

Referees: Prof. Dr. Ana Martin-Villalba

Prof. Dr. Marcus Mall

Table of contents

Abbreviations ..... **VIII**

List of figures ..... **X**

List of tables ..... **XII**

Abstract ..... **XIII**

Zusammenfassung ..... **XV**

1 Introduction **1**

1.1 Chronic airway diseases 1

1.1.1 Cystic fibrosis lung disease 1

1.1.2 Asthma 3

1.1.3 Chronic obstructive pulmonary disease 4

1.1.4 Mechanisms of impaired mucociliary clearance in chronic airway diseases 4

1.1.5 Mucociliary clearance as a therapeutic target 6

1.2 The *Scnn1b*-Tg mouse: A model to study the role of impaired mucociliary clearance in the pathogenesis of chronic airway diseases 7

1.3 Aim of the thesis 8

2 Material and Methods **10**

2.1 Experimental animals 10

2.2 Allergen exposure 10

2.3 Amiloride treatment 11

2.4 Airway hyperresponsiveness 11

2.5 Bronchoalveolar lavage, differential cell counts and cytokine measurements 12

2.6 Mucociliary clearance 13

2.7 Whole-lung and airway allergen clearance 14

2.8 Allergen uptake 15

2.9 Flow cytometry 15

2.9.1 Preparation of BAL cells for flow cytometric analysis 15

2.9.2 Preparation of single cells from lung tissue for flow cytometric analysis ... 18
2.10 Histology and morphology ... 21
2.10.1 Tissue embedding and preparation of tissue sections ... 21
2.10.2 Airway mucus content ... 21
2.10.3 Mean linear intercepts and destructive index ... 22
2.11 RNA extraction and real-time RT-PCR ... 23
2.11.1 RNA extraction ... 23
2.11.2 Real-time RT-PCR ... 23
2.12 Statistics ... 24
3 Results ... 25
3.1 Role of mucus clearance as innate defense mechanism of the lung in allergen-induced airway inflammation ... 25
3.1.1 Mucociliary clearance, whole-lung and airway allergen clearance are reduced in juvenile *Scnn1b*-Tg mice ... 25
3.1.2 Altered allergen uptake by airway macrophages and conventional dendritic cells in juvenile *Scnn1b*-Tg mice ... 27
3.1.3 Impaired mucus clearance exacerbates HDM-induced type 2 airway inflammation and AHR in juvenile *Scnn1b*-Tg mice ... 28
3.1.4 Allergen-induced type 2 airway inflammation and AHR are age-dependent and correlate with type 2 signature genes in the mouse lung ... 30
3.1.5 Pharmacological improvement of mucociliary clearance reduces allergen-induced type 2 airway inflammation and AHR in *Scnn1b*-Tg mice ... 33
3.2 Role of the adaptive immune system in chronic airway diseases ... 37
3.2.1 T and B cells are not essential for chronic airway inflammation in juvenile *Scnn1b*-Tg mice ... 37
3.2.2 Expression of *Il17a* is increased in the lungs of juvenile *Scnn1b*-Tg mice ... 38
3.2.3 The number of IL-17A-producing leukocytes is elevated in juvenile *Scnn1b*-Tg mice ... 40
3.2.4 Mucus obstruction develops independently of T and B cells in juvenile *Scnn1b*-Tg mice ... 42

3.2.5 Lack of T and B cells reduces structural lung damage in juvenile *Scnn1b*-Tg mice 44

3.2.6 Lack of T and B cells attenuates airway macrophage activation in juvenile *Scnn1b*-Tg mice 46

4 Discussion 47

4.1 Impaired mucociliary clearance exacerbates type 2 airway inflammation 47

4.2 Impaired mucociliary clearance and adaptive immunity 51

5 Conclusions 56

6 Future Perspectives 57

7 References 58

Publications from PhD studies 70

Acknowledgements 71

Abbreviations

ABPA	Allergic bronchopulmonary aspergillosis
AB-PAS	Alcian blue periodic acid-Schiff
Actb	β-Actin
Af	*Aspergillus fumigatus* allergen
AHR	Airway hyperresponsiveness
AMs	Airway macrophages
APC	Allophycocyanin
ASL	Airway surface liquid
BAL	Bronchoalveolar lavage
BV	Brilliant violet
cDCs	Conventional dendritic cells
CF	Cystic fibrosis
CFTR	Cystic fibrosis transmembrane conductance regulator
Chia	Acidic mammalian chitinase
Cl^-	Chloride ion
COPD	Chronic obstructive pulmonary disease
Cxcl1	Chemokine ligand 1
Cy	Cyanine
DCs	Dendritic cells
dd	Double distilled
DNase	Deoxyribonuclease
ENaC	Epithelial sodium channel
FACS	Fluorescence-activated cell sorting
FBS	Fetal bovine serum
FEV_1	Forced Expiratory Volume in 1 second
FITC	Fluorescein isothiocyanate
GCM	Goblet cell metaplasia
Gob5	Chloride channel accessory 1
HDM	House dust mite allergen
Ifnγ	Interferon γ
IL	Interleukin
ILC2s	Type 2 innate lymphoid cells
ILC3s	Type 3 innate lymphoid cells
MCC	Mucociliary clearance

Mmp12	Matrix metalloproteinase 12
Na^+	Sodium ion
NaCl	Sodium chloride
NK	Natural killer
PBS	Phosphate buffered saline
PCL	Periciliary liquid layer
PCR	Polymerase chain reaction
PE	Phycoerythrin
PerCP	Peridinin-chlorophyll-protein complex
PMA	Phorbol 12-myristse 13-acetate
RAG1	Recombination activating gene 1
RORγt	RAR-related orphan receptor gamma t
Rrs	Respiratory resistance
RT	Reverse transcription
Scnn1b	Gene of the β-subunit of the epithelial sodium channel
Tg	Transgenic
Th	T helper
WT	Wild-type
Ym1	Chitinase-like 3
Ym2	Chitinase-like 4

List of figures

Figure 1. Experimental setup of mucociliary clearance measurements 13
Figure 2. Gating strategy for the detection of myeloid and lymphoid cells in bronchoalveolar lavage by flow cytometry 17
Figure 3. Gating strategy for the detection of lung-derived IL-17A-producing leukocytes by flow cytometry 20
Figure 4. Impaired mucociliary clearance in *Scnn1b*-Tg mice 26
Figure 5. Mucociliary dysfunction impairs allergen clearance in juvenile *Scnn1b*-Tg mice 26
Figure 6. Reduced allergen uptake by airway macrophages in juvenile *Scnn1b*-Tg mice 27
Figure 7. Increased allergen uptake by conventional dendritic cells in juvenile *Scnn1b*-Tg mice 28
Figure 8. HDM-exposure induces elevated type 2 airway inflammation in juvenile *Scnn1b*-Tg mice 29
Figure 9. HDM-exposure exacerbates airway hyperresponsiveness in juvenile *Scnn1b*-Tg mice 30
Figure 10. Allergen-induced type 2 airway inflammation and airway hyperresponsiveness are age-dependent 31
Figure 11. Expression levels of type 2 signature genes are elevated in lungs of neonatal WT and *Scnn1b*-Tg mice 32
Figure 12. Pharmacological inhibition of ENaC reduces Af-induced type 2 airway inflammation in *Scnn1b*-Tg mice 34
Figure 13. Pharmacological inhibition of ENaC reduces HDM-induced type 2 airway inflammation in *Scnn1b*-Tg mice 35
Figure 14. Pharmacological inhibition of ENaC reduces HDM-induced airway hyperresponsiveness in *Scnn1b*-Tg mice 36
Figure 15. Chronic airway inflammation in juvenile *Scnn1b*-Tg mice develops independently of the presence of T and B cells 38
Figure 16. Lack of T and B cells reduces *Il17a* expression in lungs of juvenile *Scnn1b*-Tg mice 39
Figure 17. Increased number of IL-17A-producing leukocytes in lungs of juvenile *Scnn1b*-Tg mice 41
Figure 18. Augmented accumulation of IL-17A-producing $CD4^+$ T, γδ T cells, and ILC3s in lungs of juvenile *Scnn1b*-Tg mice 42

Figure 19. Lack of T and B cells has no effect on mucus obstruction in juvenile *Scnn1b*-Tg mice 43
Figure 20. Mucin expression is independent of the presence of T and B cells in juvenile *Scnn1b*-Tg mice 44
Figure 21. T and B cells contribute to structural lung damage in juvenile *Scnn1b*-Tg mice 45
Figure 22. T and B cells contribute to airway macrophage activation in juvenile *Scnn1b*-Tg mice 46
Figure 23. Schematic overview of impaired mucociliary clearance as a risk factor for the development of allergen-induced type 2 airway inflammation 49

List of tables

Table 1. Antibody master mix for the detection of myeloid and lymphoid cells in BAL by flow cytometry 16
Table 2. Antibody master mix for the detection of lung-derived IL-17A$^+$ leukocytes by flow cytometry 19

Abstract

Chronic airway diseases including cystic fibrosis (CF), asthma and chronic obstructive pulmonary disease (COPD) are characterized by reduced mucociliary clearance (MCC) that leads to mucus-obstructed and chronically inflamed airways and structural changes of the lung. Mice with airway-specific overexpression of the β-subunit of the epithelial sodium channel (*Scnn1b*) exhibit airway surface dehydration, mucus hyperconcentration and impaired MCC and share pathogenic key features of CF and other muco-obstructive lung diseases. Therefore, the *Scnn1b*-transgenic (Tg) mouse is a useful model to study pathophysiological mechanisms of chronic airway diseases *in vivo*. In this study, we investigated the role of MCC as an important innate defense mechanism in the pathogenesis of allergic airway disease and also aimed to understand the role of T and B cells as key cells of the adaptive immunity in chronic airway diseases.

We analyzed allergen clearance mechanisms in juvenile wild-type (WT) and *Scnn1b*-Tg mice and validated the role of impaired MCC on allergen-induced type 2 airway inflammation in a house dust mite allergen (HDM) exposure model. Further, we determined effects of impaired MCC and allergen-induced type 2 airway inflammation in adult mice. Finally, we investigated if pharmacological improvement of MCC could prevent allergen-induced type 2 airway inflammation. To investigate the role of T and B cells in the pathogenesis of chronic airway diseases *in vivo*, we crossed *Scnn1b*-Tg mice with recombination activating gene 1 (RAG1) deficient mice (*Rag1*$^{-/-}$) that lack mature T and B cells and compared inflammatory cell counts in bronchoalveolar lavage (BAL), transcript levels of T helper (Th)1, Th2 and Th17 cytokines, airway mucus obstruction and structural lung damage in juvenile *Scnn1b*-Tg mice with *Scnn1b*-Tg/*Rag1*$^{-/-}$ mice, and their WT and *Rag1*$^{-/-}$ littermates.

We found that reduced allergen clearance from the airways aggravated eosinophilic airway inflammation, secretion of type 2 signature cytokines, and airway hyperresponsiveness (AHR) in juvenile *Scnn1b*-Tg mice. Interestingly, the induction of allergen-induced type 2 airway inflammation in adult WT and *Scnn1b*-Tg mice was abrogated demonstrating an age-dependent susceptibility caused by a type 2 biased immunity during the neonatal/juvenile age. Pharmacological improvement of airway surface hydration reduced allergen-induced airway inflammation and AHR in *Scnn1b*-Tg mice. Lack of *Rag1* had no effect on elevated levels of neutrophils and eosinophils in BAL from juvenile *Scnn1b*-Tg mice. We identified elevated transcript levels of the cytokine Interleukin (IL)-17A in juvenile *Scnn1b*-Tg mice that was reduced in *Scnn1b*-Tg/*Rag1*$^{-/-}$ mice. Flow cytometry revealed γδ T, CD4^{+} T cells and type 3 innate lymphoid

cells (ILC3s) as major sources of IL-17A in lungs of *Scnn1b*-Tg mice. Increased IL-17A-production did not affect mucus plugging but might be associated with structural lung damage in juvenile *Scnn1b*-Tg mice.

In summary, our data support that impaired clearance of inhaled allergens plays an important role in the pathogenesis of type 2 airway inflammation and suggest that therapeutic improvement of MCC may be an effective strategy to prevent disease-aggravating inflammatory responses in patients with allergic asthma and other chronic airway diseases associated with mucociliary dysfunction including CF and COPD. Further, results from our study provide first insights into T and B cell-dependent mechanisms that might contribute to pathophysiological features of CF lung disease.

Zusammenfassung

Chronische Atemwegserkrankungen wie zystische Fibrose (CF), Asthma und chronisch obstruktive Lungenerkrankung (COPD) zeichnen sich durch eine reduzierte mukoziliäre Clearance aus, die zu Mukus obstruierten und chronisch entzündeten Atemwegen mit strukturellen Veränderungen der Lunge führt. Mäuse mit Atemwegs-spezifischer Überexpression der β-Untereinheit des epithelialen Natriumkanals (*Scnn1b*) weisen eine Atemwegsdehydratation, eine Mukus-Hyperkonzentration und eine beeinträchtigte mukoziliäre Clearance auf. Des Weiteren zeigen sie pathogene Hauptmerkmale von CF und anderen Mukus obstruierten Atemwegserkrankungen. Daher ist die *Scnn1b*-transgene (Tg) Maus ein geeignetes Modell, um pathophysiologische Mechanismen von chronischen Atemwegserkrankungen *in vivo* zu untersuchen. In dieser Studie untersuchten wir die Rolle von mukoziliärer Clearance als ein wichtiger angeborener Abwehrmechanismus bei der Pathogenese allergischer Atemwegserkrankungen, sowie die Rolle von T und B Zellen als Schlüsselzellen der adaptiven Immunantwort bei chronischen Atemwegserkrankungen.

Wir analysierten Mechanismen der Allergen-Clearance bei juvenilen Wildtyp (WT) und *Scnn1b*-Tg-Mäusen und validierten die Rolle von beeinträchtigter mukoziliärer Clearance bei Allergen-induzierter Typ 2 Atemwegsentzündung in einem Hausstaubmilbenallergen Expositionsmodell. Ferner haben wir die Auswirkungen von beeinträchtigter mukoziliärer Clearance und Allergen-induzierter Atemwegsentzündung des Typs 2 bei adulten Mäusen bestimmt. Schließlich untersuchten wir, ob die pharmakologische Verbesserung der mukoziliären Clearance die Allergen-induzierte Atemwegsentzündung des Typs 2 verhindern kann. Um die Rolle von T und B Zellen bei der Pathogenese von chronischen Atemwegserkrankungen *in vivo* zu untersuchen, kreuzten wir *Scnn1b*-Tg Mäuse mit *Rag1*-defizienten (*Rag1*$^{-/-}$) Mäusen, welchen reife T und B Zellen fehlen. Wir verglichen die Anzahl der Entzündungszellen in der bronchoalveolären Lavage, Genexpression von T-Helfer 1, 2 und 17 Zytokinen, Mukusobstruktion und strukturelle Lungenschäden bei juvenilen *Scnn1b*-Tg Mäusen mit denen von *Scnn1b*-Tg/*Rag1*$^{-/-}$ Mäusen, ihren WT sowie *Rag1*$^{-/-}$ Kontrollen.

Eine reduzierte Clearance von Allergenen aus den Atemwegen in juvenilen *Scnn1b*-Tg Mäusen verschlimmerte die eosinophile Atemwegsentzündung, die Sekretion von Typ 2 Signaturzytokinen und die Atemwegshyperreaktivität. Interessanterweise wurde bei adulten WT und *Scnn1b*-Tg Mäusen die Induktion einer Allergen-induzierten Typ 2 Atemwegsentzündung nicht beobachtet. Diese altersabhängige Anfälligkeit, eine Allergen-induzierte Type 2 Atemwegsentzündung zu entwickeln, wurde durch eine Typ 2

polarisierte Immunität während des neonatalen/juvenilen Alters verursacht. Die pharmakologische Verbesserung der Atemwegshydratation reduzierte die Allergen-induzierte Atemwegsentzündung und -hyperreaktivität in *Scnn1b*-Tg Mäusen. Das Fehlen von *Rag1* hatte keine Auswirkung auf das erhöhte Level von Neutrophilen und Eosinophilen in der bronchoalveolären Lavage von juvenilen *Scnn1b*-Tg Mäusen. Wir identifizierten eine erhöhte Genexpression des Zytokins Interleukin 17A in juvenilen *Scnn1b*-Tg Mäusen, welche in *Scnn1b*-Tg/*Rag1*$^{-/-}$ Mäusen reduziert war. Die Durchflusszytometrie zeigte, dass γδ T, CD4^{+} T Zellen und Typ 3 innate lymphoide Zellen Hauptquellen von Interleukin 17A in Lungen von *Scnn1b*-Tg Mäusen sind. Eine erhöhte Interleukin 17A Produktion hatte keinen Einfluss auf die Mukusobstruktion, konnte aber mit einer strukturellen Lungenschädigung bei juvenilen *Scnn1b*-Tg Mäusen assoziiert werden.

Zusammenfassend unterstützen unsere Daten, dass die gestörte Clearance von inhalierten Allergenen eine wichtige Rolle bei der Pathogenese von Typ 2 Atemwegsentzündungen spielt. Außerdem deuten sie darauf hin, dass die therapeutische Verbesserung der mukoziliären Clearance eine wirksame Strategie sein könnte, um krankheitsverschlimmernde Entzündungsreaktionen in Patienten mit allergischem Asthma und anderen chronischen Atemwegserkrankungen mit mukoziliärer Dysfunktion wie CF und COPD zu verhindern. Weiterhin liefern die Ergebnisse aus unserer Studie erste Einblicke in T und B zellabhängige Mechanismen, die zu pathophysiologischen Merkmalen der CF-Lungenkrankheit beitragen können.

1 Introduction

1.1 Chronic airway diseases

Mucus-obstructed airways are found in chronic lung diseases including rare genetic disorders such as CF and primary ciliary dyskinesia, as well as more common diseases such as COPD and asthma (Fahy and Dickey, 2010; Wanner et al., 1996). In healthy individuals, the airways are covered by a thin airway surface liquid (ASL) layer that consists of a complex mixture of mucins, proteins, lipids, ions and water (Button and Button, 2013; Fahy and Dickey, 2010). Most of these products are secreted by epithelial cells lining the airway surface as well as mucus-secreting submucosal glands in the larger airways (Livraghi and Randell, 2007). The ASL holds back invading bacteria, viruses, allergens and other environmental irritants that are constantly inhaled and deposited in the airways. By coordinated ciliary beating of ciliated cells, these noxious stimuli are removed from the lung (Button et al., 2012; Zhou-Suckow et al., 2017). Therefore, the MCC apparatus provides an important protective function and is one of the first lines of defense of the innate immune system in the lung. In mucus-obstructed airways such as CF and asthma, the MCC apparatus is impaired either by ASL dehydration due to ion imbalances and/or mucus hypersecretion and abnormal mucus rheology (Button et al., 2012; Evans et al., 2009; Hoegger et al., 2014). Consequences of impaired MCC and obstructed airways are chronic airway inflammation, bacterial/fungal colonization, airway remodeling, and structural lung damage (Zhou-Suckow et al., 2017).

1.1.1 Cystic fibrosis lung disease

CF is an autosomal recessive disease and is one of the most frequent lethal genetic diseases in Caucasian population (Welsh et al., 2001). It is a multi-organ disease, but progressive lung disease continues to be the major cause of morbidity and mortality among CF patients (Ramsey, 1996). The disease is caused by a mutation in the cystic fibrosis transmembrane conductance regulator (CFTR) gene (Kerem et al., 1989; Riordan et al., 1989; Rommens et al., 1989). The CFTR protein is a multi-domain transmembrane protein functioning as an anion channel that conducts chloride (Cl^-) and bicarbonate ions (Anderson et al., 1991; Smith and Welsh, 1992). The effects of the CFTR gene mutation vary from defective protein production, processing, regulation or Cl^- conductance to reduced amounts of functioning CFTR protein in the plasma membrane (Mall and Hartl, 2014; Welsh and Smith, 1993). In the lung, CFTR is expressed on

airway surfaces and in submucosal glands (Jiang and Engelhardt, 1998). Impaired CFTR function leads to defective Cl^- secretion and abnormal regulation of the epithelial sodium channel (ENaC) that constitutes the limiting pathway of sodium ion (Na^+) and fluid absorption (Knowles et al., 1981; Mall et al., 1998). In the airways of CF patients, Cl^- secretion is impaired and Na^+ absorption is increased due to abnormal ENaC regulation resulting in elevated water absorption and ASL dehydration (Matsui et al., 2000; Matsui et al., 1998). Consequences of ASL depletion are impaired MCC, mucus-obstructed airways, chronic airway inflammation, microbial colonization and structural lung damage (Gibson et al., 2003; Mott et al., 2012; Rosenfeld et al., 2001).

Microbial colonization of the airways by pathogens including *Pseudomonas aeruginosa* and *Aspergillus fumigatus* are a common phenomenon in patients with CF that further contributes to the severity of chronic airway inflammation (Hector et al., 2016). Some patients with CF also develop allergic bronchopulmonary aspergillosis (ABPA) which is an exaggerated response of the immune system to the fungus *Aspergillus* and is associated with type 2 immune responses that are similar to those seen in patients with allergic asthma in whom an increased risk to develop ABPA has also been observed (Knutsen and Slavin, 2011). It is assumed that impaired MCC and the emerging mucostatic environment might facilitate microbial colonization and its severe impact on chronic airway inflammation in CF and other muco-obstructive lung diseases.

Chronic airway inflammation in CF lung disease is largely driven by neutrophils (Laval et al., 2016) and pro-inflammatory molecules predominantly produced by sources of the innate immune system (Courtney et al., 2004). Lately, efforts were undertaken to investigate the contribution of the adaptive immune system to chronic airway inflammation in CF lung disease. Specifically, T cells and their pro-inflammatory molecules came into the focus (Hubeau et al., 2004). Hector *et al.* demonstrated that the function of regulatory T cells is impaired in CF patients chronically infected with *Pseudomonas aeruginosa* (Hector et al., 2015). Further, studies indicated that CF lung disease might also be driven by the Th17 pathway and a Th2-skewed cytokine profile (Hartl et al., 2006; Hubeau et al., 2001; Tan et al., 2011; Tiringer et al., 2013); however, mechanistic insights into how impaired mucociliary clearance affects adaptive immunity and its effects on chronic airway inflammation in CF are poorly understood due to limited *in vivo* analysis and lack of animal models, as CFTR knockout mice failed to develop CF-like lung disease (Grubb and Boucher, 1999).

1.1.2 Asthma

Asthma is a chronic inflammatory disease that is one of the most common chronic lung disease among children causing approximately 250,000 deaths annually (Croisant, 2014; Gregory and Lloyd, 2011). The principal cause of death from asthma is asphyxiation from obstructed airways caused by mucus plugs (Aikawa et al., 1992; Messer et al., 1960). The disease is very heterogenous and most patients, especially young children, suffer from atopic asthma (allergic asthma) that is indicated by a positive skin-prick test and the presence of IgE to common inhalant allergens, such as HDM, pollen, animal dander, and fungi (Barnes, 2008).

A typical feature of allergic asthma is type 2 airway inflammation including eosinophilic airway inflammation, increased accumulation of Th2 cells and type 2 innate lymphoid cells (ILC2s) in the lung, and elevated levels of type 2 signature cytokines including IL-4, IL-5 and IL-13 (Neill et al., 2010; Robinson et al., 1992). Type 2 airway inflammation in asthmatic patients occurs when allergens encounter the airway lumen. Dendritic cells (DCs) take up the inhaled allergen and initiate Th2 cell responses, that are supported by basophils, mast cells, ILC2s, and B cells (Lambrecht and Hammad, 2012). Further, the airway epithelium is a central player during type 2 airway inflammation. Pattern recognition receptors on the epithelium sense the allergens and activate epithelial cells. Upon activation, epithelial cells produce endogenous danger signals including members of the IL-1 family IL-1α and IL-33, that could further activate DCs thereby bridging innate and adaptive immune signals to boost type 2 airway inflammation (Lambrecht and Hammad, 2012). Consequences of chronic airway inflammation in asthma are structural changes of the lung including an increase in the smooth muscle mass that is surrounded by the airway wall, and an increase of mucus-producing goblet cells in the epithelium or submucosal glands causing mucus hypersecretion (Benayoun et al., 2003; Evans et al., 2009). Further, patients with asthma often develop airway hyperresponsiveness (AHR) which is the tendency of the airways to constrict in response to stimuli such as allergens, cold air, exercise, and other noxious stimuli (Brannan and Lougheed, 2012).

Elevated levels of IL-13 are a major trigger for AHR and mucus hypersecretion (Kuperman et al., 2002; Zhu et al., 1999). Previous studies demonstrated that asthma is associated with impaired MCC that is especially highlighted in fatal asthma cases where severe airway mucus plugging is found (Hays and Fahy, 2003; Kuyper et al., 2003); notably, in patients with mild and stable asthma reduced MCC is also present (Bateman et al., 1983; Messina et al., 1991; Pavia et al., 1985). Mucociliary dysfunction can either be caused by defects in epithelial ion/fluid transport, as seen in patients with CF, or from mucus hypersecretion under conditions of chronic airway inflammation (Button et al., 2012). Therefore, mucus hypersecretion might provide a potential mechanism as to how

mucociliary dysfunction occurs in asthma and other muco-obstructive lung diseases (Del Donno et al., 2000). Functional consequences of impaired MCC on chronic airway inflammation in patients with asthma are unknown and should not be underappreciated (Fahy and Dickey, 2010) as without an intact MCC apparatus, allergens and other noxious stimuli might accumulate and further boost chronic airway inflammation in patients with asthma.

1.1.3 Chronic obstructive pulmonary disease

COPD is one of the leading causes of morbidity and mortality worldwide (Mannino and Buist, 2007) and is especially prevalent in people with a history of tobacco smoking (Laniado-Laborin, 2009). Similar to asthma, COPD is also characterized by airway obstruction; however, in contrast to asthma, it is progressive and largely irreversible (Barnes, 2008). Characteristic pathogenic features of COPD are mucus-obstructed airways, chronic airway inflammation, and structural lung damage in the form of emphysema and chronic bronchitis (MacNee, 2005).

Most COPD patients suffer from airway neutrophilia, elevated numbers of activated macrophages and Th1 immune responses (Sutherland and Martin, 2003). The secretion of pro-inflammatory mediators including proteases and cytokines induces structural changes of the lung including goblet cell metaplasia (GCM) with mucus hypersecretion and alveolar wall destruction (Barnes, 2008).

In contrast to CF and asthma, mucus obstruction is mostly seen in the small airways of COPD patients and correlates with the increased goblet cell number and mucin gene expression (Innes et al., 2006). As in other chronic airway diseases, COPD is also associated with mucociliary dysfunction (Fahy and Dickey, 2010). Studies demonstrated that smoking tobacco inhibits CFTR function leading to an ion imbalance in the airway that facilitates ASL depletion (Raju et al., 2017). Another study demonstrated that highly concentrated mucus with increased percentage of solids and mucins caused by mucus hypersecretion resulted in ASL dehydration and mucociliary dysfunction in patients with chronic bronchitis (Anderson et al., 2015). Taken together, the underlying mechanisms leading to impaired MCC in COPD are variable but also share key mechanisms of other chronic airway diseases including CF and asthma.

1.1.4 Mechanisms of impaired mucociliary clearance in chronic airway diseases

As mentioned above, the MCC apparatus is an important innate defense mechanism of the lung. The hydration state of the ASL is crucial for an intact MCC (Button and Button, 2013). The ASL covers the airway epithelium and consists of two layers, on top there is a

mucus layer, mainly consisting of the two mucins MUC5AC and MUC5B that is responsible for entrapping inhaled particles and irritants. Below the mucus layer, there is a periciliary layer (PCL) that is occupied by membrane-spanning mucins and large mucopolysaccharides that are tethered to cilia and the epithelial surface, and facilitates ciliary beating and cephalic mucociliary transport (Knowles and Boucher, 2002).

Several mechanisms lead to impaired MCC in chronic lung diseases. A very common assumption is that ASL depletion, either caused by ion imbalances and/or by mucus hypersecretion leads to a compression of cilia resulting in impaired mucociliary transport (Button et al., 2012). In patients with CF, the ASL is depleted due to ion transport imbalances. The secretion of Cl^- from the airway epithelium is impaired due to absence or defective CFTR function (Button and Button, 2013). Conversely, Na^+ absorption is increased because of abnormal regulation of ENaC and hence water is actively absorbed from the airway lumen and the PCL and mucin layer are depleted of water leading to impaired MCC (Button et al., 2012; Clunes and Boucher, 2007). Mucus hypersecretion per se might also lead to a depletion of the ASL and impaired MCC. In asthma and COPD, elevated levels of mucus-inducing molecules including IL-13 and neutrophil elastase contribute to mucus hypersecretion (Barnes, 2008) and studies demonstrated that the increase of the osmotic pressure in the mucus layer by high mucus concentrations leads to an impairment or deformation of cilia and thus to a collapsed PCL resulting in reduced mucociliary transport (Anderson et al., 2015; Button et al., 2012).

Besides the depletion of the ASL, other mechanisms also contribute to impaired MCC in chronic lung diseases. A study by Hoegger and colleagues found that mucociliary transport was reduced in airways of CF piglets and that the reduction is associated with CF submucosal glands secreted mucus strands that remained tethered to gland ducts and failed to detach (Hoegger et al., 2014). Another study by Chen et al. demonstrated that the defects in bicarbonate ion transport, as observed in CF airways, is associated with pathologically thick and viscid mucus that is not properly cleared from the lungs (Chen et al., 2010). Abnormal crosslinking of mucus via disulfide bonds due to oxidative stress triggered by chronic airway inflammation increases mucus elasticity and is also suggested to contribute to impaired MCC (Yuan et al., 2015). Elevated levels of IL-13 is one of many key pathologies in individuals with asthma. IL-13 induces GCM and mucus hypersecretion, especially of the mucin MUC5AC (Kuperman et al., 2002; Zhu et al., 1999). Bonser *et al.* demonstrated that IL-13-induced MUC5AC expression impairs MCC in human bronchial epithelial cells due to MUC5AC-containing domains that are tethered to the airway epithelium slowing the mucociliary transport that might lead to progressive luminal accumulation of mucus and airway plugging in patients with asthma (Bonser et

al., 2016). Further, a recent study demonstrated that IL-13-induced inflammation increases Cl^- secretion via an alternative Cl^- channel. The lack of this channel was associated with mucus obstruction in IL-13-induced airway inflammation *in vivo* and a polymorphism in the gene reduced protein expression of the channel and was associated with asthma (Anagnostopoulou et al., 2012).

Collectively, these observations demonstrated that various mechanisms contribute to impaired MCC in obstructive lung diseases and that the complex mechanisms between impaired MCC and chronic airway inflammation need to be further investigated.

1.1.5 Mucociliary clearance as a therapeutic target

As mentioned above, impaired MCC and/or excessive mucus production contribute to the pathogenesis of many chronic airway diseases including CF, asthma, and COPD and several studies demonstrated that pharmacological improvement of MCC is beneficial in patients with chronic lung diseases (Fahy and Dickey, 2010).

Therapies that hydrate the ASL and thus improve MCC are very promising in patients with mucus-obstructed airways. The inhalation of 7 % hypertonic saline is a beneficial therapy already being used among patients with CF (Donaldson et al., 2006) and trials are under way for the treatment of other airway diseases including asthma and COPD. Hypertonic saline is thought to produce an osmotic gradient for water to move from the submucosa to the airway surface resulting in ASL hydration of airway surfaces (Matsui et al., 2000), thus improving MCC. Drugs that inhibit ENaC are also very promising candidates to improve ASL hydration not only in CF but also in other muco-obstructive lung diseases in which the ASL is depleted. The inhibition of ENaC leads to an increase of Na^+ concentration in the airway lumen and thus is the osmotic driving force for water to hydrate the ASL (Althaus, 2013; Zhou et al., 2008). An aerosolized ENaC blocker is currently being evaluated for the improvement of airway hydration and MCC in CF in clinical trials (Scott et al., 2017). In CF, the basic defect is impaired Cl^- secretion due to a mutation in the CFTR gene that leads to ASL dehydration and impaired MCC (Boucher, 2002). CFTR modulators that aim to improve the function of mutant CFTR are currently in use or are in clinical trials (Ramsey et al., 2011; Van Goor et al., 2011).

Besides therapies that improve ASL hydration, there are also therapies that target mucus rheology to improve MCC (Yuan et al., 2015). The breakage of disulfide bonds that convert mucin monomers to polymers and thus decreasing viscosity and elasticity of mucus seem to have an effect on MCC and need further development (Decramer and Janssens, 2010).

Many efforts were undertaken to develop new therapies that target chronic airway inflammation in asthma including the development of antibodies that target the type 2

signaling cytokines IL-4, IL-5, and IL-13 (Swedin et al., 2017). Even though, improving MCC might have a beneficial effect for patients with asthma, little attention has been obtained to develop drugs that target impaired MCC, compared to the efforts undertaken to develop therapies that reduce chronic airway inflammation (Fahy, 2015). Glucocorticoids and bronchodilators are current treatments for asthma patients. The former inhibits the formation of goblet cells and mucus hypersecretion and the latter enlarges the luminal diameter that may improve MCC (Barnes, 2006). Hydration therapies might also be beneficial in asthma as mucus hypersecretion is a characteristic feature of asthma and might lead to ASL depletion and impaired MCC (Button et al., 2012).

In summary, these studies demonstrate that improvement of MCC is a beneficial treatment strategy for several chronic lung diseases with mucus-obstructed airways; however, mechanisms of impaired MCC are variable in those diseases and treatment strategies that target MCC need to be adjusted according to the underlying clearance defect to exploit their full therapeutic benefit.

1.2 The *Scnn1b-Tg* mouse: A model to study the role of impaired mucociliary clearance in the pathogenesis of chronic airway diseases

Scnn1b-Tg mice were originally developed to study the role of abnormal airway ion transport and airway surface dehydration in the pathogenesis of CF lung disease, as the CFTR knockout mice failed to develop characteristic pathogenic features of CF lung disease (Grubb and Boucher, 1999; Mall et al., 2004). In *Scnn1b*-Tg mice, the β-subunit of ENaC is specifically overexpressed in the airway epithelium under the control of the Club cell secretory protein promoter. ENaC is expressed in the luminal membrane of the airway epithelium and consists of three subunits α, β, and γ that are encoded by the genes *Scnn1a*, *Scnn1b*, and *Scnn1c* (Canessa et al., 1994). Airway-specific overexpression of the β-subunit leads to a congenital increase of Na^+ and water absorption from the airway lumen that causes ASL depletion, mucus hyper-concentration, and reduced MCC (Mall et al., 2004; Mall et al., 2008). *Scnn1b*-Tg mice share characteristic pathological features not only of CF lung disease but also of other obstructive lung diseases including COPD and asthma. A longitudinal study by Mall *et al.* showed that *Scnn1b*-Tg mice have an increased mortality due to airway mucus plugging in the first days of life and that newborn (3 to 5-days-old) *Scnn1b*-Tg mice develop early onset of chronic airway inflammation characterized by airway neutrophilia and elevated levels of the chemokine ligand 1 (CXCL1), a functional murine homolog of the human

cytokine IL-8 (Baggiolini et al., 1994). In juvenile *Scnn1b*-Tg mice, there is robust macrophage activation and a transient type 2 airway inflammation with increased levels of eosinophils and IL-13 that is superimposed by a neutrophilic airway inflammation and wanes at adult ages (Mall et al., 2008). In the first weeks of life, *Scnn1b*-Tg mice develop airway remodeling and mucus hypersecretion that is demonstrated by GCM and increased expression of the mucins *Muc5ac* and *Muc5b* (Mall et al., 2008). Chronic airway inflammation in *Scnn1b*-Tg mice is associated with emphysema-like structural lung damage including airspace enlargement and alveolar wall destruction together with airflow obstruction, increased lung compliance and a reduced density of lung parenchyma that was demonstrated by lung function studies and chest computed tomography, respectively (Gehrig et al., 2014; Mall et al., 2008; Trojanek et al., 2014; Wielputz et al., 2011).

Data from these studies demonstrated that *Scnn1b*-Tg mice develop the full spectrum of pathophysiological phenotypes that are associated with mucus-obstructed lung diseases in humans (Boucher, 2002; Hogg, 1997; Hogg and Timens, 2009) and beyond this, provide a model to study mechanistic links between impaired MCC, mucus plugging, and chronic airway inflammation in the *in vivo* pathogenesis of chronic lung diseases.

1.3 Aim of the thesis

The overall aim of this study was to get further insights into the relationship between impaired MCC and airway inflammation in chronic airway diseases.

Therefore, the first goal of this thesis was to investigate the relationship between impaired MCC and allergen-induced type 2 airway inflammation. Previous studies demonstrated that juvenile *Scnn1b*-Tg mice, with impaired MCC due to airway surface dehydration, develop spontaneous type 2 airway inflammation (Mall et al., 2008). These findings led us to hypothesize that impaired MCC causes reduced allergen clearance and might be a risk factor for the development of allergen-induced type 2 airway inflammation. To investigate our hypothesis, we analyzed allergen clearance mechanisms in juvenile WT and *Scnn1b*-Tg mice and validated the role of impaired MCC on allergen-induced type 2 airway inflammation by using intratracheal application of the natural aeroallergen HDM. In this model, we compared effects of impaired MCC on type 2 airway inflammation including inflammatory cell counts and levels of type 2 cytokines in BAL, and AHR between juvenile WT and *Scnn1b*-Tg mice. Further, we determined effects of impaired MCC on allergen clearance and type 2 airway inflammation in adult mice. Finally, we examined, if pharmacological improvement of MCC by the inhibition of ENaC could prevent allergen-induced airway inflammation.

The second goal of this thesis was to characterize the relationship between impaired MCC and (dys)regulation of the adaptive immunity in the context of chronic airway diseases. Therefore, we crossed *Scnn1b*-Tg mice with *Rag1*$^{-/-}$ mice that lack mature T and B cells (Mombaerts et al., 1992) and analyzed juvenile *Scnn1b*-Tg/*Rag1*$^{-/-}$ double mutant mice for key pathologies of CF lung disease including airway inflammation, cytokine transcript expression and their cellular sources, mucus obstruction, and the development of structural lung damage.

2 Material and Methods

2.1 Experimental animals

All animal studies were approved by the Regierungspräsidium Karlsruhe, Germany (35-9185.81/G-26/14). *Scnn1b*-Tg mice were studied on a C57BL/6N background. *Rag1*$^{-/-}$ mice (Jackson Laboratories, Bar Harbor, Me, USA) obtained on the C57BL/6N background were intercrossed with *Scnn1b*-Tg mice to obtain *Scnn1b*-Tg/*Rag1*$^{-/-}$, *Scnn1b*-Tg, *Rag1*$^{-/-}$, and WT littermates in the F2 generation. Mice were genotyped from tail biopsies by polymerase chain reaction (PCR) as previously described or as recommended by Jackson Laboratories (Mall et al., 2004). Animal experiments were performed at neonatal (10-day-old), juvenile (2- to 3-week-old), and adult (6-week-old) ages. Mice were housed in a specific pathogen-free animal facility with a standard 12 hours day/night cycle at 22°C and had free access to food and water.

2.2 Allergen exposure

To mimic allergic airway inflammation, mice were exposed to Af extract (Hollister-Stier Laboratories, Spokane, Wash, USA) or HDM extract (Greer Laboratories, Lenoir, NC, USA) according to previously established protocols (Anagnostopoulou et al., 2010; Plantinga et al., 2013). In brief, mice were anesthetized with isoflurane (Baxter, Deerfield, Ill, USA) 3 % in oxygen and either Af or HDM dissolved in 0.9 % sodium chloride (NaCl) (B. Braun Melsungen AG, Melsungen, Germany) was administered by intratracheal instillation. In the Af protocol adult mice were intratracheally exposed to 50 µl of Af (2 mg/ml) or 0.9 % NaCl alone every 48 hours a total of 4 times and sacrificed 24 hours after the last allergen exposure. In the HDM protocol juvenile mice were intratracheally sensitized with 20 µl of HDM (0.5 mg/ml) or 0.9 % NaCl alone on two consecutive days, followed by two intratracheal challenges with 20 µl HDM (0.05 mg/ml) or 0.9 % NaCl alone on day 11 and 12 after the first HDM exposure and sacrificed 48 hours after the last HDM challenge. For Af exposure during amiloride treatment, neonatal mice were challenged intratracheally with 20 µl Af (2 mg/ml) or 0.9 % NaCl alone. For HDM exposure during amiloride treatment, neonatal mice were sensitized with 10 µl HDM (1 mg/ml) or 0.9 % NaCl alone by intranasal instillations and challenged, as described above.

2.3 Amiloride treatment

Amiloride studies were performed, as previously described (Zhou et al., 2008). In brief, newborn *Scnn1b*-Tg mice and WT littermates were treated by intranasal instillation of amiloride (10 mmol/l; 1µl/g body weight; 3 times per day) (Sigma-Aldrich, Taufkirchen, Germany) dissolved in double-distilled (dd) H_2O or equal volumes of vehicle (ddH2O) alone for a period of three weeks. During intranasal amiloride treatment, mice were weighed 3 times per day to monitor for loss of body mass because of increased diuresis caused by renal effects of systemically absorbed amiloride. Volume deficits were replaced with subcutaneous injections of 0.9 % NaCl 3 times a day, as previously described (Zhou et al., 2008). In the third week of treatment, intranasal instillation was replaced by intratracheal instillation, and mice were additionally exposed to Af or HDM, as described above and shown in Figure 12A and Figure 13A. Mice were sacrificed 12 hours after the last amiloride treatment.

2.4 Airway hyperresponsiveness

Measurements of respiratory resistance (Rrs) were performed by using a computer-controlled small animal ventilator (flexiVent, SCIREQ, Montreal, Quebec, Canada) as previously described (Goplen et al., 2009). Mice were anesthetized by intraperitoneal injection of 80 mg/kg sodium pentobarbital (cp-pharma, Burgdorf, Germany). After the mice lost their foot-pad pinch response, a tracheostomy was performed and subjects were connected to the small animal ventilator through a 19-gauge intratracheal cannula. After initiating mechanical ventilation, mice were paralyzed by intraperitoneal injection of 1.6 mg/kg pancuronium bromide (Inresa Arzneimittel GmbH, Freiburg, Germany). Animals were ventilated using the following settings: tidal volume of 10 ml/kg body weight, 150 breath/minute, and positive end-expiratory pressure approximately 2 to 3 cm H_2O. Standardization of the lung volume history was performed by two deep inflations. Subsequently, measurements of Rrs were made. Measurements of resistance were determined from a user-defined protocol by using the snapshot-150 pertubation, which is a single-frequency sinusoidal waveform at a frequency equivalent to ventilation rate (i.e. 2.5 Hz). Resultant data were fitted by using multiple linear regressions to the single compartment model, as previously described (Bates and Irvin, 2003; Irvin and Bates, 2003; Shalaby et al., 2010). Changes in Rrs were measured in response to increasing concentrations of nebulized methacholine (Sigma-Aldrich, Taufkirchen, Germany) diluted in phosphate-buffered saline (PBS) from 0 to 160 mg/ml, and delivered into the inspiratory line of the flexiVent ventilator. Previous studies demonstrated that absolute Rrs is age- and weight-dependent in developing mice (Saglani et al., 2009). To adjust for this age- and weight-dependent variability of Rrs, AHR at different methacholine

concentrations was determined from percentage change of Rrs from baseline values (0 mg/ml methacholine). In HDM-exposed *Scnn1b*-Tg mice severe airway obstruction and mucus plugging of cannulae impeded ventilation, and measurements had to be discontinued at high methacholine concentrations; > 32 mg/mL when *Scnn1b*-Tg mice were challenged with HDM alone (Figure 9) and > 80 mg/mL in studies with concurrent instillation of ddH_2O 3 times per day (Figure 14).

2.5 Bronchoalveolar lavage, differential cell counts and cytokine measurements

Mice were deeply anesthetized by intraperitoneal injection with ketamine (120 mg/kg) (Bremer Pharma GmbH, Warburg, Germany) and xylazine (16 mg/kg) (cp-pharma, Burgdorf, Germany) and sacrificed by exsanguination. The trachea was cannulated, the left main stem bronchus was ligated and the lobes of the right lung were lavaged twice with sterile PBS (Thermo Fisher Scientific, Darmstadt, Germany) supplemented with proteinase inhibitor (Sigma-Aldrich, Taufkirchen, Germany) using a weight-adjusted volume of 0.0175 ml/g body weight. This weight-adjusted lavage volume approximates the vital capacity of a developing rodent lung and was used to account for differences in lung size (Lachmann et al., 1980; Shore et al., 2000). After BAL was performed, the right lung lobes were either inflated with fixative of 4 % buffered formalin (Otto Fischar, Saarbrücken, Germany) to 25 cm of fixative pressure, stored in 4 % buffered formalin at 4°C overnight and used for measurements of distal airspace enlargement and alveolar wall destruction, or directly stored without inflation in RNAlater (Thermo Fisher Scientific, Darmstadt, Germany) at -80°C. The non-inflated left lobe from the same mouse was stored in 4 % buffered formalin at 4°C overnight and were used for measurements of airway mucus content. BAL was centrifuged at 300 x *g* for 5 minutes at 4°C (Eppendorf, Wesseling-Berzdorf, Germany) and cell-free supernatant was collected and stored at -80°C. Cells were suspended in 50 µl PBS, counted by trypan blue (Sigma-Aldrich, Taufkirchen, Germany) staining in a Neubauer counting chamber (Karl Hecht, Sondheim v. d. Rhön, Germany) and total cell counts per milliliter lavage fluid were determined by differential cell counts performed on May-Grünwald-Giemsa (Merck, Darmstadt, Germany) stained cytospin preparations, as previously described (Mall et al., 2008). For some experiments flow cytometry was used to determine differential cell counts from BAL and the method is described in detail in section 2.9.1. Concentration of cytokines IL-4, IL-5, and IL-13 were measured in BAL supernatants by using cytometric bead array-enhanced sensitivity flex set (BD Biosciences, Heidelberg, Germany) or ELISA (R&D Systems, Minneapolis, MN, USA), according to the manufacturer's instructions.

2.6 Mucociliary clearance

Mice were anesthetized with intraperitoneal injection of 80 mg/kg sodium pentobarbital (cp-pharma, Burgdorf, Germany), the trachea was exposed by a median anterior neck incision, and the anterior wall was opened longitudinally to expose the mucosal surface (Figure 1). Yellow-green fluorescent microspheres (Thermo Fisher Scientific, Darmstadt, Germany) diluted in PBS with a diameter of 1.1 µm in a 2% solids solution (approximately 3.6 x 10^{10} microspheres/ml) were applied to the mucosal surface of the pars membranacea of the distal trachea (Figure 1). MCC was determined from imaging the elimination of fluorescent beads towards the larynx by using a DFC3000 G camera (Leica, Wetzlar, Germany) coupled to a MZ10 F modular stereo microscope (Leica, Wetzlar, Germany) and analyzed with Application Suite X software (Leica, Wetzlar, Germany). For quantification of MCC, the decrease in bead-derived fluorescent intensity was measured at the area of bead application, and percentage clearance at t = i minutes was calculated as follows:

[1-fluorescence intensity at t = i minutes / fluorescence intensity at t = 0 minutes] x 100.

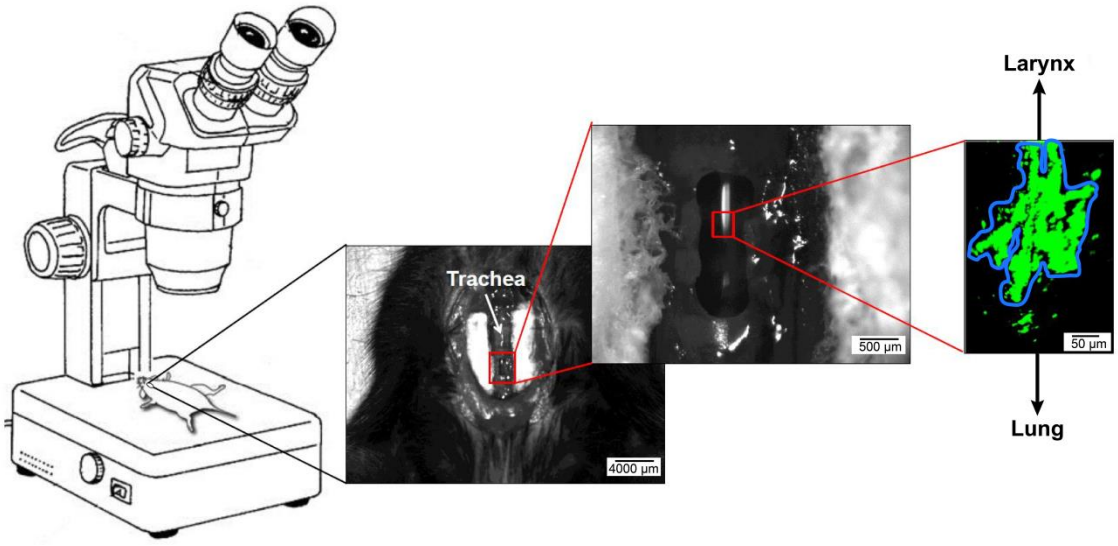

Figure 1. Experimental setup of mucociliary clearance measurements. Mice were anesthetized and the trachea was exposed and the anterior wall was opened longitudinally. Fluorescent beads were applied to the mucosal surface of the trachea and the elimination of the fluorescent beads towards the larynx was monitored by an upright microscope. Bead application area is marked with a blue line and the beads are shown in green.

2.7 Whole-lung and airway allergen clearance

Whole-lung and airway allergen clearance was assessed by measuring the elimination of fluorescently labeled Af after intratracheal instillation. Af was fluorescently labeled with Alexa Fluor 647 Microscale Protein Labeling Kit (Thermo Fisher Scientific, Darmstadt, Germany), according to the manufacturer's instructions. Mice were anesthetized with isoflurane (Baxter, Deerfield, Ill, USA) 3 % in oxygen, and 2.5 µg of fluorescently labeled Af was intratracheally administered in a volume of 20 µL dissolved in PBS. To determine whole lung allergen clearance mice were sacrificed by exsanguination after deep anesthesia through intraperitoneal injection of 120 mg/kg ketamine (Bremer Pharma GmbH, Warburg, Germany) and 16 mg/kg xylazine (cp-pharma, Burgdorf, Germany) either immediately (t = 0 hours) or 1 hour after allergen instillation. Lungs and trachea (up to but not including the larynx) were excised, placed in tubes containing 500 µl PBS supplemented with proteinase inhibitor (Sigma-Aldrich, Taufkirchen, Germany), and tissue was homogenized by a tissue homogenizer (IKA, Staufen, Germany). Homogenized material was analyzed by a plate reader (Perkin Elmer, Waltham, Mass, USA) for fluorescence intensity. Baseline (t = 0 hours) fluorescence intensity (arbitrary units) was assessed by averaging the fluorescence signal in lungs of mice euthanized immediately after instillation. These baseline values were not significantly different between WT (10,525 ± 953, n = 6) and *Scnn1b*-Tg (10,896 ± 877, n = 5, P = 0.78) mice. To determine allergen clearance from the airways, BAL was performed with a volume of 500 µl PBS supplemented with proteinase inhibitor (Sigma-Aldrich, Taufkirchen, Germany) either immediately (t = 0) or 1 hour after allergen instillation. Again baseline (t = 0 hours) intensity (arbitrary units) did not differ between WT (17,658 ± 1949, n = 6) and *Scnn1b*-Tg (17,492 ± 1677, n = 7, P = 0.87) mice. For quantification of whole lung and airway allergen clearance, the decrease in allergen-derived fluorescent intensity was measured in lung homogenates and BAL supernatants, respectively. Percentage clearance after 1 hour was calculated by the following formula:

[1 - fluorescence intensity at t = 1 hour / fluorescence intensity at t = 0 hours] x 100.

2.8 Allergen uptake

In vivo Af uptake by airway macrophages (AMs) and conventional dendritic cells (cDCs) was determined, as previously described (Lauzon-Joset et al., 2014; Soroosh et al., 2013). In brief, Mice were anesthetized with isoflurane (Baxter, Deerfield, Ill, USA) 3 % in oxygen, and 2.5 µg of fluorescently labeled Af was intratracheally administered in a volume of 20 µl dissolved in PBS. Four hours after instillation, whole lung was lavaged twice with PBS using a weight-adjusted volume of 0.035 ml/g body weight. Subsequently, BAL was processed as described in section 2.9.1. Allergen uptake by AMs and cDCs was assessed by determining the frequency of Af-Alexa Fluor 647-positive cells with a BD LSRFortessa cell analyzer (BD Biosciences, Heidelberg, Germany) and FACSDiva software v8.0.1 (BD Biosciences, Heidelberg, Germany). For *in vitro* allergen uptake, BAL was performed and centrifuged at 300 x *g* for 5 minutes at 4°C. BAL supernatant was discarded, cells were washed twice with PBS, and 50,000 cells were suspended in 100 µl RPMI-1640 medium (GE Healthcare Life Sciences, South Logan, UT, USA) and 1.25 µg labeled Af was added in a volume of 10 µl of PBS. Cells were incubated for 4 hours at 37°C and 5 % CO_2, and allergen uptake by AMs and cDCs was assessed, as described for *in vivo* allergen uptake.

2.9 Flow cytometry

2.9.1 Preparation of BAL cells for flow cytometric analysis

BAL was transferred in a 5-ml polystyrene round-bottom tube (BD Biosciences, Heidelberg, Germany) and centrifuged at 300 x *g* for 5 minutes at 4°C (Thermo Fisher Scientific, Darmstadt, Germany). Cell-free supernatant was collected and stored at -80°C. Subsequently, 500 µl of PBS and 2 ml nuclease-free H_2O (Thermo Fisher Scientific, Darmstadt, Germany) containing 10 % sputolysin (Merck, Darmstadt, Germany) were added and BAL cells were incubated for 15 minutes at room temperature, and repeatedly vortexed to release cells from mucus. A volume of 2 ml fluorescence-activated cell sorting (FACS) buffer, containing PBS substituted with 1 % inactivated fetal bovine serum (FBS) (Thermo Fisher Scientific, Darmstadt, Germany) and 0.09 % sodium azide (Sigma-Aldrich, Taufkirchen, Germany), was added and cells were centrifuged at 300 x *g* for 5 minutes at 4°C. Supernatant was discarded and cells were again washed with 4 ml FACS buffer. Finally, cells were suspended in 70 µl of FACS buffer and total cell numbers and viability were assessed by trypan blue (Sigma-Aldrich, Taufkirchen, Germany) exclusion test. Cell surface staining was performed with 50 µl of cell suspension. Before surface staining with specific monoclonal fluorochrome-conjugated antibodies or respective isotype control antibodies, cells were incubated with

1 µl FcBlock (BD Biosciences, Heidelberg, Germany) for 5 minutes at room temperature. A master mix of the antibodies listed in Table 1 was prepared, added to the cell suspension and incubated for 30 minutes at 4°C in the dark.

Table 1. Antibody master mix for the detection of myeloid and lymphoid cells in BAL by flow cytometry

Antibody	Clone	Fluorophore	Supplier	Dilution
F4/80*	BM8	Allophycocyanin (APC)-Cy7	Biolegend	1:100
MHCII	M5/114.15.2	eFluor 450	eBioscience	1:400
Siglec-F	E50-2440	Phycoerythrin (PE)-CF594	BD Biosciences	1:50
CD11c	HL3	PE-Cy7	BD Biosciences	1:200
CD11b	M1/70	Brilliant violet (BV) 605	Biolegend	1:100
CD206	MR5D3	PE	Bio-Rad	1:20
Gr1	RB-8C5	Peridinin-chlorophyll-protein complex (PerCP)-cyanine (Cy) 5.5	eBioscience	1:50
CD64*	X54-5/7.1	APC	Biolegend	1:50
CD3e	500A2	V500	BD Biosciences	1:50
CD4	RM4-5	Fluorescein isothiocyanate (FITC)	eBioscience	1:50
CD8a*	53-6.7	Alexa fluor 700	eBiosciences	1:50

*For the detection of allergen uptake by AMs and cDCs, the master mix was prepared without the antibodies against CD64, F4/80, and CD8a.

Cells were washed in FACS buffer and flow cytometry was performed on a BD LSRFortessa cell analyzer (BD Biosciences, Heidelberg, Germany) immediately after cellular staining with exclusion of debris and cell-doublets, and data were analyzed with FACSDiva software (v8.0.1; BD Biosciences, Heidelberg, Germany) or Flow Jo software (v10; TreeStar, Ashland, OR, USA) using the gating strategy shown in Figure 2.

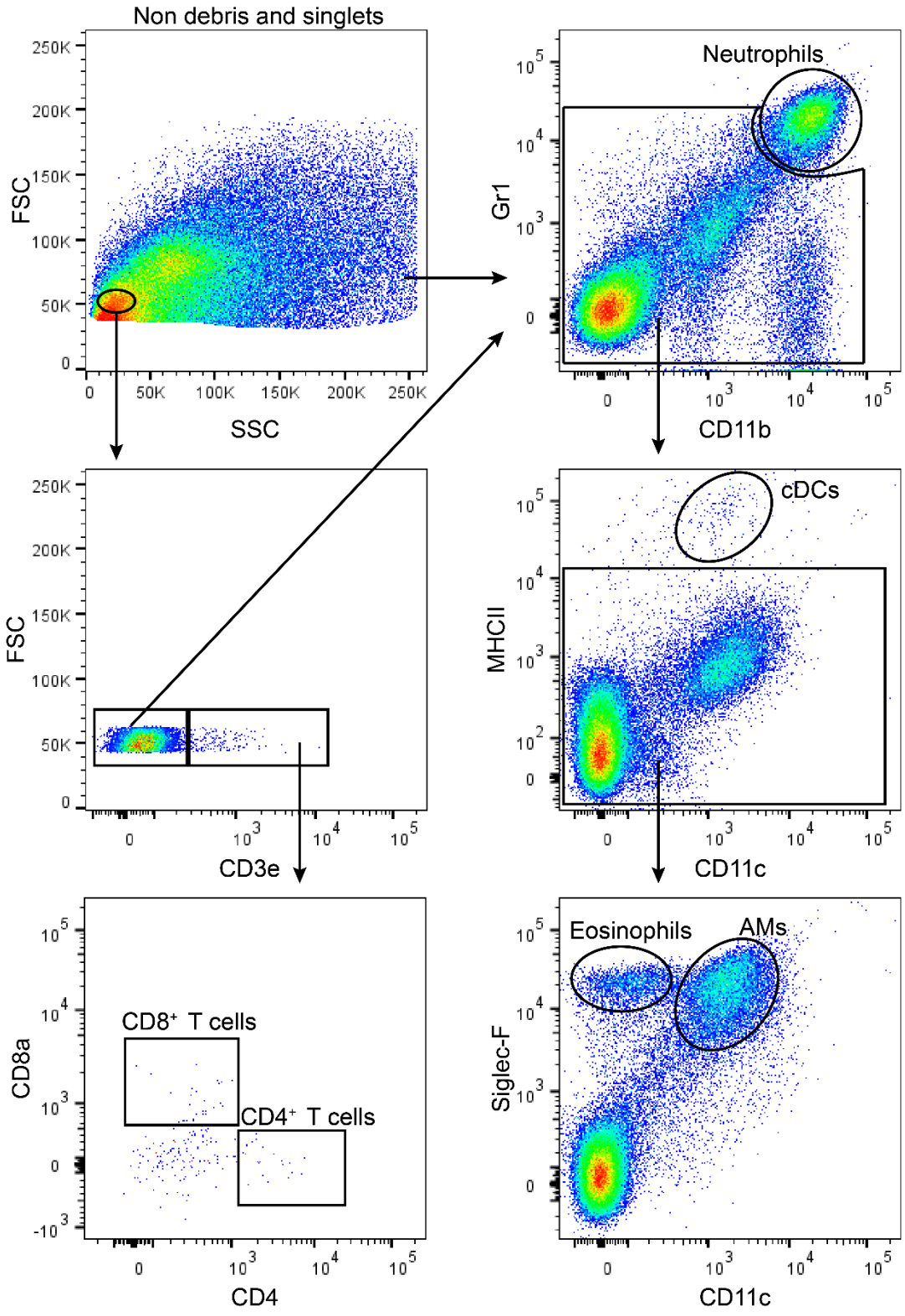

Figure 2. Gating strategy for the detection of myeloid and lymphoid cells in bronchoalveolar lavage by flow cytometry. BAL cells were prepared according to the protocol described above and applied to flow cytometry. BAL cells were characterized as follows: $CD4^+$ T cells ($CD3e^+$, $CD4^+$, $F4/80^-$, and $CD11c^-$), $CD8^+$ T cells ($CD3e^+$, $CD8a^+$, $F4/80^-$, and $CD11c^-$), neutrophils ($CD11b^+$, $Gr1^+$, $CD3^-$, and $F4/80^-$), conventional dendritic cells (cDCs) ($CD11c^+$, $MHCII^{high}$, $CD3^-$, $Gr1^-$ and $SiglecF^-$), eosinophils ($Siglec\text{-}F^+$, $CD11b^+$, $CD11c^-$, $Gr1^-$, and $CD3^-$), airway macrophages (AMs) ($Siglec\text{-}F^+$, $CD11c^+$, $MHCII^{mid}$, $CD64^+$, $F4/80^+$, and $CD3^-$).

2.9.2 Preparation of single cells from lung tissue for flow cytometric analysis

For isolation of leukocytes from the lungs, mice were deeply anesthetized through intraperitoneal injection of 120 mg/kg ketamine (Bremer Pharma GmbH, Warburg, Germany) and xylazine (16 mg/kg) (cp-pharma, Burgdorf, Germany) and killed by means of exsanguination, and the lungs were perfused trough the right ventricle of the heart with 10 ml PBS, removed, and placed in RPMI-1640 medium (GE Healthcare Life Sciences, South Logan, UT, USA) on ice for immediate processing. Each lung was removed from RPMI-1640 medium, placed into a petri dish (Greiner Bio-One, Frickenhausen, Germany) and trachea, esophagus, and connective tissue were removed from peripheral lung tissue which was then minced with scissors into pieces no larger than 2 to 3 mm, transferred to a 50-ml conical tube (Sarstedt, Nümbrecht, Germany) with 10 ml of PBS containing 300 U/ml collagenase type II (Worthington Biochemical, Lakewood, NJ, USA) and 0.15 mg/ml Deoxyribonuclease (DNase) I (Sigma-Aldrich, Taufkirchen, Germany), and incubated for 30 minutes at 37°C, as previously described (Sauer et al., 2006). Digested lung solutions were passed through a 100-µm mesh (Sigma-Aldrich, Taufkirchen, Germany) which was then rinsed with 10 ml cold PBS to stop DNase reaction. Subsequently, lung solutions were centrifuged at 300 x *g* for 5 minutes at 4°C, supernatant was discarded and cells were incubated in 5 ml of red blood cell lysis buffer (BD Biosciences, Heidelberg, Germany) for 5 minutes at room temperature and transferred through a 40-µm mesh (Sigma-Aldrich, Taufkirchen, Germany) which was then rinsed with 10 ml RPMI-1640 medium (GE Healthcare Life Sciences, South Logan, UT, USA). Single cells were finally suspended in cRPMI medium containing RPMI-1640, 10 % FBS (Thermo Fisher Scientific, Darmstadt, Germany), 0.1 % 2-Mercaptoethanol (Thermo Fisher Scientific, Darmstadt, Germany), 1 % L-Glutamin (Thermo Fisher Scientific, Darmstadt, Germany). Total cell numbers and viability were assessed by trypan blue (Sigma-Aldrich, Taufkirchen, Germany) exclusion test. For detection of intracellular IL-17A and RAR-related orphan receptor gamma t (RORγt) expression, cells were centrifuged at 300 x *g* for 5 minutes at 4°C, supernatant was discarded and cells were suspended at a concentration of 2 x 10^6 cells/190 µl in cRPMI medium containing 30 ng/ml phorbol 12-myristse 13-acetate (PMA) (Sigma-Aldrich, Taufkirchen, Germany) and 500 ng/ml ionomycin (Sigma-Aldrich, Taufkirchen, Germany). A volume of 190 µl of single-cell suspension was loaded into 96-well plates (Corning, Big Flats, NY, USA) together with 10 µl of BD Golgi-Stop (BD Biosciences, Heidelberg, Germany) and stimulated *in vitro* for 4 hours at 37°C and 5 % CO_2. Cells were then gently removed from wells and transferred to 5-ml polystyrene round-bottom

tube (BD Biosciences, Heidelberg, Germany), 1 ml FACS buffer was added, centrifuged at 300 x *g* for 5 minutes at 4°C and finally resuspended in 100 µl FACS buffer. Before surface staining with specific monoclonal fluorochrome-conjugated antibodies or respective isotype control antibodies, cells were incubated with 1 µl FcBlock (BD Biosciences, Heidelberg, Germany) for 5 minutes at room temperature. For surface staining, a master mix of the antibodies listed in Table 2 was prepared, added to the cell suspension and incubated for 30 minutes at 4°C in the dark.

Table 2. Antibody master mix for the detection of lung-derived IL-17A$^+$ leukocytes by flow cytometry

Antibody	Clone	Fluorophore	Supplier	Dilution
CD45	30-F11	V500	BD Biosciences	1:100
CD4	RM4-5	FITC	eBioscience	1:100
CD8a	53-6.7	PE-CF594	BD Biosciences	1:100
CD3e	145-211	BV421	BD Biosciences	1:100
NK1.1	PK136	BV605	BD Biosciences	1:100
γδTCR	GL3	APC	eBioscience	1:100
Lineage Marker:				
CD19	1D3		BD Biosciences	1:100
GR1	RB6-8C5	Alexa Fluor 700	BD Biosciences	1:100
CD11c	HL3		BD Biosciences	1:100
CD11b	M1/70		eBioscience	1:100

Cells were then washed with 2 ml PBS and resuspended in 1ml PBS and 0.75 µl fixable viability dye eFluor 780 (eBioscience, Darmstadt, Germany) was added and incubated for 25 minutes at 4°C in the dark. After two washing steps with 2 ml FACS buffer each, cells were fixed and permeabilized with Foxp3/Transcription factor staining buffer set (eBioscience, Darmstadt, Germany) according to manufacturer's instructions and subsequently incubated with 1 µl IL-17A-PE (clone TC11-18H10) (BD Biosciences, Heidelberg, Germany) and 1 µl of 1:5 pre-diluted in FACS buffer RORγt-PerCP-eFluor 710 (clone B2D) (eBioscience, Darmstadt, Germany) antibody for 30 minutes at room temperature. Finally, cells were washed in FACS buffer and flow cytometry was performed on a BD LSRFortessa cell analyzer (BD Biosciences, Heidelberg, Germany) and data were analyzed with FACSDiva software (v8.0.1; BD Biosciences, Heidelberg, Germany) or Flow Jo software (v10; TreeStar, Ashland, OR, USA) and the following gating strategy (Figure 3) was applied to identify IL-17A producing leukocytes.

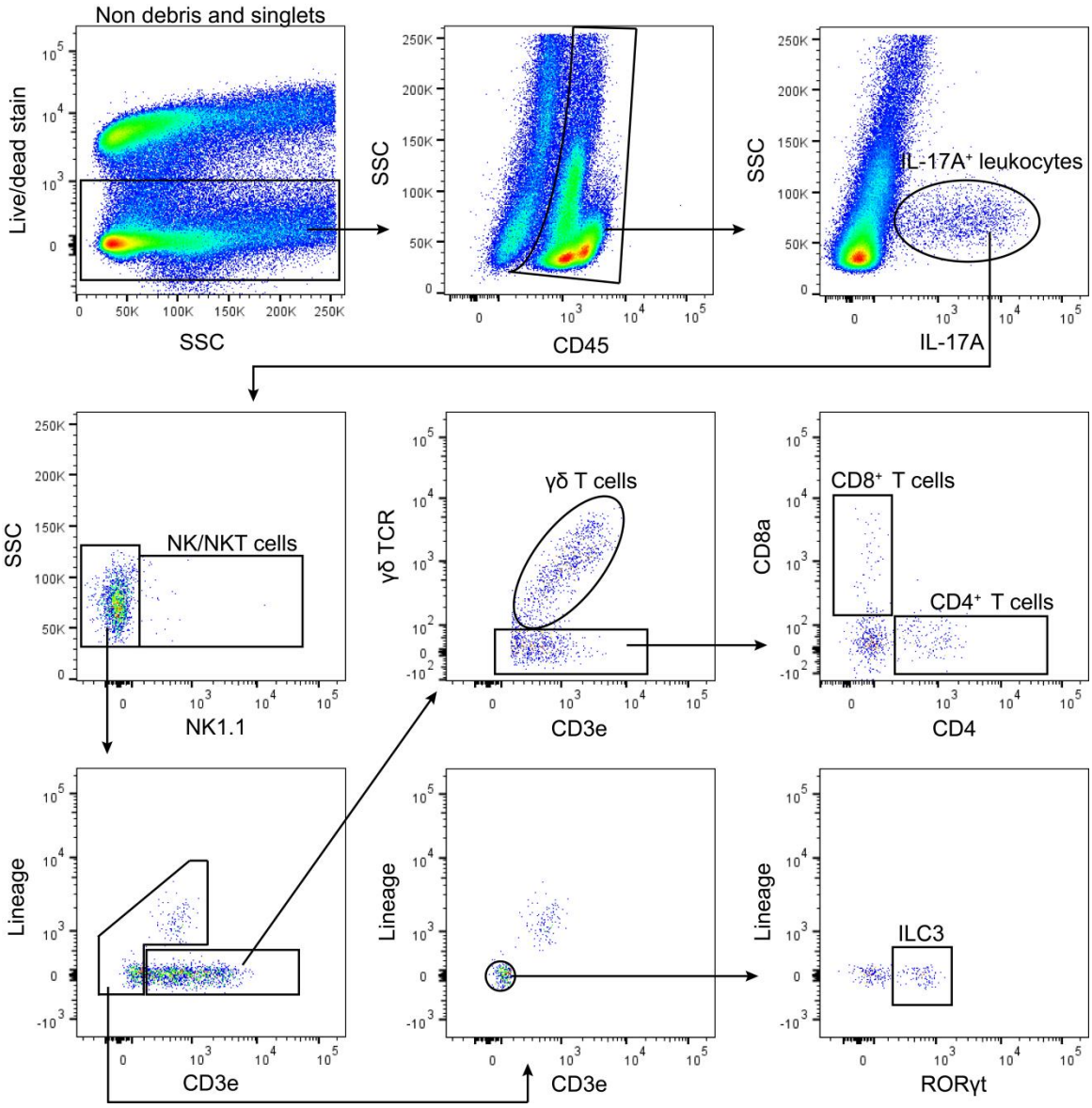

Figure 3. Gating strategy for the detection of lung-derived IL-17A-producing leukocytes by flow cytometry. Single cell suspension from lungs of mice was prepared, stimulated with PMA and ionomycin, and stained according to the protocol described above. IL-17A producing leukocytes were described as follows: Natural killer(NK) and NKT cells ($CD45^+$, $IL\text{-}17A^+$, and $NK1.1^+$), γδ T cells ($CD45^+$, $IL\text{-}17A^+$, $CD3e^+$, $\gamma\delta TCR^+$, and $NK1.1^-$), $CD4^+$ T cells ($CD45^+$, $IL\text{-}17A^+$, $CD3e^+$, $CD4^+$, $NK1.1^-$, $\gamma\delta TCR^-$, and $CD8a^-$), $CD8^+$ T cells ($CD45^+$, $IL\text{-}17A^+$, $CD3e^+$, $CD8a^+$, $NK1.1^-$, $\gamma\delta TCR^-$, and $CD4^-$), ILC3s ($CD45^+$, $IL\text{-}17A^+$, $ROR\gamma t^+$, $lineage^-$, $NK1.1^-$, and $CD3^-$). Lineage marker includes CD19, Gr1, CD11c, and CD11b.

2.10 Histology and morphology

2.10.1 Tissue embedding and preparation of tissue sections

Fixed lungs were washed in PBS and either stored in 70 % ethanol (Carl Roth, Karlsruhe, Germany) at 4°C or directly processed for paraffin embedding. In brief, the apical part of the fixed lungs was cropped transversally and lungs were placed in embedding cassettes (Steinbrenner Laborsysteme, Wiesenbach, Germany) and dehydrated 2 x 30 minutes in 96 % ethanol (Carl Roth, Karlsruhe, Germany), 2 x 45 minutes in 100 % ethanol (Carl Roth, Karlsruhe, Germany), and 12 to 16 hours in xylene (Carl Roth, Karlsruhe, Germany). Samples were then submerged in paraffin (Carl Roth, Karlsruhe, Germany) and vacuum was applied for 2 hours followed by 1 hour at atmospheric pressure. Afterwards, lungs were placed in embedding molds with the cropped surface facing downwards to ensure correct orientation of embedded tissue. Paraffin blocks were kept for 12 to 16 hours at 4°C to harden completely. Left lungs were cut with a microtome (Leica Microsystems, Nussloch, Germany) to 5 µm and were sectioned transversally at the level of the proximal intra-pulmonary main axial airway near the hilus. Right lung lobes were cut to sections of 5 µm. Lung sections were deparaffinized in xylene (Carl Roth, Karlsruhe, Germany) and rehydrated 2 x 10 minutes in 100 % ethanol (Carl Roth, Karlsruhe, Germany), 2 x 2 minutes in 96 % ethanol (Carl Roth, Karlsruhe, Germany), 2 minutes in 70 % ethanol (Carl Roth, Karlsruhe, Germany), and finally rinsed in ddH_2O.

2.10.2 Airway mucus content

For morphometric analysis of airway mucus content, 5 µm sections from the left lung lobe were stained with Alcian blue periodic acid-Schiff (AB-PAS). In brief, tissue sections were placed in Alcian blue solution containing 3 % acetic acid (Carl Roth, Karlsruhe, Germany), 1 % Alcian Blue 8GX (Sigma-Aldrich, Taufkirchen, Germany), and 2 to 3 crystals of Thymol (Sigma-Aldrich, Taufkirchen, Germany) for 30 minutes, rinsed 2 minutes in tab water, and transferred to 0.5 % periodic acid solution (Sigma-Aldrich, Taufkirchen, Germany) for 5 minutes. Subsequently, sections were rinsed 3 x in ddH_2O, placed 15 minutes in Schiff's reagent (Sigma-Aldrich, Taufkirchen, Germany) and 1 minute in sulfur solution containing 1 % 5 M HCl (Merck, Darmstadt, Germany), 0.6 % sodium metabisulfit (Sigma-Aldrich, Taufkirchen, Germany). Tissue was again rinsed with tab water and dehydrated 1 minute in 96 % ethanol (Carl Roth, Karlsruhe, Germany), followed by 2 x 1 minute in 100 % ethanol (Carl Roth, Karlsruhe, Germany) and 3 minutes in xylene (Carl Roth, Karlsruhe, Germany), and finally mounted with permanent mounting medium (Sigma-Aldrich, Taufkirchen, Germany). Images of stained

airway sections were taken with an Olympus IX-71 microscope (Olympus, Hamburg, Germany) interfaced with a DP73 camera (Olympus, Hamburg, Germany) and analyzed using Cell F imaging software (OSIS, Münster, Germany). Intraluminal airway mucus content was determined in 5 µm sections, as previously described (Harkema et al., 1987). In brief, the area of luminal AB-PAS positive material in the airway was quantified using a defined threshold and related to the area of the airway, which was derived from the length of the luminal membrane of the airway epithelium. This ratio was then normalized to the surface area per unit volume (Harkema et al., 1987; Mall et al., 2008; Weibel, 1963).

2.10.3 Mean linear intercepts and destructive index

The 4 right lung lobes were washed in PBS and connective tissue, trachea, and esophagus were removed. Right lung lobes were either stored in 70 % ethanol (Carl Roth, Karlsruhe, Germany) at 4°C or directly processed for paraffin embedding, sectioned, deparaffinized, and rehydrated, as described above. Lung sections were then stained with hematoxylin and eosin to determine mean linear intercepts as a measure of distal airspace enlargement and destructive index as a measure of alveolar wall destruction. In brief, tissue slides were placed 3 minutes in hematoxylin (Sigma-Aldrich, Taufkirchen, Germany), rinsed with ddH_2O and placed 1 minute in HCl/ethanol solution containing 50 % ethanol (Carl Roth, Karlsruhe, Germany) and 1.3 % 5 M HCl (Merck, Darmstadt, Germany), and subsequently washed with tab water. Slides were then transferred to the eosin solution containing 0.1 % Eosin (Carl Roth, Karlsruhe, Germany), 63 % ethanol (Carl Roth, Karlsruhe, Germany), and 1 % acetic acid (Carl Roth, Karlsruhe, Germany), for 45 seconds before rinsing again in ddH_2O. Tissue sections were then dehydrated, and mounted with permanent mounting medium (Sigma-Aldrich, Taufkirchen, Germany), as described above. For measurement of alveolar airspace enlargement and alveolar wall destruction, images of randomly selected airway sections were taken with an Olympus IX-71 microscope (Olympus, Hamburg, Germany) interfaced with a DP73 camera (Olympus, Hamburg, Germany) at 10x magnification. Images were analyzed using Cell F image analysis software (OSIS, Münster, Germany). For the analysis of mean linear intercepts the line counting tool beginning at a randomly selected point was used. Mean linear intercepts were determined by dividing the sum of the lengths of all lines in all frames by the number of intercepts between alveolar septi and counting lines, as previously described (Dunnill, 1962). For each animal, we measured a minimum of 200 intercepts sampled in 10 fields in different lobes. The destructive index was determined using a grid of 72 points overlying images of lung sections. The points were classified to lie within destructed (D) or intact (N, normal)

alveolar ducts in the lung parenchyma and the destructive index was calculated by the formula: 100 x D / (D + N) as previously described (Saetta et al., 1985). For each animal, a minimum of 250 points was sampled and classified in 10 fields in different lobes.

2.11 RNA extraction and real-time RT-PCR

2.11.1 RNA extraction

Lungs were transferred in 1 ml Trizol reagent (Thermo Fisher Scientific, Darmstadt, Germany) and tissue was homogenized by a tissue homogenizer (IKA, Staufen, Germany). Samples were left at room temperature for 20 minutes. Subsequently, 200 µl chloroform (Sigma-Aldrich, Taufkirchen, Germany) was added and samples were vortexed for 15 seconds, left at room temperature for 2 to 3 minutes, and centrifuged at 14,000 x *g* for 20 minutes at 4°C. Upper aqueous phase was transferred to a fresh tube and 500 µl isopropanol (Carl Roth, Karlsruhe, Germany) was added and vortexed thoroughly for 10 seconds, following incubation for 30 minutes at -20°C. Samples were then centrifuged at 16,000 x *g* for 10 minutes at 4°C and supernatant was discarded. Pellet was washed with 1 ml 80 % ethanol (Carl Roth, Karlsruhe, Germany) and centrifuged at 16,000 x *g* for 5 minutes at 4°C. Supernatant was again discarded and pellets were air-dried before dissolving them in nuclease-free H_2O (Thermo Fisher Scientific, Darmstadt, Germany). RNA concentration and purity were measured by a spectrophotometer (DeNovix, Wilmington, DE, USA).

2.11.2 Real-time RT-PCR

cDNA was obtained by performing reverse transcription (RT) of 2 µg of total RNA with Superscript III reverse transcriptase (Thermo Fisher Scientific, Darmstadt, Germany) according to manufacturer's instructions. Real-time quantitative PCR was performed on an Applied Biosystems 7500 Real Time PCR system with TaqMan Universal PCR master mix and inventoried TaqMan gene expression assays (Applied Biosystems, Darmstadt, Germany) for *Muc5ac* (Mm01276718_m1), *Muc5b* (Mm00466391_m1), chloride channel accessory 1 (*Gob5*) (Mm01320697_m1), Interferon γ (*Ifnγ*) (Mm01168134_m1), *Il6* (Mm00446190_m1), *Cxcl1* (Mm04207460_m1), *Il4* (Mm00445259_m1), *Il5* (Mm00439646_m1), *Il13* (Mm00434204_m1), *Il17a* (Mm00439618_m1), matrix metalloproteinase 12 (*Mmp12*) (Mm00500554_m1), acitic mammalian chitinase (*Chia*) (Mm00458221_m1), chitinase-like 3 (*Ym1*) (Mm00657889_mH), chitinase-like 4 (*Ym2*) (Mm00840870_m1), arginase 1 (*Arg1*) (Mm00475988_m1), and β-Actin (*Actb*) (Mm00607939_s1) according to manufacturer's instructions (purchased all from Thermo Fisher Scientific, Darmstadt, Germany). Relative fold changes in target gene expression were calculated from the efficiency of the PCR

reaction and the crossing point deviation between samples from the different genotypes in relation to wild-type controls and normalization to the expression of the reference gene *Actb*, as previously described (Pfaffl, 2001).

2.12 Statistics

Data were derived from at least 3 independent experiments and were analyzed with SigmaPlot version 12.5 software (Systat Software, Erkrath, Germany) and reported as mean ± SEM. Statistical analysis was performed with one-way ANOVA and Tukey's post hoc test, Kruskal-Wallis ANOVA and Dunn's post hoc test, unpaired t-test, and Mann Whitney U test, as appropriate. $P < 0.05$ was accepted to indicate statistical significance.

3 Results

3.1 Role of mucus clearance as innate defense mechanism of the lung in allergen-induced airway inflammation

Previous studies demonstrated that asthma is associated with impaired MCC (Bateman et al., 1983; Messina et al., 1991; Wanner et al., 1996) and studies from our group showed that impaired MCC in juvenile *Scnn1b*-Tg mice produces spontaneous type 2 airway inflammation, including increased levels of the type 2 signature cytokine IL-13, airway eosinophilia and mucus hypersecretion (Mall et al., 2008). In preliminary studies, we observed that a short-term allergen challenge protocol consisting of 4 Af challenges, induces an exaggerated type 2 airway inflammation with increased levels of the type 2 signature cytokines IL-4, IL-5 and IL-13, airway eosinophilia, and AHR in juvenile *Scnn1b-Tg* mice (Fritzsching et al., 2017). To investigate the effects of impaired MCC on allergen clearance and type 2 airway inflammation, we analyzed allergen clearance mechanisms in WT and *Scnn1b-Tg* mice and evaluated the role of impaired MCC in another allergen model by using a protocol consisting of HDM sensitization and challenge in juvenile WT and *Scnn1b-Tg* mice. Further, we tested age-dependent susceptibility of allergen-induced type 2 airway inflammation. Finally, as a proof of concept, we examined if pharmacological improvement of MCC might be an effective therapeutic strategy to reduce allergic airway inflammation.

3.1.1 Mucociliary clearance, whole-lung and airway allergen clearance are reduced in juvenile *Scnn1b*-Tg mice

To assess MCC in WT and *Scnn1b*-Tg mice, we used an *in vivo* fluorescent bead assay which was based on the elimination of fluorescent microspheres from the trachea. Consistent with previously published results (Mall et al., 2008), we observed a reduced MCC in *Scnn1b*-Tg mice (Figure 4). To determine the effects of mucociliary dysfunction on allergen clearance, we instilled fluorescently labeled Af in juvenile naïve WT and *Scnn1b*-Tg mice and measured the allergen clearance from the whole lung and airway lumen. Both whole-lung and airway allergen clearance were decreased in *Scnn1b*-Tg mice (Figure 5). Overall, these data demonstrate that impaired MCC leads to reduced allergen clearance from the lungs of *Scnn1b*-Tg mice.

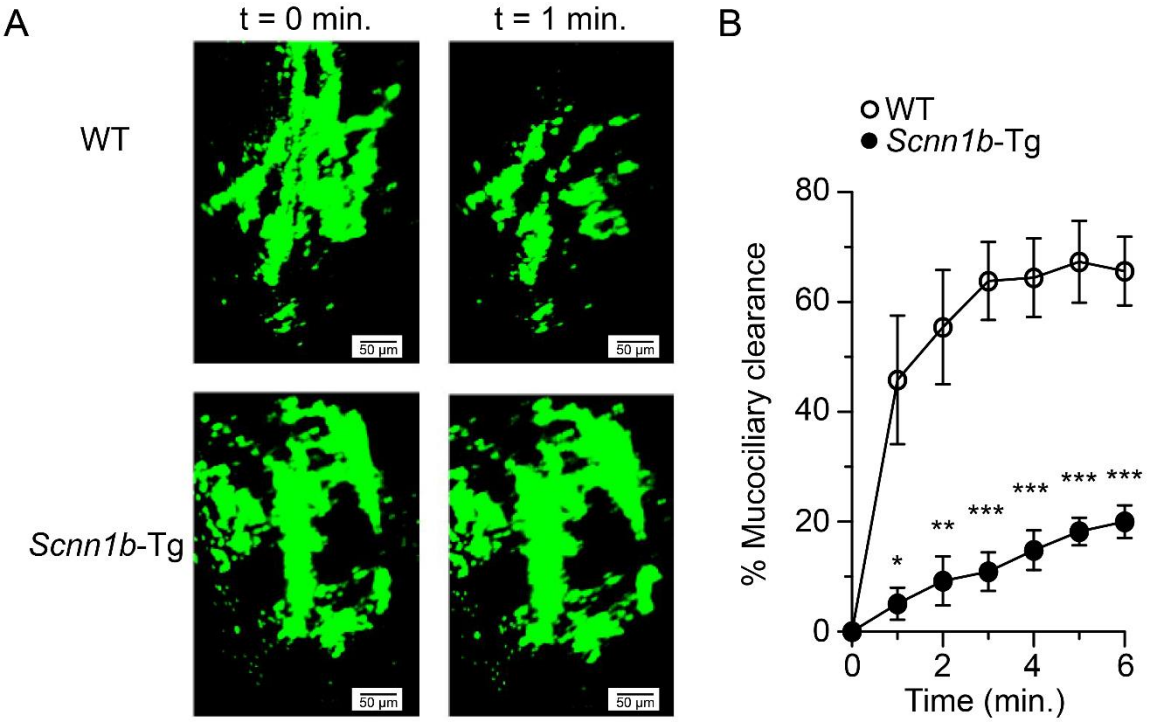

Figure 4. Impaired mucociliary clearance in *Scnn1b*-Tg mice. (A and B) Mice were anesthetized, the trachea was exposed and the anterior wall was opened longitudinally to expose the mucosal surface. Fluorescent microspheres were applied to the mucosal surface and mucociliary clearance was determined from imaging the elimination of fluorescent beads toward the larynx. (A) Microscopic images of fluorescent beads (green) at t = 0 minutes (min.) and t = 1 min. in WT and *Scnn1b*-Tg mice. (B) Percent of cleared fluorescent beads over a period of 6 min. in WT and *Scnn1b*-Tg mice. n = 4 mice for each group. *P < 0.05, **P < 0.01, and ***P < 0.001 compared with WT mice.

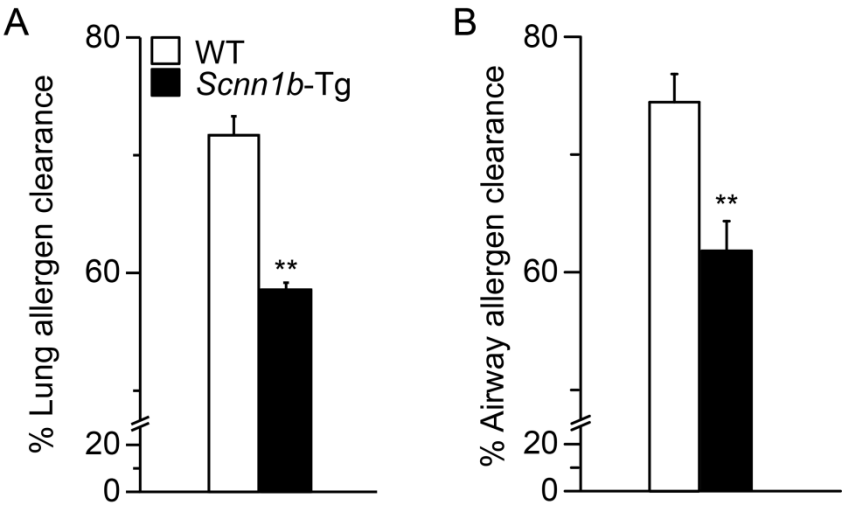

Figure 5. Mucociliary dysfunction impairs allergen clearance in juvenile *Scnn1b*-Tg mice. (A and B) Fluorescently labeled Af was intratracheally instilled in juvenile WT and *Scnn1b*-Tg mice and elimination from either whole-lung (A) or airways (B) was measured after 1 hour. n = 6-7 mice for each group. **P < 0.01 compared with WT mice.

3.1.2 Altered allergen uptake by airway macrophages and conventional dendritic cells in juvenile *Scnn1b*-Tg mice

AMs and cDCs are one of the first cell types encountered by aeroallergens in the airways and are important for the removal and the presentation of the allergen to T cells (Balhara and Gounni, 2012; Hammad and Lambrecht, 2008). Because whole-lung and airway allergen clearance are impaired in *Scnn1b*-Tg mice, we investigated the capacity of allergen uptake by AMs and cDCs *in vivo* and *in vitro*. Af was fluorescently labeled and either instilled by intratracheal application in juvenile WT and *Scnn1b*-Tg mice for *in vivo* allergen uptake or incubated together with BAL cells for *in vitro* allergen uptake and flow cytometry was performed to analyze the capacity of allergen uptake by cDCs and AMs. The uptake of fluorescently labeled Af by AMs from naïve *Scnn1b*-Tg mice was impaired and significantly decreased compared with that in WT mice *in vivo* and *in vitro* (Figure 6).

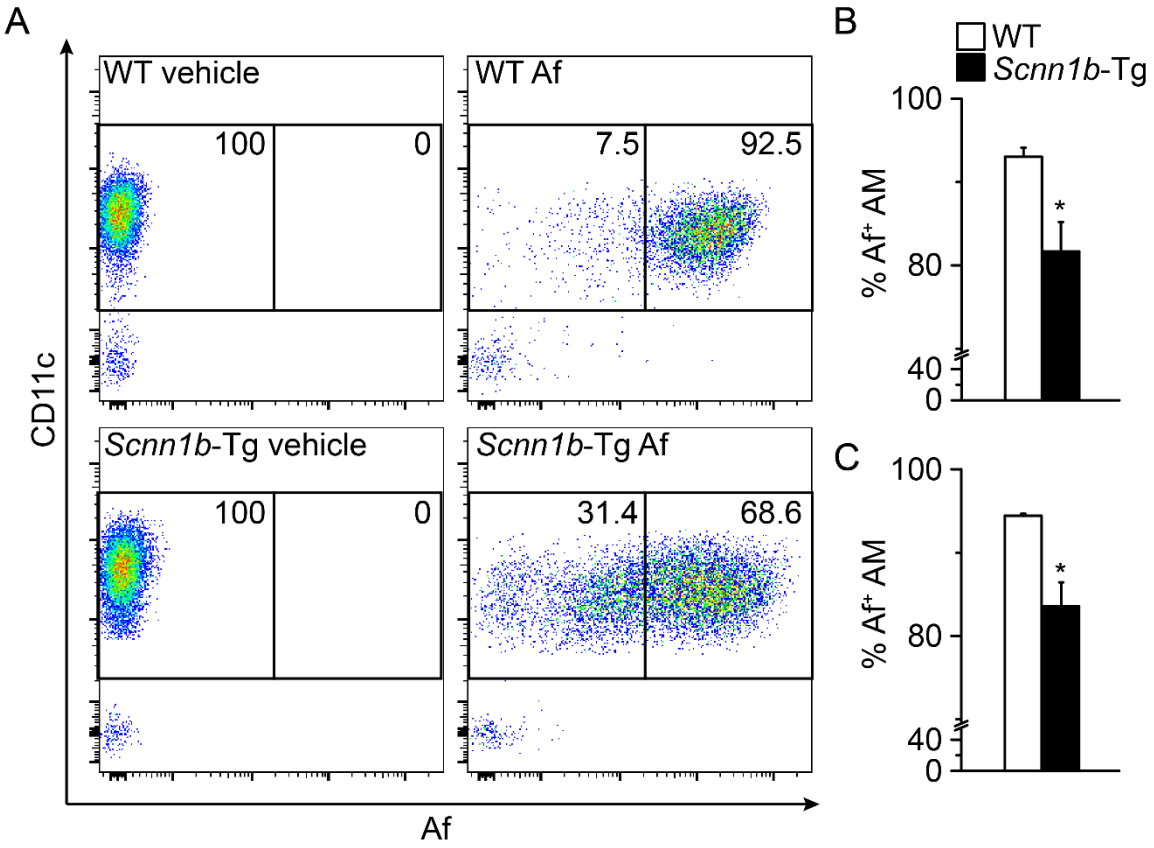

Figure 6. Reduced allergen uptake by airway macrophages in juvenile *Scnn1b*-Tg mice. (A-C) Allergen uptake by airway macrophages (AMs) was assessed by determining the frequency of Af-Alexa Fluor 647-positive cells by flow cytometry in juvenile WT and *Scnn1b*-Tg mice. (A) Representative dot plots of WT and *Scnn1b*-Tg AMs (Siglec-F$^+$/CD11c$^+$/MHCII^{mid}) and lymphocytes (Siglec-F$^-$/CD11c$^-$). Number in rectangles represents percentage of AMs that are positive or negative for Af. (B and C) Percentage of BAL fluid-derived AMs from WT and *Scnn1b*-Tg mice positive for fluorescently labeled Af after intratracheal application *in vivo* (B) or incubation *in vitro* (C). n = 5-6 mice for each group. *P < 0.05 compared with WT mice.

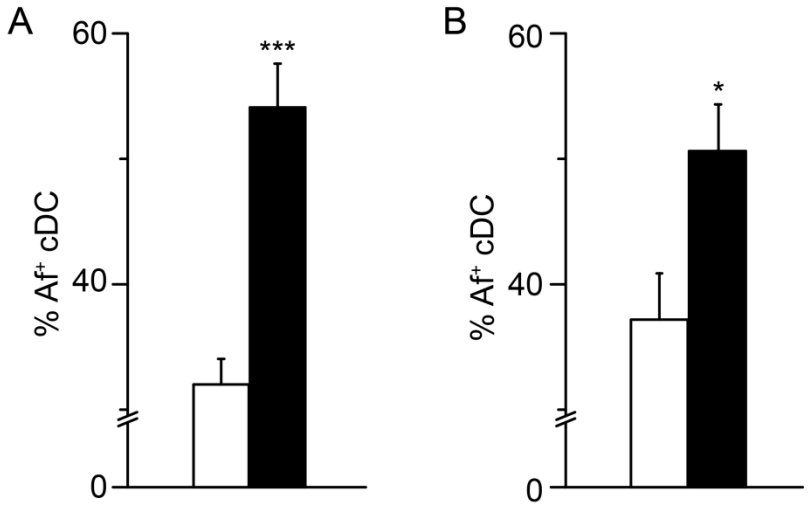

Figure 7. Increased allergen uptake by conventional dendritic cells in juvenile *Scnn1b*-Tg mice. (A and B) Allergen uptake by conventional dendritic cells (cDCs) was assessed by determining the frequency of Af-Alexa Fluor 647-positive cells by flow cytometry and the percentage of BAL fluid-derived cDCs ($CD11c^+/MHCII^{high}/Siglec\text{-}F^-$) from juvenile WT and *Scnn1b*-Tg mice positive for fluorescently labeled Af after intratracheal application *in vivo* (A) or incubation *in vitro* (B). n = 5-6 mice for each group. *P < 0.05 and ***P < 0.001 compared with WT mice.

Conversely, uptake of Af by lung cDCs was significantly enhanced in *Scnn1b*-Tg mice (Figure 7). Collectively, these data show that impaired MCC facilitates reduced allergen clearance resulting in altered allergen uptake of AMs and cDCs.

3.1.3 Impaired mucus clearance exacerbates HDM-induced type 2 airway inflammation and AHR in juvenile *Scnn1b*-Tg mice

Previous studies by our group showed that a short-term Af challenge protocol induces aggravated type 2 airway inflammation in juvenile *Scnn1b*-Tg mice (Fritzsching et al., 2017). To evaluate the role of impaired MCC in the context of type 2 airway inflammation and to further determine the effects in an independent allergen model, we used a protocol consisting of intratracheal sensitization and challenge with the aeroallergen HDM. In detail, we sensitized and challenged 2- to 3-week-old juvenile WT and *Scnn1b*-Tg mice with intratracheal application of the natural aeroallergen HDM or vehicle alone and compared inflammatory cell counts, levels of the type 2 cytokines IL-4, IL-5, and IL-13 in BAL fluid, and AHR. In WT mice HDM induced a modest increase in BAL eosinophil counts, $CD4^+$ T cells and IL-4, IL-5 and IL-13 levels (Figure 8A-E). In *Scnn1b*-Tg mice BAL fluid eosinophil counts and IL-4, IL-5, and IL-13 levels were spontaneously increased, as described previously (Livraghi et al., 2009; Mall et al., 2008), and HDM triggered elevated levels of AMs, robust airway eosinophilia and production of IL-4, IL-5,

and IL-13 that was significantly increased compared with allergen-induced responses in WT mice (Figure 8A-E).

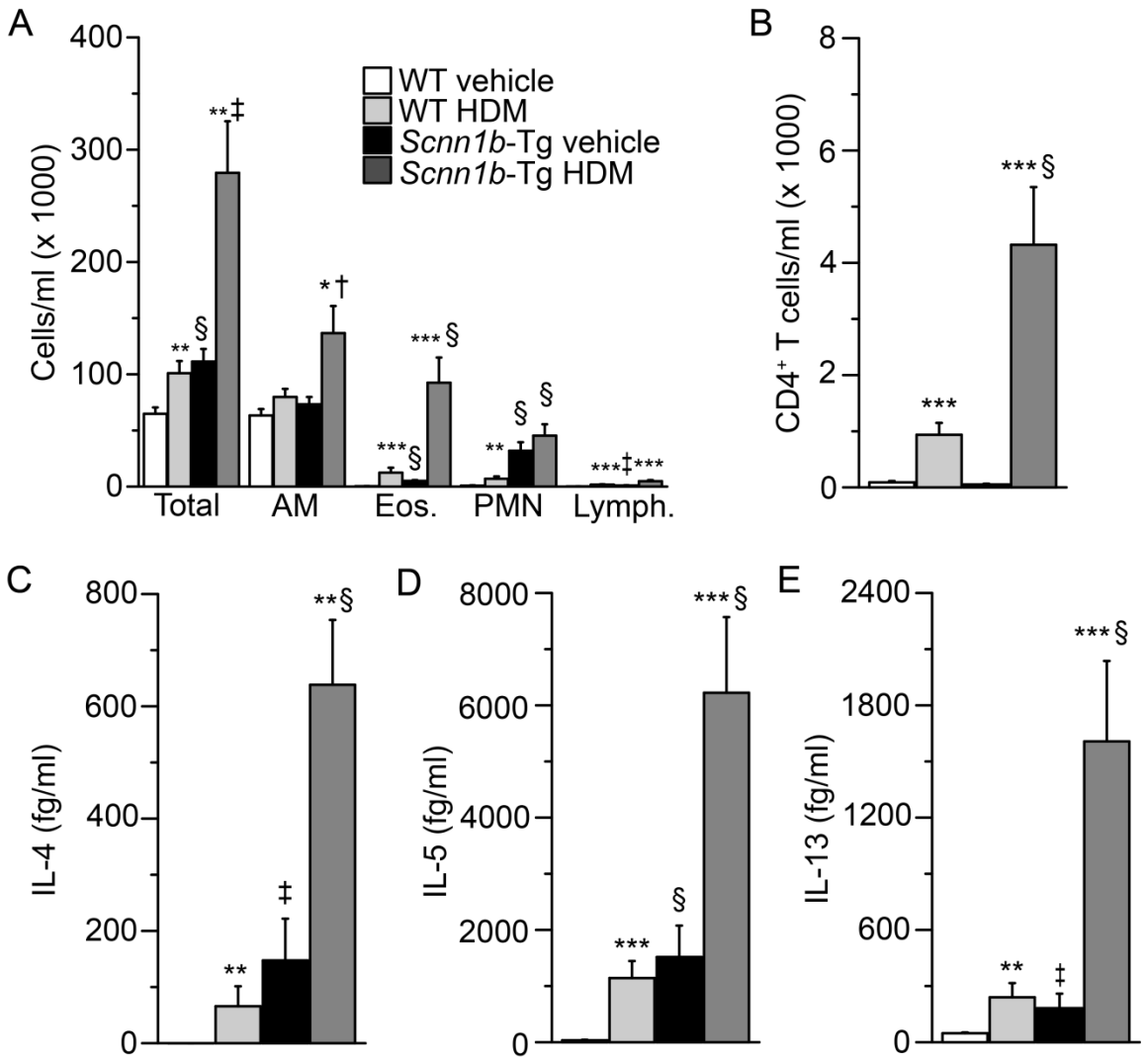

Figure 8. HDM-exposure induces elevated type 2 airway inflammation in juvenile *Scnn1b*-Tg mice. (A-E) Juvenile WT and *Scnn1b*-Tg mice were sensitized and challenged with HDM or vehicle alone. (A) BAL cell counts (Airway macrophages [AM], eosinophils [Eos.], neutrophils [PMN], and lymphocytes [Lymph.]). (B) Airway $CD4^+$ T cell counts. (C-E) IL-4 (C), IL-5 (D), and IL-13 (E) in BAL fluid. n = 13-23 mice for each group. *P < 0.05, **P < 0.01, and ***P < 0.001 compared with vehicle-treated mice of the same genotype. †P < 0.05, ‡P < 0.01, and §P < 0.001 compared with mice with the same treatment but different genotype.

Invasive pulmonary function testing demonstrated spontaneous AHR in naive juvenile *Scnn1b*-Tg versus WT mice (Figure 9) and HDM challenge increased AHR in juvenile WT and *Scnn1b*-Tg mice and was significantly aggravated in *Scnn1b*-Tg mice compared to WT littermates (Figure 9). In summary, these results demonstrate that impaired allergen clearance from the airways induces robust type 2 airway inflammation together with AHR in juvenile *Scnn1b*-Tg mice.

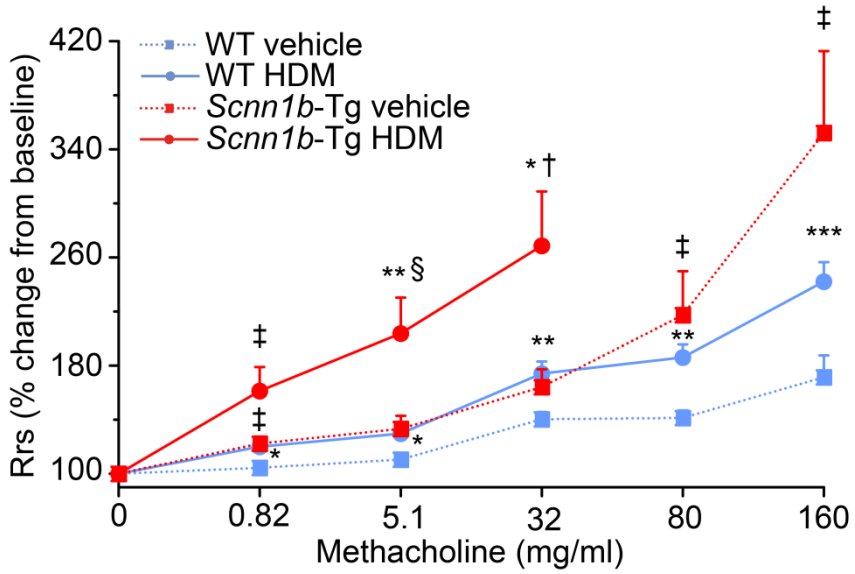

Figure 9. HDM-exposure exacerbates airway hyperresponsiveness in juvenile *Scnn1b*-Tg mice. Juvenile WT and *Scnn1b*-Tg mice were sensitized and challenged with HDM or vehicle alone and AHR was assessed by measuring respiratory resistance (Rrs). In HDM-exposed *Scnn1b*-Tg mice severe airway obstruction and mucus plugging of cannulae impeded ventilation, and measurements had to be discontinued at methacholine concentrations of greater than 32 mg/ml. n = 13-23 for each group. *P < 0.05, **P < 0.01, and ***P < 0.001 compared with vehicle-treated mice of the same genotype. †P < 0.05 and ‡P < 0.01 compared with mice with the same treatment but different genotype.

3.1.4 Allergen-induced type 2 airway inflammation and AHR are age-dependent and correlate with type 2 signature genes in the mouse lung

So far, our data demonstrated that juvenile *Scnn1b*-Tg mice with mucociliary dysfunction exhibit impaired allergen clearance that aggravates type 2 airway inflammation and AHR. Next, we were interested to determine the effects of impaired allergen clearance in adult mice. Therefore, we used our previously established short-term treatment protocol consisting of 4 Af challenges (Fritzsching et al., 2017), and exposed adult WT and *Scnn1b*-Tg mice to Af or vehicle alone and again compared inflammatory cell counts, IL-13 levels in BAL, and AHR. In comparison to vehicle-treated juvenile *Scnn1b*-Tg mice (Figure 8A and E), vehicle-treated adult *Scnn1b*-Tg mice did not show airway eosinophilia and increased IL-13 levels in BAL (Figure 10A and B) and consistent with previous studies airway inflammation was dominated by neutrophils (Figure 10A) (Gehrig et al., 2014; Mall et al., 2008). In adult WT and *Scnn1b*-Tg mice, Af-challenge neither induced type 2 airway inflammation nor AHR (Figure 10) and this is in contrast to previously published results in which Af-challenge triggered moderate type 2 airway inflammation in juvenile WT mice that was exacerbated in juvenile *Scnn1b*-Tg mice

(Fritzsching et al., 2017). These data suggest an age-dependent susceptibility to develop allergen-induced type 2 airway inflammation.

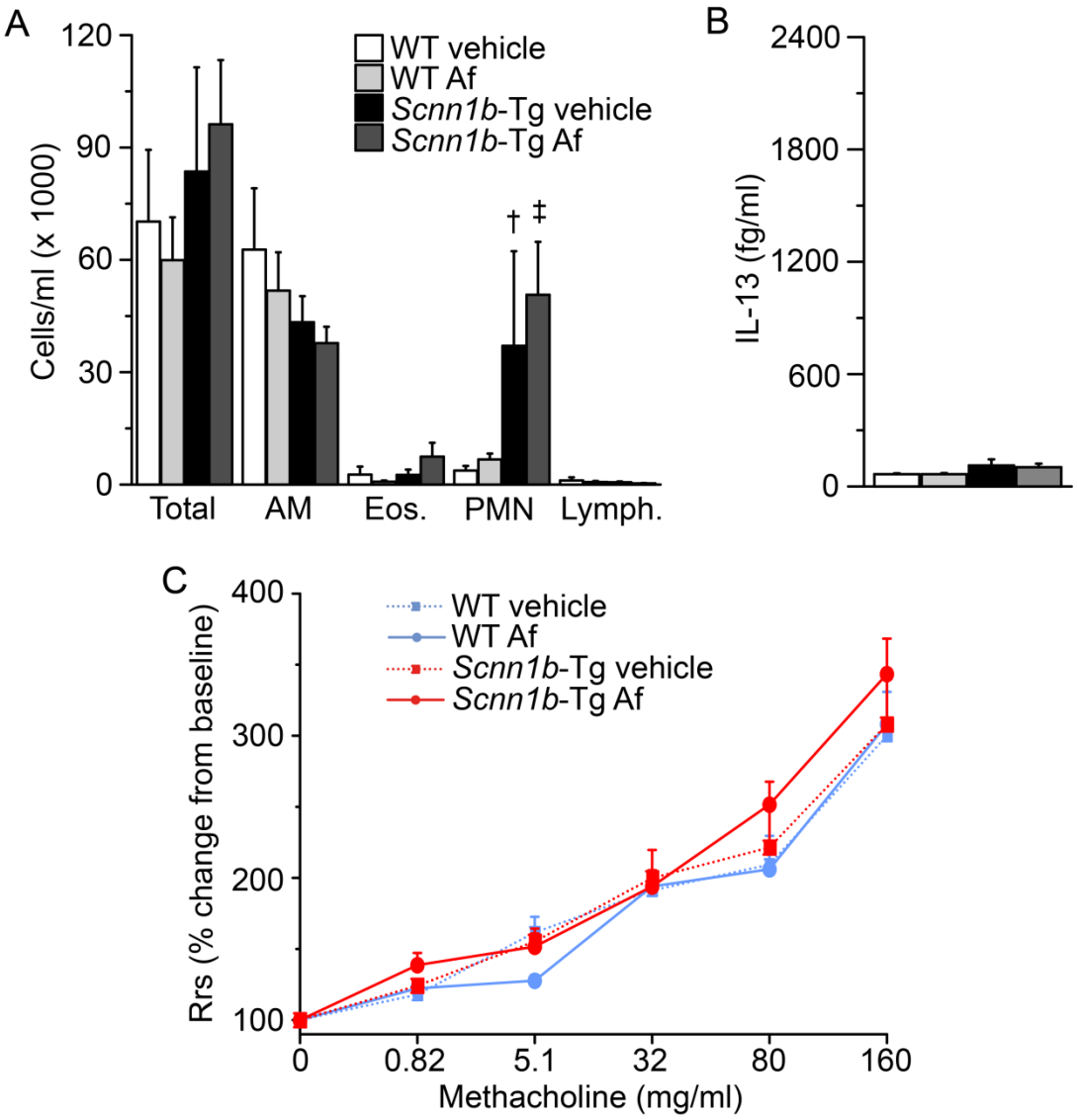

Figure 10. Allergen-induced type 2 airway inflammation and airway hyperresponsiveness are age-dependent. (A-C) Adult WT and *Scnn1b*-Tg mice were challenged with Af or vehicle alone and BAL inflammatory cell counts (Airway macrophages [AM], eosinophils [Eos.], neutrophils [PMN], and lymphocytes [Lymph.]) (A), IL-13 levels in BAL (B), and AHR by measuring respiratory resistance (Rrs) (C) were determined. n = 7-17 mice for each group). †P < 0.05 and ‡P < 0.01 compared with mice with the same treatment but different genotype.

Previous studies indicated that the immune system in neonatal mice is biased towards a type 2 immunity (Adkins et al., 2004; Saglani et al., 2009) that could facilitate increased susceptibility to develop type 2 airway inflammation upon allergen exposure. To investigate the relationship between the age-dependent susceptibility to allergen challenge and reported skewing towards type 2 immunity in neonatal mice, we compared

expression levels of a set of type 2 signature genes including *Il13*, *Muc5ac*, *Gob5*, *Arg1*, *Mmp12*, *Ym1*, *Ym2*, and *Chia* (Lewis et al., 2009) in lung tissues from WT and *Scnn1b*-Tg mice at neonatal, juvenile, and adult ages (Figure 11).

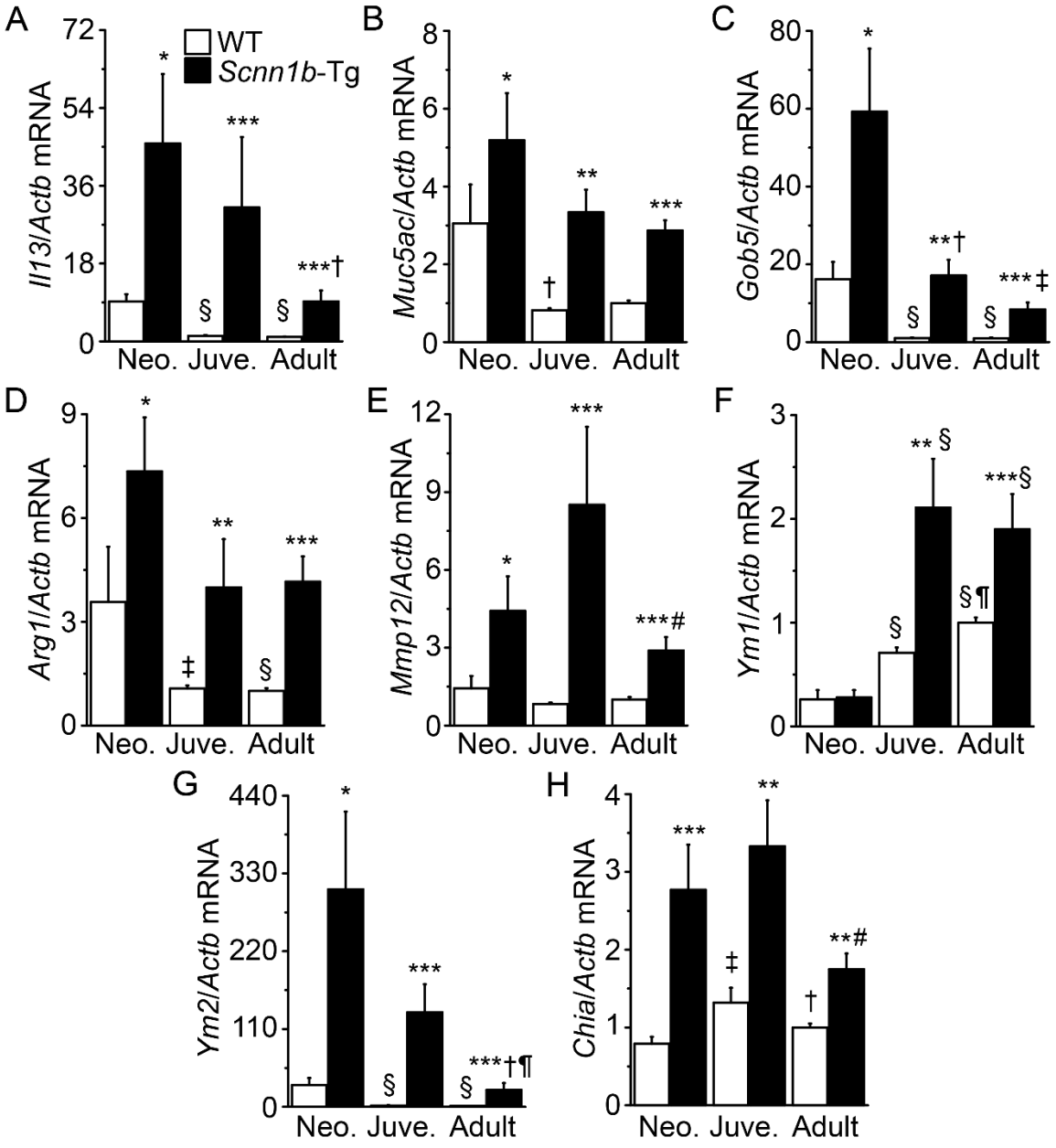

Figure 11. Expression levels of type 2 signature genes are elevated in lungs of neonatal WT and *Scnn1b*-Tg mice. (A-H) Expression of the type 2 signature genes *Il13* (A), *Muc5ac* (B), *Gob5* (C), *Arg1* (D), *Mmp12* (E), *Ym1* (F), *Ym2* (G), and *Chia* (H) in naïve neonatal (10-day-old), juvenile (Juve.) (3-week-old), and adult (6-week-old) WT and *Scnn1b*-Tg mice. n = 7-16 mice for each group. *P < 0.05, **P < 0.01, and ***P < 0.001 compared with mice with the same age but different genotype. †P < 0.05, ‡P < 0.01, and §P < 0.001 compared with neonatal mice with the same genotype. #P < 0.05 and ¶P < 0.01 compared with juvenile mice with the same genotype.

Several type 2 signature genes (*Il13*, *Muc5ac*, *Gob5*, *Arg1*, and *Ym2*) in lungs of neonatal WT mice were significantly elevated compared with older WT mice (Figure 11). At all age groups, expression levels of investigated type 2 signature genes in *Scnn1b*-Tg mice were significantly increased compared to WT mice, however, these differences in expression waned for most of the signatures at adult ages (Figure 11). Taken together, these results confirm that the immune system in neonatal/juvenile mouse lungs is skewed towards a type 2 immunity and support that this bias is associated with the increased susceptibility to allergen-induced type 2 airway inflammation in juvenile WT mice, as well as exacerbated responses in juvenile *Scnn1b*-Tg mice with impaired allergen clearance.

3.1.5 Pharmacological improvement of mucociliary clearance reduces allergen-induced type 2 airway inflammation and AHR in *Scnn1b*-Tg mice

As a proof of concept, we were interested if improvement of MCC can reduce allergen-induced type 2 airway inflammation. In previous studies, preventive treatment with the ENaC blocker amiloride improved airway surface hydration, MCC, and simultaneously decreases spontaneous type 2 airway inflammation in juvenile *Scnn1b*-Tg mice (Zhou et al., 2008). To investigate if improvement of airway surface hydration by ENaC inhibition has an effect on allergen-induced type 2 airway inflammation, we treated newborn WT and *Scnn1b*-Tg mice with airway instillations of amiloride or vehicle alone for 3 weeks and superimposed with an allergen provocation of Af or HDM in the presence of this treatment regime (Figure 12A and Figure 13A). Preventive amiloride treatment slightly reduced Af-induced airway eosinophilia (Figure 12C) but had no beneficial effects on HDM-induced type 2 airway inflammation including airway eosinophilia (Figure 13C), IL-13 levels in BAL (Figure 13D), and AHR in WT mice (Figure 14A). In contrast to WT mice, preventive amiloride treatment significantly reduced exaggerated Af- and HDM-induced airway eosinophilia (Figure 12C and Figure 13C) and IL-13 levels in BAL (Figure 12D and Figure 13D) in *Scnn1b*-Tg mice. Further, amiloride also prevented HDM-induced AHR in *Scnn1b*-Tg mice (Figure 14B). In summary, these data demonstrate that pharmacological improvement of airway surface hydration protects juvenile *Scnn1b*-Tg mice from allergen-induced type 2 airway inflammation.

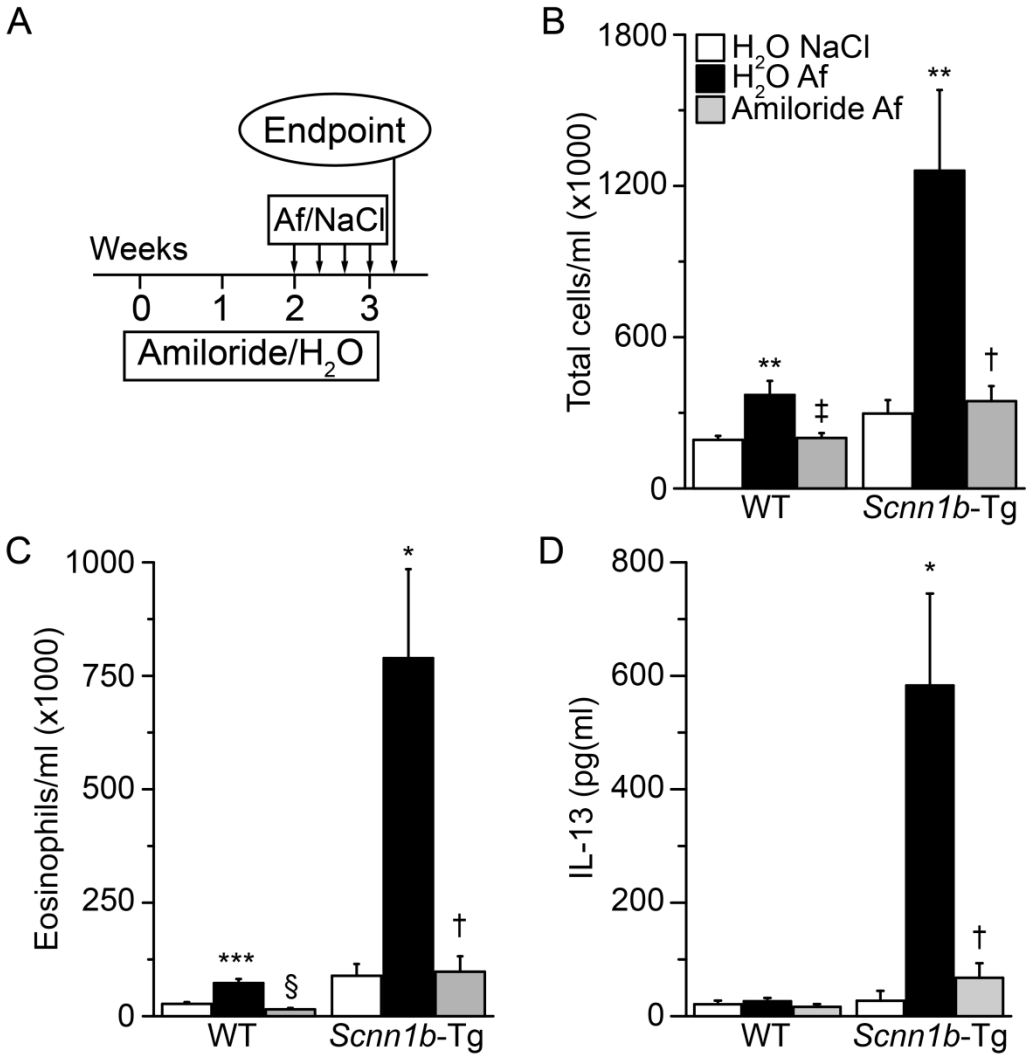

Figure 12. Pharmacological inhibition of ENaC reduces Af-induced type 2 airway inflammation in *Scnn1b*-Tg mice. (A-D) Newborn WT and *Scnn1b*-Tg mice were treated with airway instillation of amiloride or vehicle (ddH_2O) alone from the first day of life for a period of 3 weeks. Challenge with Af or vehicle (NaCl 0.9 %) alone was superimposed to amiloride treatment in juvenile mice (A), and BAL fluid total cell counts (B), eosinophil counts (C), and IL-13 levels (D) were determined. n = 14-49 in WT groups and n = 4-9 in *Scnn1b*-Tg groups. *P < 0.05, **P < 0.01, and ***P < 0.001 compared with vehicle-treated (ddH_2O and NaCl 0.9 %) mice of the same genotype. †P < .05, ‡P < .01, and §P < .001 compared with vehicle-treated (H_2O) Af-induced mice of same genotype.

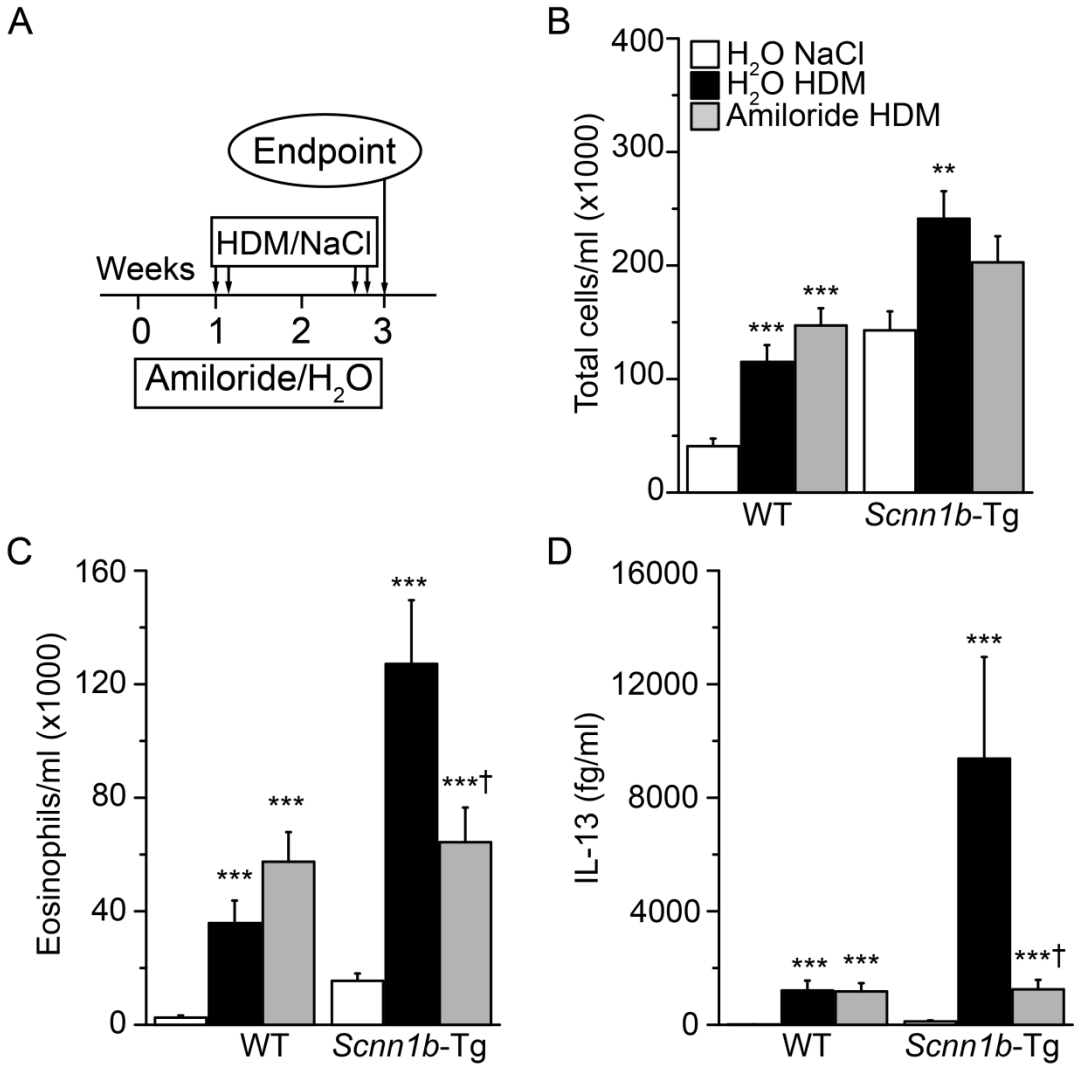

Figure 13. Pharmacological inhibition of ENaC reduces HDM-induced type 2 airway inflammation in *Scnn1b*-Tg mice. (A-D) Newborn WT and *Scnn1b*-Tg mice were treated with airway instillation of amiloride or vehicle (ddH_2O) alone from the first day of life for a period of 3 weeks. Sensitization and challenge with HDM or vehicle (NaCl 0.9 %) alone was superimposed to amiloride treatment in juvenile mice (A), and BAL fluid total cell counts (B), eosinophil counts (C), and IL-13 levels (D) were determined. n = 13-23 in WT groups and n = 16-28 in *Scnn1b*-Tg groups. **P < 0.01 and ***P < 0.001 compared with vehicle-treated (ddH_2O and NaCl 0.9 %) mice of the same genotype. †P < 0.05 compared with vehicle-treated (H_2O) HDM-induced mice of same genotype.

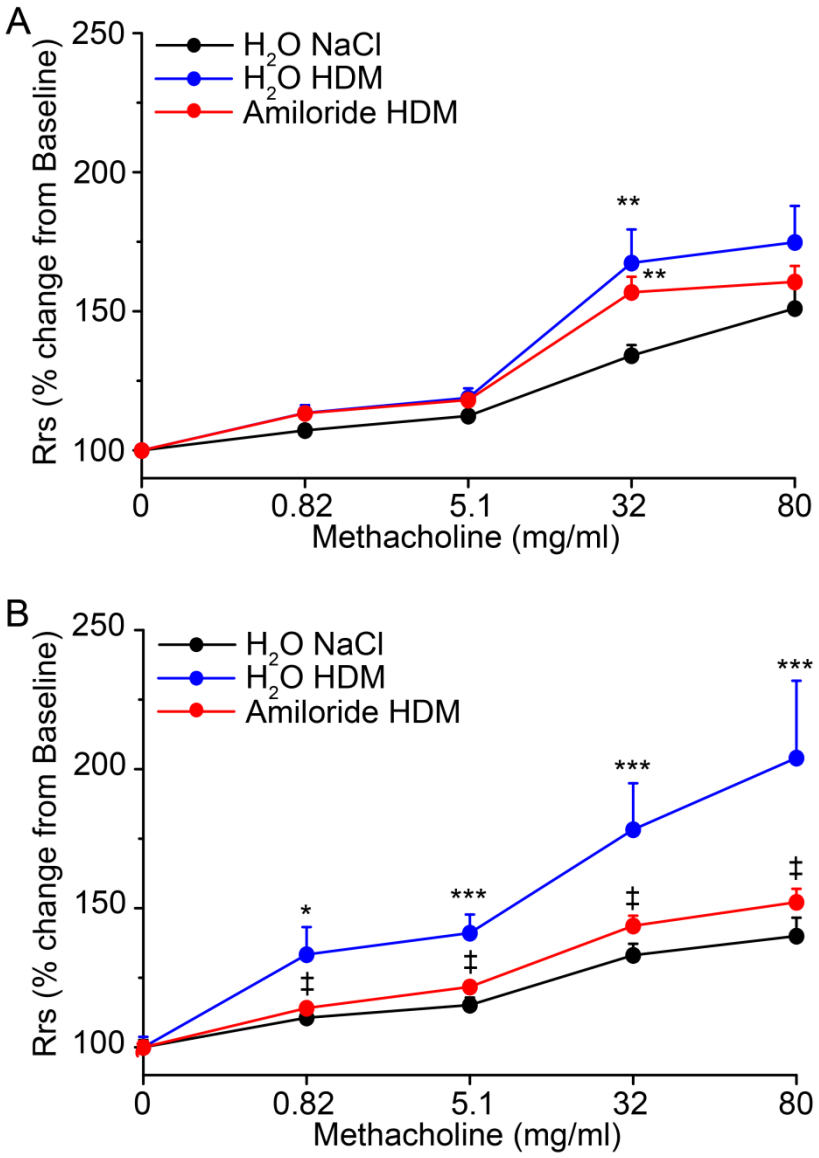

Figure 14. Pharmacological inhibition of ENaC reduces HDM-induced airway hyperresponsiveness in *Scnn1b*-Tg mice. (A and B) Newborn WT and *Scnn1b*-Tg mice were treated with airway instillation of amiloride or vehicle (ddH_2O) alone from the first day of life for a period of 3 weeks. Sensitization and challenge with HDM or vehicle (NaCl 0.9 %) alone was superimposed to amiloride treatment in juvenile mice and AHR by measuring respiratory resistance (Rrs) was determined in WT (A) and *Scnn1b*-Tg (B) mice. n = 13-23 in WT groups and n = 16-28 in *Scnn1b*-Tg groups. *P < 0.05, **P < 0.01, and ***P < 0.001 compared with vehicle-treated (ddH_2O and NaCl 0.9 %) mice of the same genotype. ‡P < 0.01 compared with vehicle-treated (H_2O) HDM-induced mice of same genotype.

3.2 Role of the adaptive immune system in chronic airway diseases

Our study and previous published data demonstrated that the immune system in neonatal/juvenile mice is skewed towards a type 2 immunity (Adkins et al., 2004; Li et al., 2004) and that the mucostatic environment in lungs of juvenile *Scnn1b*-Tg mice aggravates this bias (Fritzsching et al., 2017; Zhou-Suckow et al., 2017). Patients with CF lung disease suffer from a predominant neutrophilic airway inflammation (Conese et al., 2003) that is mostly triggered by signals from innate immune sources; however, there are also studies demonstrating that adaptive immunity including Th1-, Th2- and Th17-mediated inflammatory mechanisms contribute to chronic airway inflammation in lungs of CF patients.(Hartl et al., 2006; Hubeau et al., 2001; Tiringer et al., 2013). Further, it was shown that end-stage CF patients had an abnormal number of lymphoid follicles in their lungs that are rich in T and B cells (Lammertyn et al., 2017) and those were also found in *Scnn1b*-Tg mice with impaired MCC (Livraghi et al., 2009). Together these findings suggest a crucial role of the adaptive immune system contributing to these inflammatory processes. So far pathogenic mechanisms in CF lung disease that drive adaptive immune responses and their implications are only partially understood. To better understand these mechanisms in the development of CF lung diseases *in vivo*, we used *Scnn1b*-Tg mice as a model for CF-like lung disease and crossed them with *Rag1*$^{-/-}$ mice, that lack mature T and B cells (Mombaerts et al., 1992), and studied the lung phenotype of juvenile *Scnn1b*-Tg, double mutant *Scnn1b*-Tg/*Rag1*$^{-/-}$, and WT and *Rag1*$^{-/-}$ littermates.

3.2.1 T and B cells are not essential for chronic airway inflammation in juvenile *Scnn1b*-Tg mice

To determine the role of T and B cells in the pathogenesis of chronic airway inflammation in mice with CF-like lung disease, BAL was performed and inflammatory cell counts were compared between juvenile WT, *Rag1*$^{-/-}$, *Scnn1b*-Tg, and *Scnn1b*-Tg/*Rag1*$^{-/-}$ mice. In line with previous studies (Mall et al., 2008), total inflammatory cells were significantly elevated in BAL fluid of juvenile *Scnn1b*-Tg mice compared to WT littermates (Figure 15A). The lack of T and B cells had no effect on total inflammatory cells in *Scnn1b*-Tg mice (Figure 15A). The level of AMs was significantly increased in *Scnn1b*-Tg mice compared to WT controls (Figure 15B). In *Scnn1b*-Tg/*Rag1*$^{-/-}$ mice, AMs tended to be reduced compared to *Scnn1b*-Tg mice (Figure 15B), but, this difference did not reach statistical significance. BAL neutrophils and eosinophils were significantly increased in *Scnn1b*-Tg and *Scnn1b*-Tg/*Rag1*$^{-/-}$ mice compared to their WT and *Rag1*$^{-/-}$ littermates

and did not differ between *Scnn1b*-Tg and *Scnn1b*-Tg/*Rag1*$^{-/-}$ mice (Figure 15C and D). Collectively, these data indicate that chronic airway inflammation develops independently of the presence of T and B cells in juvenile *Scnn1b*-Tg mice.

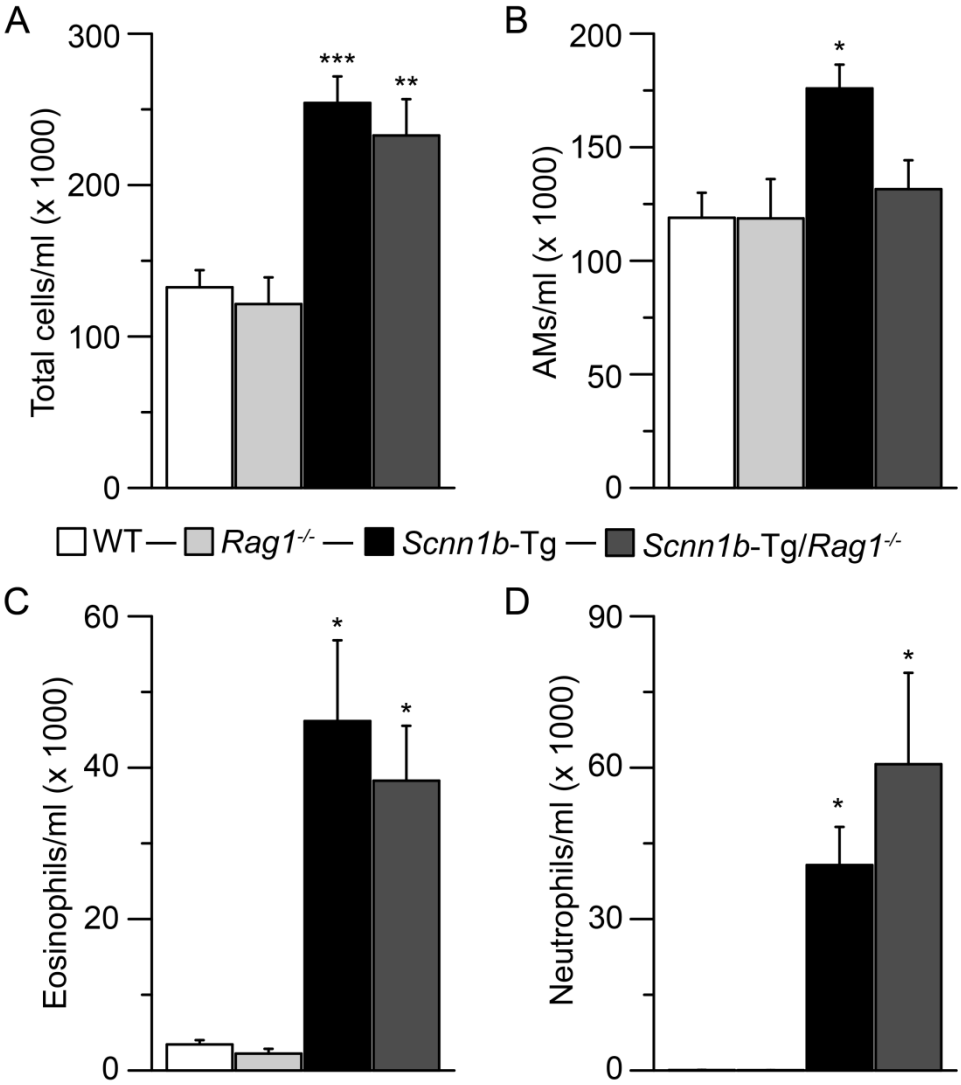

Figure 15. Chronic airway inflammation in juvenile *Scnn1b*-Tg mice develops independently of the presence of T and B cells. Total cell (A), airway macrophage (AM) (B), eosinophil (C), and neutrophil (D) counts in BAL fluid were determined by flow cytometry in juvenile WT, *Rag1*$^{-/-}$, *Scnn1b*-Tg, and double-mutant *Scnn1b*-Tg/*Rag1*$^{-/-}$ mice. n = 14-16 mice for each group. *P < 0.05, **P < 0.01 and ***P < 0.001 compared with WT mice.

3.2.2 Expression of *Il17a* is increased in the lungs of juvenile *Scnn1b*-Tg mice

Studies in patients with CF demonstrated that i) Th1 cytokines, such as IFNγ ii) Th2 cytokines, such as IL-4, IL-5 and IL-13, and iii) IL-17A and Th17-related cytokines, such as IL-6 and IL-8 are elevated in BAL fluid compared to healthy individuals (Tiringer et al.,

2013). To investigate whether T and B cells are predominant sources and inducers of these cytokines in lungs of *Scnn1b*-Tg mice, we isolated RNA from lung tissue, performed real-time RT-PCR, and compared expression levels of *Ifnγ*, *Il6*, *Cxcl1* (a functional mouse homolog for human *Il8*), *Il4*, *Il5*, *Il13*, and *Il17a*, between juvenile WT, *Rag1*$^{-/-}$, *Scnn1b*-Tg, and *Scnn1b*-Tg/*Rag1*$^{-/-}$ mice (Figure 16).

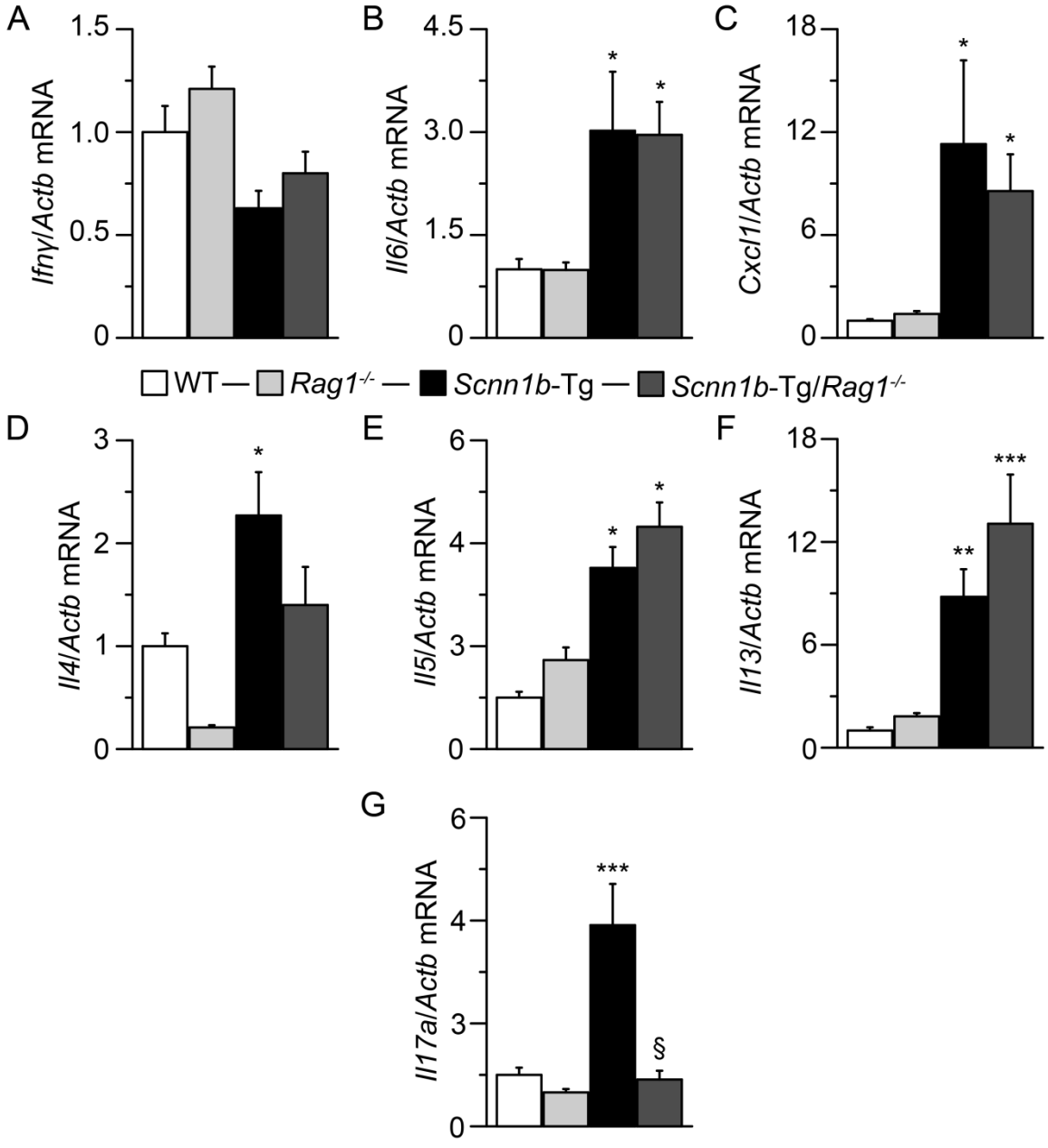

Figure 16. Lack of T and B cells reduces *Il17a* expression in lungs of juvenile *Scnn1b*-Tg mice. (A-G) Gene expression of key Th1-, Th2-, and Th17-related cytokines in lungs of juvenile WT, *Rag1*$^{-/-}$, *Scnn1b*-Tg, and *Scnn1b*-Tg/*Rag1*$^{-/-}$ mice. Expression levels of *Ifnγ* (A), *Il6* (B), *Cxcl1* (C), *Il4* (D), *Il5* (E), *Il13* (F), and *Il17a* (G) were determined by real-time RT-PCR. n = 7-12 mice for each group. *P < 0.05, **P < 0.01 and ***P < 0.001 compared with WT mice. §P < 0.001 compared with Scnn1b-Tg mice.

The expression level of *Ifnγ* was not different in lung tissues of juvenile WT, *Rag1*$^{-/-}$, *Scnn1b*-Tg, and *Scnn1b*-Tg/*Rag1*$^{-/-}$ mice (Figure 16A), but showed a trend to a somewhat decreased expression in lungs of *Scnn1b*-Tg, and *Scnn1b*-Tg/*Rag1*$^{-/-}$ mice. Th17-related genes *Il6*, *Cxcl1* and Th2 signature genes *Il4*, *Il5*, and *Il13* were elevated in *Scnn1b*-Tg mice compared to their WT and *Rag1*$^{-/-}$ littermates and deletion of *Rag1* showed no effect on the expression of these genes in *Scnn1b*-Tg mice (Figure 16B-F). Of note, gene expression of *Il17a* was significantly increased in lungs from *Scnn1b*-Tg mice compared to WT, *Rag1*$^{-/-}$, and *Scnn1b*-Tg/*Rag1*$^{-/-}$ littermates (Figure 16G). Taken together, these data demonstrate a skewing towards a Th2- and Th17-associated cytokine profile in juvenile *Scnn1b*-Tg mice that correlates with findings previously observed in patients with CF lung disease (Tiringer et al., 2013) but also indicate that innate rather than adaptive immunity is a predominant source of these cytokines *in vivo,* with the exception of *Il17a*.

3.2.3 The number of IL-17A-producing leukocytes is elevated in juvenile *Scnn1b*-Tg mice

Because *Il17a* expression is increased in lungs of juvenile *Scnn1b*-Tg mice, and because different T cell populations are known to produce IL-17A, we next determined the cellular sources of IL-17A expression. According to the literature, CD4$^+$ T, CD8$^+$ T, γδ T and natural killer (NK)T cells are able to produce IL-17A. Besides T cells, NK cells and the recently discovered ILC3s are also capable of producing IL-17A (Cua and Tato, 2010; Dubin and Kolls, 2011; Miossec and Kolls, 2012). Based on this information, we performed flow cytometry with intracellular staining against the cytokine IL-17A and developed a gating strategy (Figure 3) to identify these IL-17A producing cell types in the lungs of juvenile WT, *Rag1*$^{-/-}$, *Scnn1b*-Tg, and *Scnn1b*-Tg/*Rag1*$^{-/-}$ mice. We found that the percentage and total number of IL-17A positive leukocytes was significantly increased in *Scnn1b*-Tg mice compared to WT, *Rag1*$^{-/-}$, *Scnn1b*-Tg/*Rag1*$^{-/-}$ littermates (Figure 17). Further, in *Scnn1b*-Tg/*Rag1*$^{-/-}$ mice the percentage and total number of IL-17A$^+$ leukocytes were elevated compared to *Rag1*$^{-/-}$ littermates (Figure 17) suggesting that T cells are not the only source for increased IL-17A secretion in *Scnn1b*-Tg mice. The number of lung-derived IL-17A-producing CD8$^+$ T- and NKT cells did not differ between WT and *Scnn1b*-Tg mice (data not shown) nor did the number of lung-derived IL-17A-producing NK cells (data not shown). Interestingly, we detected significantly increased numbers of IL-17A$^+$ CD4$^+$ T and γδ T cells in lungs of *Scnn1b*-Tg mice compared to WT controls and in both groups the number of lung-derived IL-17A$^+$ γδ T cells was about 6-fold higher than the number of IL-17A-producing CD4$^+$ T cells (Figure 18A and B). The number of IL-17A$^+$ ILC3s that are defined by the absence of

RAG-dependent rearranged antigen receptor, the lack of myeloid cell and dendritic cell phenotypical markers and expression of the transcription factor RORγt (Artis and Spits, 2015; Spits et al., 2013), was significantly elevated in lungs of *Scnn1b*-Tg and *Scnn1b*-Tg/*Rag1*$^{-/-}$ mice compared to WT and *Rag1*$^{-/-}$ controls (Figure 18C). This result indicates that besides T cells other cells, namely ILC3s, contribute to the augmented IL-17A secretion in juvenile *Scnn1b*-Tg mice. In summary, these data demonstrate an increased accumulation of IL-17A-producing, CD4^{+} T, γδ T cells, and ILC3s in lungs of juvenile *Scnn1b*-Tg mice and indicate that γδ T cells are the predominant source of IL-17A in both WT and *Scnn1b*-Tg mice.

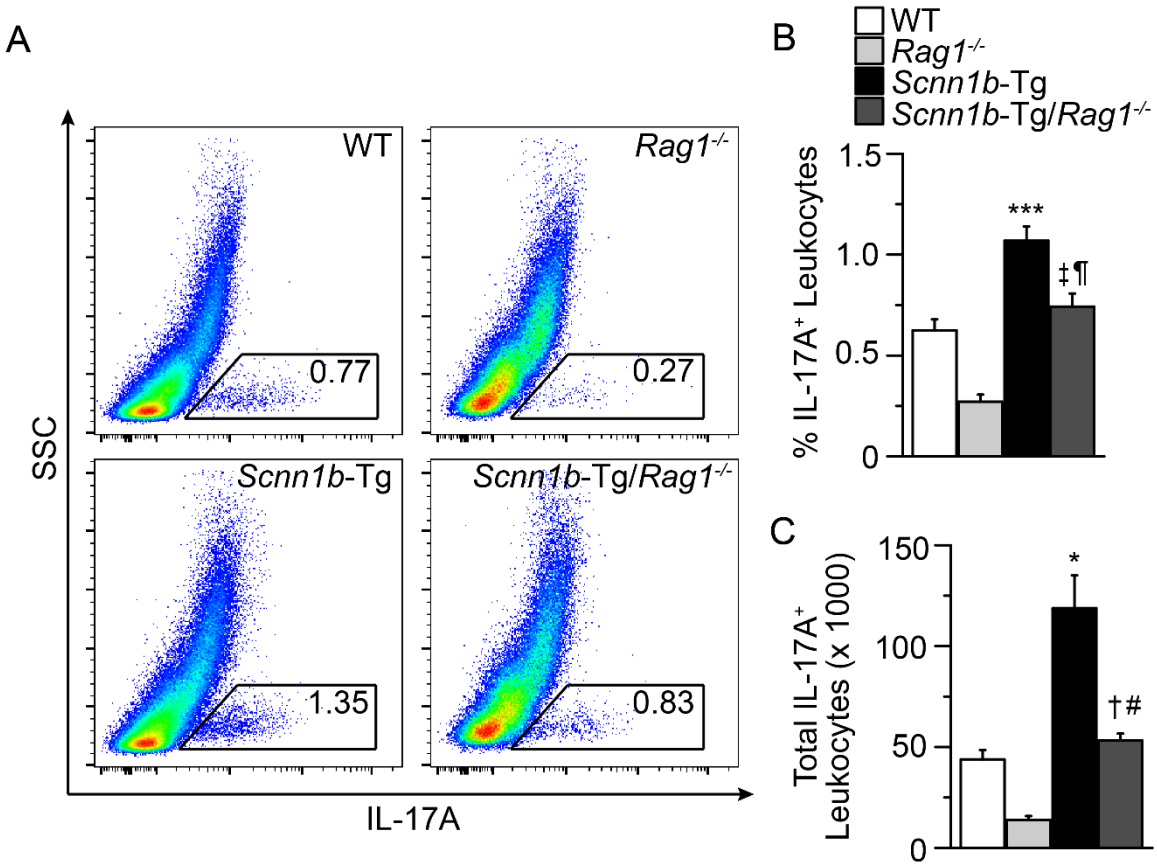

Figure 17. Increased number of IL-17A-producing leukocytes in lungs of juvenile *Scnn1b*-Tg mice. (A-C) Number of IL-17A expressing leukocytes that were isolated from lungs of juvenile WT, *Rag1*$^{-/-}$, *Scnn1b*-Tg, and *Scnn1b*-Tg/*Rag1*$^{-/-}$ mice and determined by flow cytometry after *in vitro* stimulation. (A) Representative dot plots of WT, *Rag1*$^{-/-}$, *Scnn1b*-Tg, and *Scnn1b*-Tg/*Rag1*$^{-/-}$ leukocytes (CD45^{+}). Number in rectangles represents percentage of IL-17A^{+} leukocytes. Percentage (B) and total number (C) of IL-17^{+} leukocytes in lungs of WT, *Rag1*$^{-/-}$, *Scnn1b*-Tg, and *Scnn1b*-Tg/*Rag1*$^{-/-}$ mice. n = 10-11 mice for each group. *P < 0.05 and ***P < 0.001 compared with WT mice. ¶P < 0.05 and #P < 0.001 compared with *Rag1*$^{-/-}$ mice. †P < 0.05 and ‡P < 0.01 compared with *Scnn1b*-Tg mice.

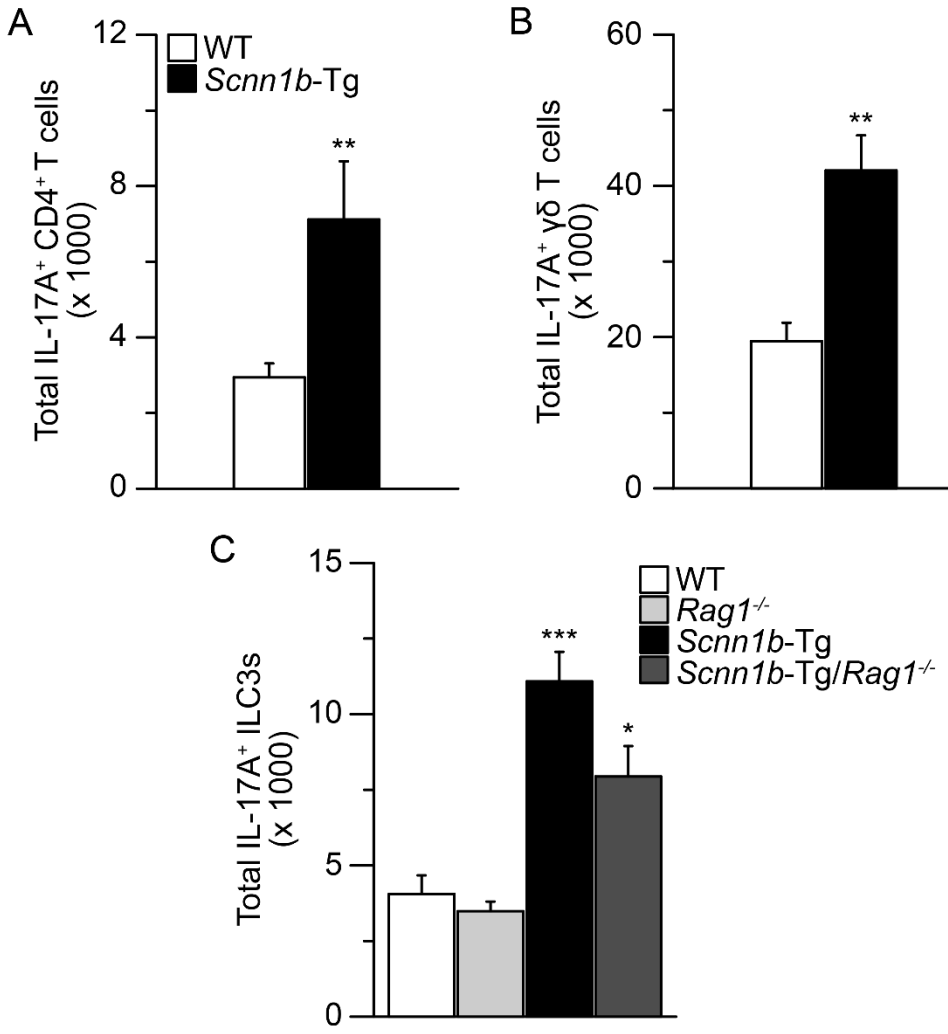

Figure 18. Augmented accumulation of IL-17A-producing CD4⁺ T, γδ T cells, and ILC3s in lungs of juvenile *Scnn1b*-Tg mice. (A-C) Single cells were isolated from lungs of mice, stimulated with PMA and ionomycin *in vitro*, and stained with the appropriate antibodies for the detection of intracellular IL-17A expression by flow cytometry. (A and B) The total number of lung-derived IL-17A⁺ CD4⁺ T (A) and IL-17A⁺ γδ T (B) cells isolated from juvenile WT and *Scnn1b*-Tg mice. Due to the fact that *Rag1*$^{-/-}$ and *Scnn1b*-Tg/*Rag1*$^{-/-}$ mice lack T cells, they were not detected in those genotypes. (C) Total number of lung-derived IL-17A⁺ ILC3s isolated from juvenile WT, *Rag1*$^{-/-}$, *Scnn1b*-Tg, and *Scnn1b*-Tg/*Rag1*$^{-/-}$ mice. n = 5-11 mice for each group. *P < 0.05, **P < 0.01 and ***P < 0.001 compared with WT mice.

3.2.4 Mucus obstruction develops independently of T and B cells in juvenile *Scnn1b*-Tg mice

Previous studies demonstrated that juvenile *Scnn1b*-Tg mice suffer from severe mucus plugging which is a result of the combination of airway surface dehydration, impaired mucus clearance, and mucin overexpression that is driven by the chronic inflammatory milieu (Livraghi-Butrico et al., 2017). The understanding of the role of T and B cells in relation to impaired mucus clearance and mucus overproduction during chronic airway inflammation is limited (Cohn et al., 1997; Justice et al., 2002). Studies by Fujisawa et al.

showed that IL-17A could induce the expression of *Muc5ac* and *Muc5b* from airway epithelial cells *ex vivo* (Chen et al., 2003; Fujisawa et al., 2011; Fujisawa et al., 2009). Our results indicate that IL-17A production is increased in lungs of juvenile *Scnn1b*-Tg mice and that the lack of T cells, specifically γδ T cells, resulted in reduced *Il17a* expression (Figure 16 and Figure 18). Based on these findings, we investigated the effects of the depletion of T and B cells on airway mucus obstruction and mucin hypersecretion in juvenile *Scnn1b*-Tg mice *in vivo*. Therefore, we determined mucus obstruction by histological analysis, and expression of the mucins *Muc5ac* and *Muc5b* and the expression of the goblet cell marker gene *Gob5* in lungs of juvenile WT, *Rag1*$^{-/-}$, *Scnn1b*-Tg, and *Scnn1b*-Tg/*Rag1*$^{-/-}$ mice.

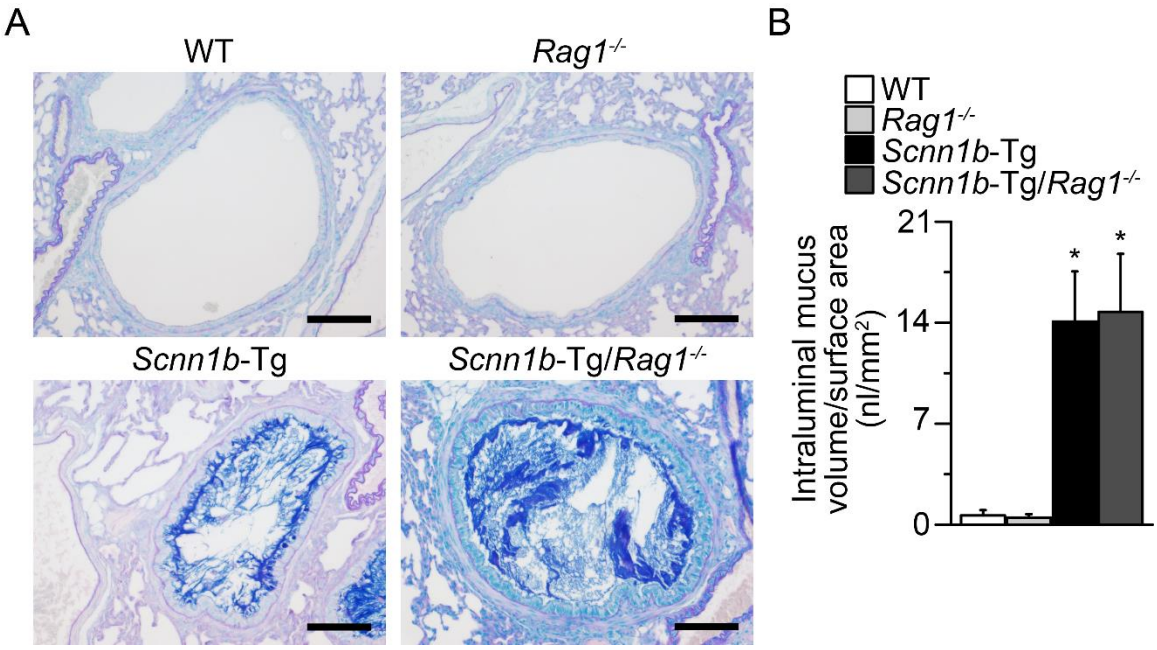

Figure 19. Lack of T and B cells has no effect on mucus obstruction in juvenile *Scnn1b*-Tg mice. (A and B) Lung histology of AB-PAS stained sections from juvenile WT, *Rag1*$^{-/-}$, *Scnn1b*-Tg, and *Scnn1b*-Tg/*Rag1*$^{-/-}$ mice. Lungs were sectioned at the level of the proximal main axial airway. (A) Morphology of AB-PAS stained sections. Scale bars: 100 µm. (B) Summary of airway mucus content determined by the quantification of AB-PAS positive material in the airway lumen. n = 8-12 mice for each group. *P < 0.05 compared with WT mice.

The airways of WT and *Rag1*$^{-/-}$ mice were free of mucus, whereas obstructed airways were observed in *Scnn1b*-Tg, and *Scnn1b*-Tg/*Rag1*$^{-/-}$ mice at similar levels (Figure 19A and B). In addition to airway mucus obstruction, *Muc5ac* and *Muc5b* expression were significantly increased to similar levels in *Scnn1b*-Tg and *Scnn1b*-Tg/*Rag1*$^{-/-}$ mice compared to WT and *Rag1*$^{-/-}$ mice (Figure 20A and B). The expression of the goblet cell

marker gene *Gob5* was not changed between *Scnn1b*-Tg and *Scnn1b*-Tg/*Rag1*$^{-/-}$ mice but was elevated compared to their WT and *Rag1*$^{-/-}$ controls (Figure 20C).

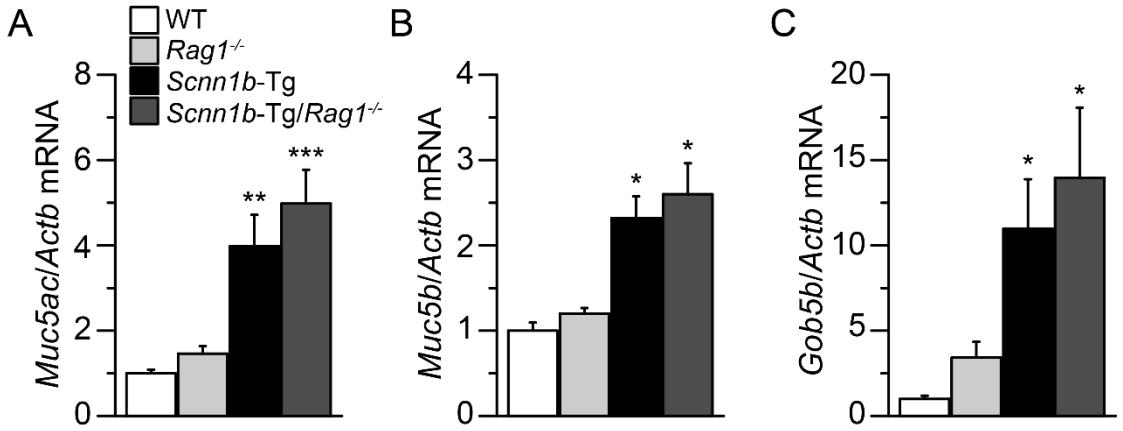

Figure 20. Mucin expression is independent of the presence of T and B cells in juvenile *Scnn1b*-Tg mice. Expression levels of *Muc5ac* (A), *Muc5b* (B), and *Gob5* (C) were determined by real-time RT-PCR in juvenile WT, *Rag1*$^{-/-}$, *Scnn1b*-Tg, and *Scnn1b*-Tg/*Rag1*$^{-/-}$ mice. n = 7-8 mice for each group. *P < 0.05, **P < 0.01 and ***P < 0.001 compared with WT mice.

Collectively, these data indicate that T and B cells do not mediate mucus obstruction and mucin expression in lungs of juvenile *Scnn1b*-Tg mice although secretion of the mucus-inducing cytokine IL-17A that is mainly produced by T cells is increased in juvenile *Scnn1b*-Tg mice.

3.2.5 Lack of T and B cells reduces structural lung damage in juvenile *Scnn1b*-Tg mice

Scnn1b-Tg mice develop structural lung damage which is mediated through increased protease activity associated with chronic inflammation (Fritzsching et al., 2015; Gehrig et al., 2014; Trojanek et al., 2014). Elevated secretion of IL-17A in the lung has also been associated with structural lung damage and emphysematous lesions in COPD (Kurimoto et al., 2013; Muir et al., 2016; Tan et al., 2011) and there is evidence that IL-17A can activate airway neutrophils through direct or indirect mechanisms leading to increased elastase activity on neutrophils that facilitates structural lung damage (Linden and Adachi, 2002). To determine if the lack of T and B cells affects structural lung damage in juvenile *Scnn1b*-Tg mice, mean linear intercepts and destructive index were compared between juvenile WT, *Rag1*$^{-/-}$, *Scnn1b*-Tg, and *Scnn1b*-Tg/*Rag1*$^{-/-}$ mice.

Consistent with previous results (Trojanek et al., 2014), mean linear intercepts and destructive index were significantly increased in lungs of *Scnn1b*-Tg mice versus WT littermates (Figure 21). Interestingly, we found that the lack of T and B cells in *Scnn1b*-Tg mice significantly reduces structural lung damage, as shown by an

attenuation of mean linear intercepts and destructive index in *Scnn1b*-Tg/*Rag1*$^{-/-}$ mice (Figure 21).

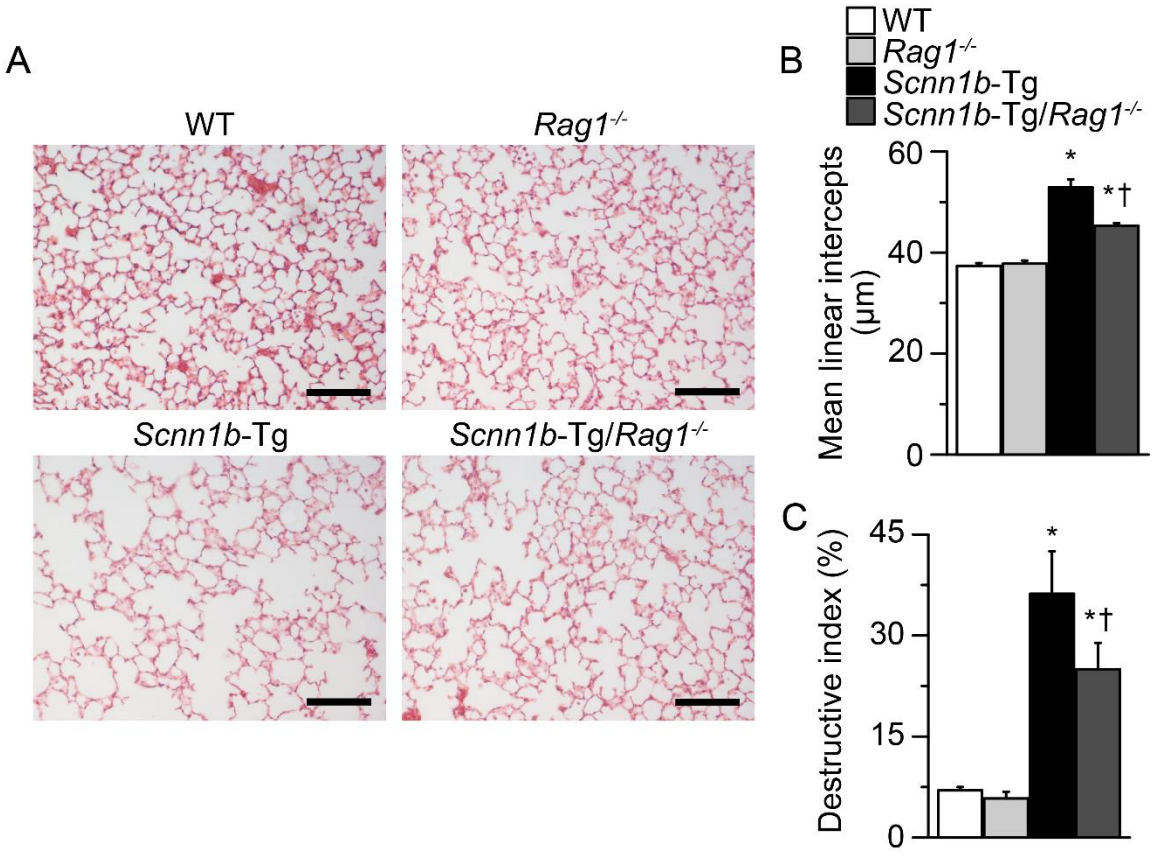

Figure 21. T and B cells contribute to structural lung damage in juvenile *Scnn1b*-Tg mice. (A-C) Lung histology of hematoxylin and eosin-stained sections from juvenile WT, *Rag1*$^{-/-}$, *Scnn1b*-Tg, and *Scnn1b*-Tg/*Rag1*$^{-/-}$ mice. (A) Morphology of hematoxylin and eosin-stained sections. Scale bars: 100 µm. (B and C) Mean linear intercepts (B) were determined by the distances between alveolar walls, and destructive index (C) were determined by the percent of destructed alveoli. n = 6-12 mice for each group. *P < 0.05 compared with WT mice. †P < 0.05 compared with *Scnn1b*-Tg mice

Taken together, the data demonstrate that the lack of T and B cells reduces distal airspace enlargement and alveolar wall destruction in juvenile *Scnn1b*-Tg mice and suggest that T cell mediated IL-17A secretion might be implicated in this process in CF-like lung disease.

3.2.6 Lack of T and B cells attenuates airway macrophage activation in juvenile *Scnn1b*-Tg mice

Previous studies demonstrated elevated activation of AMs that is associated with emphysema formation and structural lung damage in *Scnn1b*-Tg mice (Trojanek et al., 2014). IL-17A could stimulate the recruitment and activation of AMs via direct or indirect mechanisms (Gaffen, 2008). To investigate the role of AM activation on reduced emphysema formation in *Scnn1b*-Tg/*Rag1*$^{-/-}$ mice, flow cytometry was performed and the population of AMs positive for the activation marker CD11b (Fritzsching et al., 2017) was determined in BAL of juvenile WT, *Rag1*$^{-/-}$, *Scnn1b*-Tg, and *Scnn1b*-Tg/*Rag1*$^{-/-}$ mice.

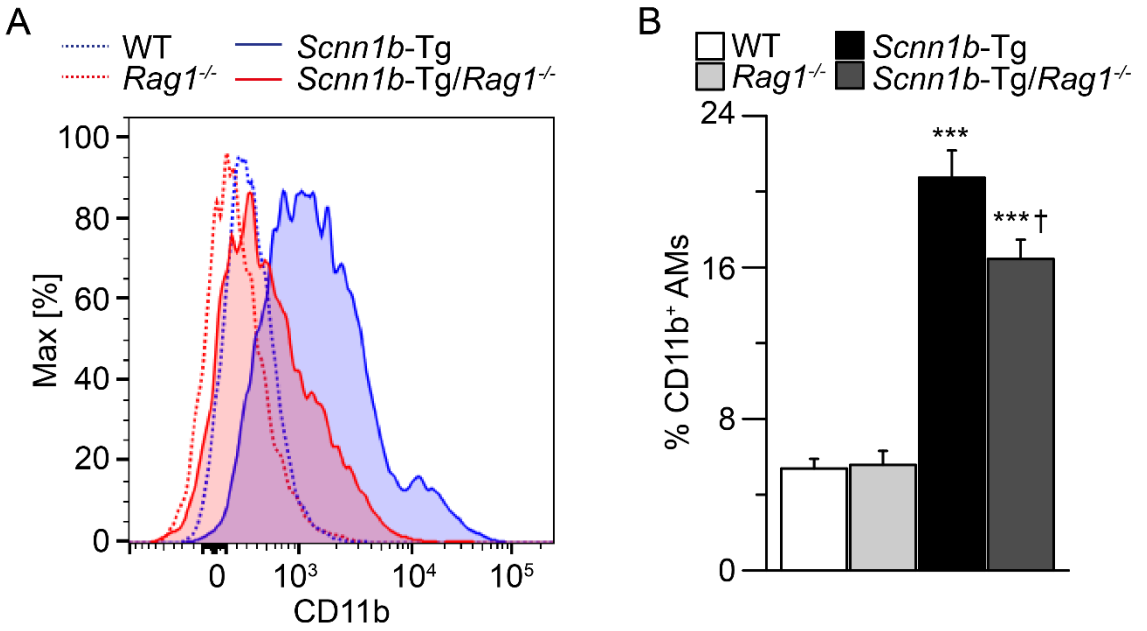

Figure 22. T and B cells contribute to airway macrophage activation in juvenile *Scnn1b*-Tg mice. (A and B) BAL was performed and the percentage of CD11b^{+} airway macrophages (AMs) was determined by flow cytometry in juvenile WT, *Rag1*$^{-/-}$, *Scnn1b*-Tg, and *Scnn1b*-Tg/*Rag1*$^{-/-}$ mice. (A) Representative histogram plot of WT, *Rag1*$^{-/-}$, *Scnn1b*-Tg, and *Scnn1b*-Tg/*Rag1*$^{-/-}$ AMs (Siglec-F^{+}, CD11c^{+}, MHCII^{mid}, CD64^{+}, F4/80^{+}, and CD3^{-}). Y-axis represents the percentage of the maximum count of AMs for each genotype. (B) Percentage of CD11b^{+} AMs in BAL of WT, *Rag1*$^{-/-}$, *Scnn1b*-Tg, and *Scnn1b*-Tg/*Rag1*$^{-/-}$ mice. n = 15-17 mice for each group. ***P < 0.001 compared with WT mice. †P < 0.05 compared with *Scnn1b*-Tg mice.

Consistent with previous studies (Fritzsching et al., 2017), we observed an increased activation of AMs in juvenile *Scnn1b*-Tg mice compared to WT littermates (Figure 22). In *Scnn1b*-Tg/*Rag1*$^{-/-}$ mice, AM activation was significantly reduced compared to *Scnn1b*-Tg mice, but remained significantly elevated when compared to WT and *Rag1*$^{-/-}$ mice (Figure 22). These data indicate that T and B cells contribute to macrophage activation and that IL-17A may be implicated in this process.

4 Discussion

The MCC apparatus is an important innate defense mechanism of the lung. It provides a highly effective defense against continuously inhaled noxious stimuli such as bacteria, viruses, allergens and other environmental irritants that are properly cleared from the airways by an intact MCC (Zhou-Suckow et al., 2017). Impaired MCC and/or excessive mucus secretion contribute to the pathogenesis of many chronic lung diseases including CF, asthma, and COPD (Fahy and Dickey, 2010). Chronic airway inflammation is a characteristic pathogenic feature of these lung diseases; however, mechanistic insights that unravel the relationship between impaired MCC and chronic airway inflammation and its functional consequences are limited. In this study, we focused on the role of MCC as an important innate defense mechanism in the pathogenesis of allergen-induced type 2 airway inflammation and further investigated the role of T and B cells as key cells of the adaptive immunity in chronic airway diseases.

4.1 Impaired mucociliary clearance triggers type 2 airway inflammation

Previous studies demonstrated that asthma is associated with impaired MCC (Bateman et al., 1983; Messina et al., 1991) and the principal cause of death from asthma is asphyxiation from intraluminal airway obstruction caused by mucus plugs (Aikawa et al., 1992; Messer et al., 1960). Type 2 airway inflammation including increased levels of eosinophils, type 2 signature cytokines, and AHR is a characteristic feature of allergen-induced asthma (Lambrecht and Hammad, 2015). Type 2 inflammation not only contributes to disease severity in allergen-induced asthma but also in other chronic lung diseases with impaired MCC such as CF and COPD (Postma and Rabe, 2015; Tiringer et al., 2013). Many CF and COPD patients develop ABPA, a hypersensitivity against antigens of the fungi *Aspergillus fumigatus*, that is associated with increased type 2 immune responses similar to those observed in allergen-induced asthma (Agarwal et al., 2010; Jin et al., 2014; Knutsen and Slavin, 2011). However, underlying risk factors and mechanisms that trigger type 2 airway inflammation remain poorly understood. Based on these findings and reports we investigated the relationship between impaired MCC and allergen-induced type 2 airway inflammation.

In this study, for the first time, we could link impaired MCC with reduced clearance of aeroallergens as a risk factor for the development of allergen-induced type 2 airway inflammation. By using a model that induces allergic asthma by intratracheal application

of the aeroallergen HDM, we showed that juvenile *Scnn1b*-Tg mice with reduced MCC develope an aggravated type 2 airway inflammation with airway eosinophilia, elevated levels of the type 2 signature cytokines IL-4, IL-5, and IL-13, and AHR (Figure 8 and Figure 9). These findings were further supported by previously published data from our group in which we used a short-term allergen challenge protocol consisting of 4 intratracheal Af challenges in juvenile WT and *Scnn1b*-Tg mice (Fritzsching et al., 2017). This allergen-inducing asthma protocol triggered an aggravated type 2 airway inflammation together with GCM and AHR that was similar to that induced by the HDM sensitization and challenge protocol in juvenile *Scnn1b*-Tg mice (Figure 8 and Figure 9). Further, in this work, we demonstrated that transcript expression of *Il33* and *Il13* were strongly upregulated at baseline and after allergen challenge in airway epithelial cells of juvenile *Scnn1b*-Tg mice compared to WT littermates and that IL-33 could induce *Il13* expression in primary airway epithelial cells (Fritzsching et al., 2017). These findings showed a mechanism in which the airway epithelium is a considerable source for IL-13 production and contributes to the orchestration of allergen-induced type 2 airway inflammation. Besides the induction of IL-13 from airway epithelial cells by IL-33, several other studies demonstrated that the release of IL-33 from the airway epithelium induces the production of IL-5 and IL-13 from ILC2s (Halim et al., 2012) and activation of AMs and Th2 cells (Kurowska-Stolarska et al., 2009; Louten et al., 2011) that were also identified to be one of the main IL-13 sources in juvenile Af-challenged *Scnn1b*-Tg mice (Fritzsching et al., 2017). A schematic overview of the relation between impaired MCC and the induction of allergen-induced type 2 airway inflammation is shown in Figure 23.

AMs and cDCs are crucial cell types involved in asthma pathogenesis (Balhara and Gounni, 2012; van Rijt et al., 2005). Due to the fact that impaired MCC leads to reduced allergen clearance from the lungs and the airways of *Scnn1b*-Tg mice (Figure 4 and Figure 5), we were also interested whether the allergen uptake of AMs and cDCs is affected. We found a reduced allergen uptake by AMs in juvenile *Scnn1b*-Tg mice (Figure 6). In combination with impaired MCC, decreased allergen uptake by AMs might further contribute to impaired allergen clearance and thus to the overall burden of allergens in the lungs of *Scnn1b*-Tg mice. In contrast to the decreased allergen uptake by AMs, we found that the uptake by cDCs was significantly elevated in *Scnn1b*-Tg mice compared with WT littermates (Figure 7). This finding suggests that the enhanced allergen uptake by cDCs might be due to a more active phenotype of cDCs in the pro-inflammatory milieu and/or an increased allergen load in mucostatic airways of *Scnn1b*-Tg mice and thus might contribute to an elevated priming of effector T cells in *Scnn1b*-Tg mice (Figure 8B).

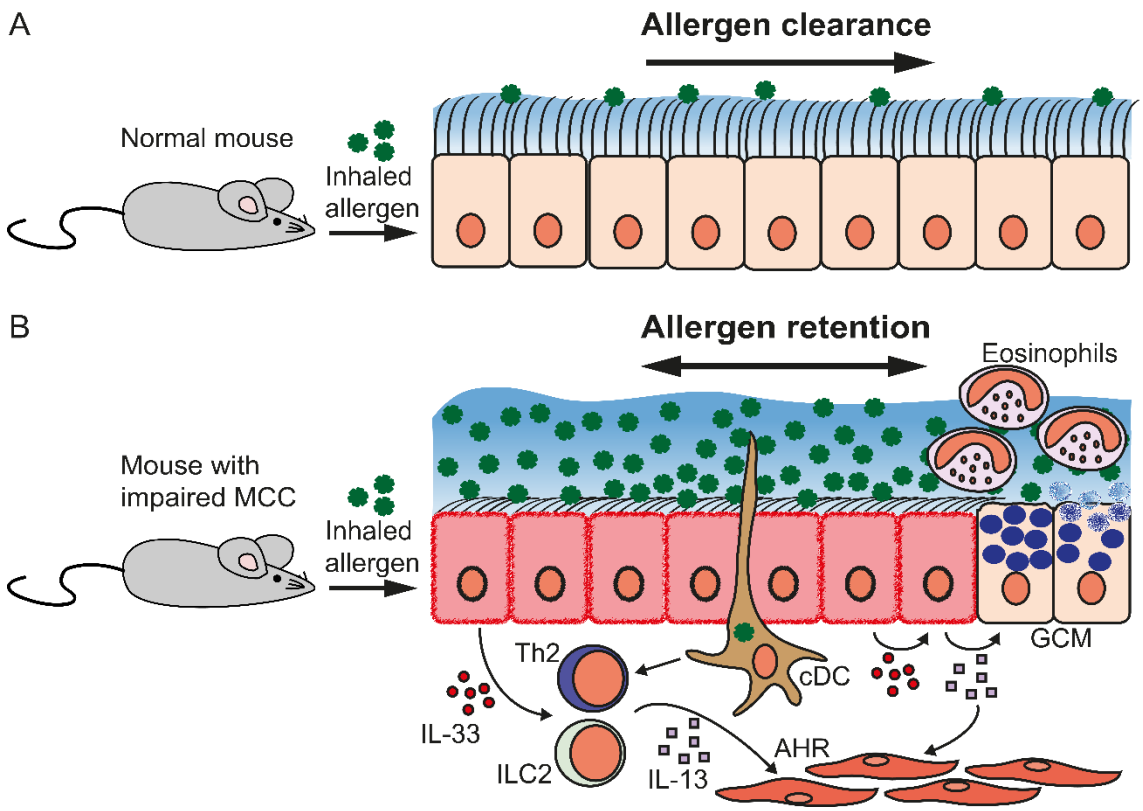

Figure 23. Schematic overview of impaired mucociliary clearance as a risk factor for the development of allergen-induced type 2 airway inflammation. (A) In healthy airways, the MCC apparatus functions normally and inhaled allergens and other environmental particles are properly cleared. (B) If MCC is impaired due to ASL dehydration and/or mucus hypersecretion, inhaled allergens are retained. This results in an activation of the airway epithelium and conventional dendritic cells (cDCs). The activated airway epithelium releases the cytokine IL-33 that leads to an autocrine activation as well as an activation and accumulation of Th2 cells and type 2 innate lymphoid cells (ILC2) and the secretion of IL-13 and other type 2 cytokines driving key features of allergic airway inflammation including airway eosinophilia, goblet cell metaplasia (GCM) and mucus hypersecretion and airway hyperrespnsiveness (AHR). Figure is adapted from the publication by Fritzsching et al., 2017 and Zhou-Suckow et al., 2017.

An interesting finding in our study was the age-dependent susceptibility of mice to develop allergen-induced type 2 airway inflammation in the context of impaired MCC. We found that a short-term allergen challenge protocol with Af neither induced type 2 airway inflammation nor AHR in adult WT and *Scnn1b*-Tg mice (Figure 10). In contrast, results from previous published work by our group showed that the same protocol induces airway eosinophilia, increased levels of type 2 signature cytokines in juvenile Af-challenged WT mice that were exacerbated and associated with AHR in juvenile Af-challenged *Scnn1b*-Tg mice (Fritzsching et al., 2017). We speculate that this age-dependent susceptibility to develop allergen-induced type 2 airway inflammation originates from a type 2 biased immunity in the first weeks of life that makes the host susceptible to the development of allergen-induced type 2 airway inflammation. This

assumption is supported by several studies (de Kleer et al., 2016; Mall et al., 2008; Saglani et al., 2009; Steer et al., 2017). First, Saglani et al. observed that WT mice exposed to HDM from the first days of life developed an allergen-induced airway eosinophilia with elevated levels of type 2 cytokines that peaked at the juvenile age and waned at the adult age (Saglani et al., 2009). Second, Mall et al. observed that naïve WT and *Scnn1b*-Tg mice exhibit spontaneous increased eosinophil counts, IL-13 levels, and goblet cell counts in juvenile mice that were further enhanced in juvenile *Scnn1b*-Tg mice and waned in both genotypes at adult ages (Mall et al., 2008). Third, de Kleer et al. demonstrated that ILC2s, eosinophils, basophils, and mast cells spontaneously accumulate in juvenile WT mice in an IL-33-dependent manner and HDM exposure further increases levels of IL-33 that boost cytokine production in ILC2s and activates cDCs and thus facilitates enhanced neonatal/juvenile Th2 responses (de Kleer et al., 2016). Fourth, a study similar to that from de Kleer et al., showed that elevated levels of IL-33 activates ILC2s in the neonatal/juvenile lung which then promote innate as well as adaptive type 2 immunity (Steer et al., 2017).

The notion that juvenile mice are more susceptible to develop allergen-induced type 2 airway inflammation than adults was further substantiated in our study by comprehensive analyses of a spectrum of type 2 signature genes, including *Il13*, *Muc5ac*, *Gob5*, *Arg1*, *Mmp12*, *Ym1*, *Ym2*, and *Chia* (Lewis et al., 2009) (Figure 11). We observed that the expression levels of most of the type 2 signature genes were upregulated in neonatal WT mice compared with older WT mice and this age-dependent type 2 pattern was exacerbated in *Scnn1b*-Tg mice (Figure 11). A similar type 2 biased immunity was observed in human subjects (Li et al., 2004; Prescott et al., 1998) and might explain why the onset of allergic asthma is observed especially in young children (Sennhauser et al., 2005); however, future studies are needed to identify relationships between impaired MCC, allergen-induced type 2 airway inflammation, and age-dependent susceptibility in patients with allergic asthma.

To test if pharmacological improvement of airway surface hydration and thus MMC might be an effective therapeutic target to reduce allergen-induced type 2 airway inflammation, we pretreated newborn WT and *Scnn1b*-Tg mice with the ENaC blocker amiloride and superimposed this treatment regime with Af or HDM challenges (Figure 12A and Figure 13A). As mentioned before, ENaC is responsible for Na^+ and fluid absorption from the airways (Knowles et al., 1981; Mall et al., 1998) and airway surface dehydration either because of ion imbalances between Cl^- secretion and Na^+ absorption or by mucus hypersecretion has been shown to be responsible for impaired MCC in many chronic lung diseases including asthma (Anagnostopoulou et al., 2012; Bonser et al., 2016;

Button et al., 2012; Evans et al., 2009). Amiloride and other hydration therapies have been applied in patients with CF and other chronic inflammatory lung diseases demonstrating an improvement of MCC (Daviskas et al., 1996; Houtmeyers et al., 1999; Kohler et al., 1986); however, the effects of this therapy on allergen-induced airway inflammation remain unknown. A previous study demonstrated that pharmacologic inhibition of ENaC from the first day of life reduced mucus obstruction and spontaneous type 2 airway inflammation in juvenile *Scnn1b*-Tg mice (Zhou et al., 2008). Therefore, the inhibition of ENaC is a pharmacological approach to improve airway surface hydration and MCC, and to test effects on allergic airway inflammation. Indeed, in our study amiloride treatment prevented exaggerated airway eosinophilia and IL-13 production in *Scnn1b*-Tg mice and this finding was independent of the allergen that was applied (Figure 12 and Figure 13). Of note, preventive amiloride treatment also protected *Scnn1b*-Tg mice from allergen-induced AHR (Figure 14). The data from our study provides the first proof of concept that pharmacologic improvement of airway surface hydration and MCC in a susceptible host can reduce allergen-induced type 2 airway inflammation. Further, it shows that improvement of MCC might be an effective therapeutic approach to decrease or prevent chronic airway inflammation in patients with allergic asthma and other chronic airway diseases including CF and COPD that are associated with mucociliary dysfunction.

4.2 Impaired mucociliary clearance and adaptive immunity

Chronic airway inflammation is a pathogenic feature of many mucus-obstructed lung diseases (Barnes, 2008; Elizur et al., 2008). Specifically, in CF dehydrated mucus leads to impaired MCC and mucus plugging that drives chronic airway inflammation that is characterized by a neutrophil-dominated inflammation and bacterial/fungal infections (Elizur et al., 2008). Studies in *Scnn1b*-Tg mice mimicking the pathology of CF-like lung disease demonstrated that neutrophilic airway inflammation is triggered through epithelial necrosis due to mucus plug-induced hypoxia and the release of innate cytokines including IL-1α and IL-1β (Fritzsching et al., 2015), but also through increased activity of the protease neutrophil elastase and increased levels of the chemokine CXCL1 (Gehrig et al., 2014). All of these mechanisms were also connected to human CF patients. Also, bacterial and fungal infections activate pattern recognition receptors on airway epithelial and other innate immune cells leading to the release of pro-inflammatory molecules including IL-1β, IL-6 and IL-8 that further boost neutrophilic airway inflammation in CF (Hartl et al., 2012). Much research has been done to unravel mechanisms that contribute to chronic airway inflammation in CF, mainly focusing on innate immune responses and its signal transducing molecules (Courtney et al., 2004;

Hartl et al., 2012; Laval et al., 2016). However, the effects of innate immune responses on adaptive immunity and its pathophysiological contribution in CF lung disease are poorly understood. Lately, efforts have been undertaken to investigate the contribution of the adaptive immune system to the chronic airway inflammation (Ratner and Mueller, 2012), thereby showing that mechanisms triggered by Th2 and Th17 immunity might be implicated in chronic airway inflammation in CF (Hubeau et al., 2004; Tan et al., 2011; Tiringer et al., 2013). Another study showed that the function of regulatory T cells is impaired in CF patients chronically infected with *Pseudomonas aeruginosa* (Hector et al., 2015). Further, lymphoid follicles that are rich in T and B cells were found in patients with end-stage CF lung disease (Lammertyn et al., 2017). Based on these results and reports, we investigated the role of the adaptive immune system in the development of chronic airway inflammation in *Scnn1b*-Tg mice. Therefore, we crossed *Rag1*$^{-/-}$ mice with *Scnn1b*-Tg mice and studied the lung phenotype of *Scnn1b*-Tg mice that lack mature T and B cells. We investigated the pulmonary phenotype at the juvenile age because at this period we expected the most prominent changes concerning Th2-related mechanisms when T and B cells are lacking. This assumption was based on the facts that juvenile mice have a type 2 biased immune system as we have shown before (Figure 11) and that *Scnn1b*-Tg mice at this age develop a spontaneous type 2 airway inflammation in addition to airway neutrophilia (Mall et al., 2008).

We found that the development of chronic airway inflammation was not mediated by T and B cells in juvenile *Scnn1b*-Tg mice as the inflammatory cells including AMs, eosinophils, and neutrophils in BAL did not change between *Scnn1b*-Tg and *Scnn1b*-Tg/*Rag1*$^{-/-}$ mice (Figure 15). Elevated levels of IL-5 and IL-13 are strong indicators for eosinophilic airway inflammation (Pope et al., 2001) whereas increased levels of IL-6 and CXCL1 correlate with neutrophilic airway inflammation (Fielding et al., 2008; Hammond et al., 1995). Transcript expression of these molecules was increased in *Scnn1b*-Tg and *Scnn1b*-Tg/*Rag1*$^{-/-}$ mice compared to WT and *Rag1*$^{-/-}$ littermates and associated with elevated levels of airway eosinophils and neutrophils in *Scnn1b*-Tg and *Scnn1b*-Tg/*Rag1*$^{-/-}$ mice (Figure 15 and Figure 16). These findings demonstrate that chronic airway inflammation is largely driven by innate inflammatory mechanisms in juvenile *Scnn1b*-Tg mice including the production of IL-5 and IL-13 by ILC2s and the airway epithelium (Fritzsching et al., 2017; Halim et al., 2012) and IL-6 and CXCL1 by AMs and the airway epithelium (Kotloff et al., 1990; Marini et al., 1992; Mukaida, 2003).

As mentioned above, previous studies demonstrated a Th2- and Th17-skewed cytokine profile in patients with CF (Tiringer et al., 2013). In our study, we were interested if there

is such a Th2- and Th17-skewed cytokine profile in juvenile *Scnn1b*-Tg mice that correlates with that found in CF patients and whether these cytokines are predominantly expressed by innate or adaptive immune cells. To address these questions, we measured transcript expression levels of Th1- (*Ifnγ*), Th2- (*Il4*, *Il5*, and *Il13*) and Th17-related (*Il6*, *Cxcl1*, and *Il17a*) cytokines in lung homogenates of juvenile WT, *Rag1*$^{-/-}$, *Scnn1b*-Tg and *Scnn1b*-Tg/*Rag1*$^{-/-}$ mice (Figure 16). Nearly all of the cytokines including *Il4*, *Il5*, *Il13*, *Il6*, *Cxcl1*, and *Il17a* were upregulated in *Scnn1b*-Tg mice (Figure 16B-G) and this correlates with findings in CF patients (Tiringer et al., 2013). The transcript expression of most cytokines including *Ifnγ*, *Il4*, *Il5*, *Il13*, *Il6*, and *Cxcl1* was not changed between *Scnn1b*-Tg and *Scnn1b*-Tg/*Rag1*$^{-/-}$ mice (Figure 16A-F) demonstrating that the expression of these cytokines is mediated by innate rather than by adaptive mechanisms including T and B cells.

An interesting finding was that the transcript expression of *Il17a*, a cytokine that is associated with activation and migration of neutrophils, bacterial defense and structural lung damage, was upregulated in juvenile *Scnn1b*-Tg mice compared to WT and *Rag1*$^{-/-}$ littermates and was significantly downregulated to levels of WT mice when T and B cells were lacking as seen for *Scnn1b*-Tg/*Rag1*$^{-/-}$ mice (Figure 16G). This result indicates that IL-17A is a major source of T and/or B cells in juvenile *Scnn1b*-Tg mice and correlates with previous findings in CF patients showing increased levels of IL-17A (Tan et al., 2011; Tiringer et al., 2013).

According to the literature, T cells rather than B cells are able to produce IL-17A. CD4^{+} T, CD8^{+} T, γδ T and NKT cells are subclasses of T cells that have been shown to produce IL-17A and besides T cells, innate cells including NK cells and the recently discovered ILC3s are also capable of producing IL-17A (Cua and Tato, 2010; Dubin and Kolls, 2011; Miossec and Kolls, 2012). In our study, we identified significantly elevated numbers of IL-17A-producing leukocytes in lungs of juvenile *Scnn1b*-Tg mice (Figure 17). Specifically, increased levels of IL-17A-expressing CD4^{+} T and γδ T cells were identified in *Scnn1b*-Tg mice (Figure 18A and B) and this is in line with previous findings in CF patients (Chan et al., 2013; Tan et al., 2011). An interesting finding was that the number of IL-17A^{+} ILC3s was increased in *Scnn1b*-Tg mice and *Scnn1b*-Tg/*Rag1*$^{-/-}$ mice compared to WT and *Rag1*$^{-/-}$ littermates and did not differ between *Scnn1b*-Tg and *Scnn1b*-Tg/*Rag1*$^{-/-}$ mice (Figure 18C). These results suggest that besides T cells, ILC3s might be a considerable source of elevated IL-17A expression in CF lung disease. Further, we noted that the number of IL-17A-producing γδ T cells derived from WT and *Scnn1b*-Tg mice was about 4 to 6-fold higher than the number of IL-17A^{+} CD4^{+} T cells and ILC3s indicating that γδ T cells are a predominant source of IL-17A and might contribute to

pathogenic features of CF lung disease (Papotto et al., 2017; Tan et al., 2011). In summary, our data demonstrate increased numbers of IL-17A-producing $CD4^+$ T, γδ T cells and ILC3s in lungs of juvenile *Scnn1b*-Tg mice and indicate that IL-17A might be an important player in CF lung disease. Further studies are needed to investigate IL-17A signaling and its impact on pathogenic features in CF lung disease.

Besides other mucus-inducing molecules including IL-1β, IL-6, IL-13, and neutrophil elastase (Chen et al., 2003; Fritzsching et al., 2015; Gehrig et al., 2014; Zhu et al., 1999), IL-17A is also known for its mucus-inducing function (Chen et al., 2003; Fujisawa et al., 2011; Fujisawa et al., 2009). Previous studies demonstrated that *Scnn1b*-Tg mice suffer from airway mucus plugging that is caused by airway surface dehydration, impaired MCC and mucus hypersecretion (Mall et al., 2008). However, mucus plugging could also occur in the absence of mucus hypersecretion in *Scnn1b*-Tg mice (Gehrig et al., 2014), thus indicating that mucus hypersecretion alone is not always associated with mucus obstruction under conditions of well hydrated airway surfaces (Button and Button, 2013). We hypothesized that the removal of T cells via *Rag1*-deficiency and the associated loss of a major source of IL-17A, might lead to reduced mucus secretion and plugging in *Scnn1b*-Tg mice. Our results showed that the lack of T cells did not affect mucus plugging (Figure 19A and B) or mucin hypersecretion of the two mucins *Muc5ac* (Figure 20A) and *Muc5b* (Figure 20B) in juvenile *Scnn1b*-Tg mice. Further, we detected similar elevated expression levels of the goblet cell marker *Gob5* in *Scnn1b*-Tg and *Scnn1b*-Tg/*Rag1*$^{-/-}$ mice (Figure 20C). These results suggest that either elevated secretion of IL-17A by ILC3s still maintains mucus hypersecretion and plugging in juvenile *Scnn1b*-Tg/*Rag1*$^{-/-}$ mice or, which is more likely, that other mucus-inducing molecules including IL-1β, IL-13 and neutrophil elastase are more potent than IL-17A to induce mucus hypersecretion and plugging in juvenile *Scnn1b*-Tg mice (Fritzsching et al., 2015; Gehrig et al., 2014; Zhu et al., 1999).
Collectively, these results demonstrate that T cell mediated IL-17A expression rather plays a minor role in the context of mucin hypersecretion and mucus plugging, in comparison to IL-1β, IL-13 and neutrophil elastase in juvenile *Scnn1b*-Tg mice and thus maybe also in patients with CF lung disease.

Previous studies demonstrated that IL-17A is involved in structural lung damage and emphysema formation (Kurimoto et al., 2013; Muir et al., 2016) and B cell-mediated emphysema formation was demonstrated in mice with cigarette smoke-induced COPD (van der Strate et al., 2006). *Scnn1b*-Tg mice develop structural lung damage and emphysema that was linked to elevated protease activity (Gehrig et al., 2014; Mall et al.,

2008; Trojanek et al., 2014). By the lack of T and B cells due to *Rag1* deficiency, we speculated that structural lung damage and emphysema formation might be reduced in *Scnn1b*-Tg mice. Indeed, we observed a reduction of destructive index, a measure for alveolar wall destruction, and mean linear intercept, a measure for alveolar airspace enlargement, in *Scnn1b*-Tg/*Rag1*$^{-/-}$ mice compared to *Scnn1b*-Tg mice (Figure 21). We speculate that the reduction in structural lung damage is linked to the absence of T cell-produced IL-17A rather than the lack of B cell-mediated mechanisms in *Scnn1b*-Tg/*Rag1*$^{-/-}$ mice because a study by John-Schuster et al. demonstrated that elastase-induced emphysema still develops in B cell-deficient mice and was as severe as in WT mice (John-Schuster et al., 2014). Several mechanisms might contribute to IL-17A-induced structural lung damage in *Scnn1b*-Tg mice. First, IL-17A could induce neutrophil recruitment to the lung and might also enhance neutrophil activation by increasing elastase activity (Linden and Adachi, 2002). In our study, we did not observe a reduction in neutrophil counts in the BAL of *Scnn1b*-Tg/*Rag1*$^{-/-}$ mice (Figure 15D) and this suggests that other mechanisms including elevated levels of the neutrophil attractants IL-6 (Figure 16B) and CXCL1 (Figure 16C) might compensate the effects of potentially decreased IL-17A-induced neutrophil recruitment in *Scnn1b*-Tg/*Rag1*$^{-/-}$ mice. Thus, these findings argue that neutrophil activation rather than recruitment might play a role in IL-17A-induced structural lung damage in *Scnn1b*-Tg mice. Second, IL-17A could also recruit macrophages to the lung via direct or indirect mechanisms (Bozinovski et al., 2015; Gaffen, 2008; Voss et al., 2015) and has the potential to stimulate the release of matrix metalloproteinases from AMs that contribute to structural lung damage and emphysema formation (Gaffen, 2008; Jovanovic et al., 2000; Prause et al., 2004; Trojanek et al., 2014). In our study, we observed a trend towards a reduced level of AMs in BAL of *Scnn1b*-Tg/*Rag1*$^{-/-}$ mice compared to *Scnn1b*-Tg mice (Figure 15A). Further, we measured activation of AMs through the expression of CD11b that might mediate inflammation by regulating leukocyte adhesion and migration (Solovjov et al., 2005). We observed a reduced AM activation phenotype in *Scnn1b*-Tg/*Rag1*$^{-/-}$ mice compared to *Scnn1b*-Tg mice (Figure 22).

Collectively, these findings indicate that reduced structural lung damage and emphysema formation in juvenile *Scnn1b*-Tg/*Rag1*$^{-/-}$ mice might be associated with the lack of T cell mediated IL-17A expression; however, further studies are required to elucidate IL-17A-dependent mechanisms triggering structural lung damage in CF-like chronic airway inflammation.

5 Conclusions

Patients with mucus-obstructed lung diseases including CF, asthma and COPD develop chronic airway inflammation that differ in their immune responses. The understanding of mechanisms and risk factors that lead to chronic airway inflammation and their pathophysiological contributions in muco-obstructive lung diseases is crucial to allow the design of effective treatment strategies. In this work, we investigated the role of MCC as an important innate defense mechanism in the pathogenesis of allergic airway disease and also aimed to understand the role of T and B cells as key cells of the adaptive immunity in chronic airway diseases in context of CF-like lung disease.

For the first time, this study demonstrates that mucociliary dysfunction causing reduced clearance of inhaled allergens from the airways represents an important risk factor for the development of allergen-induced type 2 airway inflammation. Further, our results demonstrated that allergen-induced airway inflammation is related to an age-dependent susceptibility that is most likely caused by a type 2 biased immune system in early life. Finally, we showed that pharmacological improvement of airway surface hydration and MCC reduces allergen-induced type 2 airway inflammation and AHR in a susceptible host.

Analyzing the lung phenotype of juvenile *Scnn1b*-Tg/*Rag1*$^{-/-}$ mice gave first insights into the pathophysiological contribution of the adaptive immune system and its interaction between innate immunity in CF-like lung disease. Our data showed that chronic airway inflammation is rather mediated by innate than adaptive immune responses in *Scnn1b*-Tg mice. We found that many of the cytokines orchestrating chronic airway inflammation in CF are produced by innate cellular sources in juvenile *Scnn1b*-Tg mice and confirmed a Th2- and Th17-skewed cytokine profile previously found in CF patients (Tiringer et al., 2013). The identification of increased levels of IL-17A predominantly produced by CD4^{+} T, γδ T cells and ILC3s in lungs of *Scnn1b*-Tg mice showed no effect on mucus plugging but seem to be implicated in the development of structural lung damage.

In summary, our data support that impaired clearance of inhaled allergens plays an important role in the pathogenesis of type 2 airway inflammation and suggest that therapeutic improvement of MCC may be an effective novel therapeutic target in patients with allergen-induced asthma and potentially other chronic airway diseases associated with mucociliary dysfunction including CF and COPD. Further, results from our study provided first insights into T and B cell-dependent mechanisms that might contribute to pathophysiological features of CF lung disease.

6 Future Perspectives

We identified impaired MCC with reduced allergen clearance as a risk factor for the development of type 2 airway inflammation. Reduced uptake of allergens by AMs contributed to the increased burden of allergens in the airways of juvenile *Scnn1b*-Tg mice. Mechanisms of reduced allergen uptake by AMs were not investigated in this study as this was beyond the scope of this project; however, the identification of such mechanisms could lead to a better understanding of the development of allergen-induced type 2 airway inflammation. Conversely, we observed elevated allergen uptake by cDCs that suggested an enhanced allergen presentation to T cells and a further boost of type 2 airway inflammation. This assumption could be addressed by *in vitro* co-culture experiments of allergen primed cDCs and T cells from juvenile WT and *Scnn1b*-Tg mice. The observation that allergen-induced type 2 airway inflammation is mediated by an age-dependent susceptibility that is likely due to a type 2 biased immunity at neonatal/juvenile age is an interesting result. Some genes of the type 2 signature pattern including *Muc5ac* and *Gob5* that were elevated at neonatal/juvenile age are exclusively derived from airway epithelial cells supporting an important role of the airway epithelium in the age-dependent susceptibility. Transcriptomic and proteomic analyses of airway epithelial cells from neonatal, juvenile and adult WT and *Scnn1b*-Tg mice might lead to further important insights concerning this issue. Pharmacological improvement of airway surface hydration and MCC reduced allergen-induced type 2 airway inflammation and AHR demonstrating that improving MCC might be a potential therapeutic strategy in patients with allergen-induced asthma. Effects of other ENaC blockers targeting MCC should be tested *in vivo* in context of allergen-induced type 2 airway inflammation. Also, the effects of reducing agents breaking disulfide bonds of mucus polymers should be tested. These drugs thin mucus making it less sticky and easier to clear thereby having a potential therapeutic effect on MCC and allergen-induced type 2 airway inflammation that might be similar to that of hydration therapies with ENaC blockers.

By the investigation of the pathogenic contribution of the adaptive immunity in *Scnn1b*-Tg mice, we found that the lack of T and B cells is associated with reduced structural lung damage and that IL-17A may be implicated in this process. To determine the role of IL-17A in more detail *in vivo*, IL-17A-knockout mice should be crossed with *Scnn1b*-Tg mice. The confirmation of our current observations and findings of new pathogenic IL-17A-dependent mechanisms in these mice might give new insights into the complex network of chronic airway inflammation in CF lung disease. In addition, translational studies to confirm the significance of our findings in patient tissues are still needed.

7 References

Adkins, B., Leclerc, C., and Marshall-Clarke, S. (2004). Neonatal adaptive immunity comes of age. Nat Rev Immunol *4*, 553-564.

Agarwal, R., Hazarika, B., Gupta, D., Aggarwal, A.N., Chakrabarti, A., and Jindal, S.K. (2010). Aspergillus hypersensitivity in patients with chronic obstructive pulmonary disease: COPD as a risk factor for ABPA? Med Mycol *48*, 988-994.

Aikawa, T., Shimura, S., Sasaki, H., Ebina, M., and Takishima, T. (1992). Marked goblet cell hyperplasia with mucus accumulation in the airways of patients who died of severe acute asthma attack. Chest *101*, 916-921.

Althaus, M. (2013). ENaC inhibitors and airway re-hydration in cystic fibrosis: state of the art. Curr Mol Pharmacol *6*, 3-12.

Anagnostopoulou, P., Dai, L., Schatterny, J., Hirtz, S., Duerr, J., and Mall, M.A. (2010). Allergic airway inflammation induces a pro-secretory epithelial ion transport phenotype in mice. Eur Respir J *36*, 1436-1447.

Anagnostopoulou, P., Riederer, B., Duerr, J., Michel, S., Binia, A., Agrawal, R., Liu, X., Kalitzki, K., Xiao, F., Chen, M.*, et al.* (2012). SLC26A9-mediated chloride secretion prevents mucus obstruction in airway inflammation. J Clin Invest *122*, 3629-3634.

Anderson, M.P., Gregory, R.J., Thompson, S., Souza, D.W., Paul, S., Mulligan, R.C., Smith, A.E., and Welsh, M.J. (1991). Demonstration that CFTR is a chloride channel by alteration of its anion selectivity. Science *253*, 202-205.

Anderson, W.H., Coakley, R.D., Button, B., Henderson, A.G., Zeman, K.L., Alexis, N.E., Peden, D.B., Lazarowski, E.R., Davis, C.W., Bailey, S.*, et al.* (2015). The Relationship of Mucus Concentration (Hydration) to Mucus Osmotic Pressure and Transport in Chronic Bronchitis. Am J Respir Crit Care Med *192*, 182-190.

Artis, D., and Spits, H. (2015). The biology of innate lymphoid cells. Nature *517*, 293-301.

Baggiolini, M., Dewald, B., and Moser, B. (1994). Interleukin-8 and related chemotactic cytokines--CXC and CC chemokines. Adv Immunol *55*, 97-179.

Balhara, J., and Gounni, A.S. (2012). The alveolar macrophages in asthma: a double-edged sword. Mucosal Immunol *5*, 605-609.

Barnes, P.J. (2006). New therapies for asthma. Trends Mol Med *12*, 515-520.

Barnes, P.J. (2008). Immunology of asthma and chronic obstructive pulmonary disease. Nat Rev Immunol *8*, 183-192.

Bateman, J.R., Pavia, D., Sheahan, N.F., Agnew, J.E., and Clarke, S.W. (1983). Impaired tracheobronchial clearance in patients with mild stable asthma. Thorax *38*, 463-467.

Bates, J.H., and Irvin, C.G. (2003). Measuring lung function in mice: the phenotyping uncertainty principle. J Appl Physiol (1985) *94*, 1297-1306.

Benayoun, L., Druilhe, A., Dombret, M.C., Aubier, M., and Pretolani, M. (2003). Airway structural alterations selectively associated with severe asthma. Am J Respir Crit Care Med *167*, 1360-1368.

Bonser, L.R., Zlock, L., Finkbeiner, W., and Erle, D.J. (2016). Epithelial tethering of MUC5AC-rich mucus impairs mucociliary transport in asthma. J Clin Invest *126*, 2367-2371.

Boucher, R.C. (2002). An overview of the pathogenesis of cystic fibrosis lung disease. Adv Drug Deliv Rev *54*, 1359-1371.

Bozinovski, S., Seow, H.J., Chan, S.P., Anthony, D., McQualter, J., Hansen, M., Jenkins, B.J., Anderson, G.P., and Vlahos, R. (2015). Innate cellular sources of interleukin-17A regulate macrophage accumulation in cigarette- smoke-induced lung inflammation in mice. Clin Sci (Lond) *129*, 785-796.

Brannan, J.D., and Lougheed, M.D. (2012). Airway hyperresponsiveness in asthma: mechanisms, clinical significance, and treatment. Front Physiol *3*, 460.

Button, B., Cai, L.H., Ehre, C., Kesimer, M., Hill, D.B., Sheehan, J.K., Boucher, R.C., and Rubinstein, M. (2012). A periciliary brush promotes the lung health by separating the mucus layer from airway epithelia. Science *337*, 937-941.

Button, B.M., and Button, B. (2013). Structure and function of the mucus clearance system of the lung. Cold Spring Harb Perspect Med *3*.

Canessa, C.M., Schild, L., Buell, G., Thorens, B., Gautschi, I., Horisberger, J.D., and Rossier, B.C. (1994). Amiloride-sensitive epithelial Na+ channel is made of three homologous subunits. Nature *367*, 463-467.

Chan, Y.R., Chen, K., Duncan, S.R., Lathrop, K.L., Latoche, J.D., Logar, A.J., Pociask, D.A., Wahlberg, B.J., Ray, P., Ray, A.*, et al.* (2013). Patients with cystic fibrosis have inducible IL-17+IL-22+ memory cells in lung draining lymph nodes. J Allergy Clin Immunol *131*, 1117-1129, 1129 e1111-1115.

Chen, E.Y., Yang, N., Quinton, P.M., and Chin, W.C. (2010). A new role for bicarbonate in mucus formation. Am J Physiol Lung Cell Mol Physiol *299*, L542-549.

Chen, Y., Thai, P., Zhao, Y.H., Ho, Y.S., DeSouza, M.M., and Wu, R. (2003). Stimulation of airway mucin gene expression by interleukin (IL)-17 through IL-6 paracrine/autocrine loop. J Biol Chem *278*, 17036-17043.

Clunes, M.T., and Boucher, R.C. (2007). Cystic Fibrosis: The Mechanisms of Pathogenesis of an Inherited Lung Disorder. Drug Discov Today Dis Mech *4*, 63-72.

Cohn, L., Homer, R.J., Marinov, A., Rankin, J., and Bottomly, K. (1997). Induction of airway mucus production By T helper 2 (Th2) cells: a critical role for interleukin 4 in cell recruitment but not mucus production. J Exp Med *186*, 1737-1747.

Conese, M., Copreni, E., Di Gioia, S., De Rinaldis, P., and Fumarulo, R. (2003). Neutrophil recruitment and airway epithelial cell involvement in chronic cystic fibrosis lung disease. J Cyst Fibros *2*, 129-135.

Courtney, J.M., Ennis, M., and Elborn, J.S. (2004). Cytokines and inflammatory mediators in cystic fibrosis. J Cyst Fibros *3*, 223-231.

Croisant, S. (2014). Epidemiology of asthma: prevalence and burden of disease. Adv Exp Med Biol *795*, 17-29.

Cua, D.J., and Tato, C.M. (2010). Innate IL-17-producing cells: the sentinels of the immune system. Nat Rev Immunol *10*, 479-489.

Daviskas, E., Anderson, S.D., Gonda, I., Eberl, S., Meikle, S., Seale, J.P., and Bautovich, G. (1996). Inhalation of hypertonic saline aerosol enhances mucociliary clearance in asthmatic and healthy subjects. Eur Respir J *9*, 725-732.

de Kleer, I.M., Kool, M., de Bruijn, M.J., Willart, M., van Moorleghem, J., Schuijs, M.J., Plantinga, M., Beyaert, R., Hams, E., Fallon, P.G.*, et al.* (2016). Perinatal Activation of the Interleukin-33 Pathway Promotes Type 2 Immunity in the Developing Lung. Immunity *45*, 1285-1298.

Decramer, M., and Janssens, W. (2010). Mucoactive therapy in COPD. Eur Respir Rev *19*, 134-140.

Del Donno, M., Bittesnich, D., Chetta, A., Olivieri, D., and Lopez-Vidriero, M.T. (2000). The effect of inflammation on mucociliary clearance in asthma: an overview. Chest *118*, 1142-1149.

Donaldson, S.H., Bennett, W.D., Zeman, K.L., Knowles, M.R., Tarran, R., and Boucher, R.C. (2006). Mucus clearance and lung function in cystic fibrosis with hypertonic saline. N Engl J Med *354*, 241-250.

Dubin, P.J., and Kolls, J.K. (2011). IL-17 in cystic fibrosis: more than just Th17 cells. Am J Respir Crit Care Med *184*, 155-157.

Dunnill, M.S. (1962). Quantitative methods in the study of pulmonary pathology. Thorax *17*, 320-328.

Elizur, A., Cannon, C.L., and Ferkol, T.W. (2008). Airway inflammation in cystic fibrosis. Chest *133*, 489-495.

Evans, C.M., Kim, K., Tuvim, M.J., and Dickey, B.F. (2009). Mucus hypersecretion in asthma: causes and effects. Curr Opin Pulm Med *15*, 4-11.

Fahy, J.V. (2015). Type 2 inflammation in asthma--present in most, absent in many. Nat Rev Immunol *15*, 57-65.

Fahy, J.V., and Dickey, B.F. (2010). Airway mucus function and dysfunction. N Engl J Med *363*, 2233-2247.

Fielding, C.A., McLoughlin, R.M., McLeod, L., Colmont, C.S., Najdovska, M., Grail, D., Ernst, M., Jones, S.A., Topley, N., and Jenkins, B.J. (2008). IL-6 regulates neutrophil trafficking during acute inflammation via STAT3. J Immunol *181*, 2189-2195.

Fritzsching, B., Hagner, M., Dai, L., Christochowitz, S., Agrawal, R., van Bodegom, C., Schmidt, S., Schatterny, J., Hirtz, S., Brown, R.*, et al.* (2017). Impaired mucus clearance exacerbates allergen-induced type 2 airway inflammation in juvenile mice. J Allergy Clin Immunol *140*, 190-203 e195.

Fritzsching, B., Zhou-Suckow, Z., Trojanek, J.B., Schubert, S.C., Schatterny, J., Hirtz, S., Agrawal, R., Muley, T., Kahn, N., Sticht, C.*, et al.* (2015). Hypoxic epithelial necrosis triggers neutrophilic inflammation via IL-1 receptor signaling in cystic fibrosis lung disease. Am J Respir Crit Care Med *191*, 902-913.

Fujisawa, T., Chang, M.M., Velichko, S., Thai, P., Hung, L.Y., Huang, F., Phuong, N., Chen, Y., and Wu, R. (2011). NF-kappaB mediates IL-1beta- and IL-17A-induced MUC5B expression in airway epithelial cells. Am J Respir Cell Mol Biol *45*, 246-252.

Fujisawa, T., Velichko, S., Thai, P., Hung, L.Y., Huang, F., and Wu, R. (2009). Regulation of airway MUC5AC expression by IL-1beta and IL-17A; the NF-kappaB paradigm. J Immunol *183*, 6236-6243.

Gaffen, S.L. (2008). An overview of IL-17 function and signaling. Cytokine *43*, 402-407.

Gehrig, S., Duerr, J., Weitnauer, M., Wagner, C.J., Graeber, S.Y., Schatterny, J., Hirtz, S., Belaaouaj, A., Dalpke, A.H., Schultz, C., and Mall, M.A. (2014). Lack of neutrophil elastase reduces inflammation, mucus hypersecretion, and emphysema, but not mucus obstruction, in mice with cystic fibrosis-like lung disease. Am J Respir Crit Care Med *189*, 1082-1092.

Gibson, R.L., Burns, J.L., and Ramsey, B.W. (2003). Pathophysiology and management of pulmonary infections in cystic fibrosis. Am J Respir Crit Care Med *168*, 918-951.

Goplen, N., Karim, M.Z., Liang, Q., Gorska, M.M., Rozario, S., Guo, L., and Alam, R. (2009). Combined sensitization of mice to extracts of dust mite, ragweed, and Aspergillus species breaks through tolerance and establishes chronic features of asthma. J Allergy Clin Immunol *123*, 925-932 e911.

Gregory, L.G., and Lloyd, C.M. (2011). Orchestrating house dust mite-associated allergy in the lung. Trends Immunol *32*, 402-411.

Grubb, B.R., and Boucher, R.C. (1999). Pathophysiology of gene-targeted mouse models for cystic fibrosis. Physiol Rev *79*, S193-214.

Halim, T.Y., Krauss, R.H., Sun, A.C., and Takei, F. (2012). Lung natural helper cells are a critical source of Th2 cell-type cytokines in protease allergen-induced airway inflammation. Immunity *36*, 451-463.

Hammad, H., and Lambrecht, B.N. (2008). Dendritic cells and epithelial cells: linking innate and adaptive immunity in asthma. Nat Rev Immunol *8*, 193-204.

Hammond, M.E., Lapointe, G.R., Feucht, P.H., Hilt, S., Gallegos, C.A., Gordon, C.A., Giedlin, M.A., Mullenbach, G., and Tekamp-Olson, P. (1995). IL-8 induces neutrophil chemotaxis predominantly via type I IL-8 receptors. J Immunol *155*, 1428-1433.

Harkema, J.R., Plopper, C.G., Hyde, D.M., and St George, J.A. (1987). Regional differences in quantities of histochemically detectable mucosubstances in nasal, paranasal, and nasopharyngeal epithelium of the bonnet monkey. J Histochem Cytochem *35*, 279-286.

Hartl, D., Gaggar, A., Bruscia, E., Hector, A., Marcos, V., Jung, A., Greene, C., McElvaney, G., Mall, M., and Doring, G. (2012). Innate immunity in cystic fibrosis lung disease. J Cyst Fibros *11*, 363-382.

Hartl, D., Griese, M., Kappler, M., Zissel, G., Reinhardt, D., Rebhan, C., Schendel, D.J., and Krauss-Etschmann, S. (2006). Pulmonary T(H)2 response in Pseudomonas aeruginosa-infected patients with cystic fibrosis. J Allergy Clin Immunol *117*, 204-211.

Hays, S.R., and Fahy, J.V. (2003). The role of mucus in fatal asthma. Am J Med *115*, 68-69.

Hector, A., Kirn, T., Ralhan, A., Graepler-Mainka, U., Berenbrinker, S., Riethmueller, J., Hogardt, M., Wagner, M., Pfleger, A., Autenrieth, I.*, et al.* (2016). Microbial colonization and lung function in adolescents with cystic fibrosis. J Cyst Fibros *15*, 340-349.

Hector, A., Schafer, H., Poschel, S., Fischer, A., Fritzsching, B., Ralhan, A., Carevic, M., Oz, H., Zundel, S., Hogardt, M.*, et al.* (2015). Regulatory T-cell impairment in cystic fibrosis patients with chronic pseudomonas infection. Am J Respir Crit Care Med *191*, 914-923.

Hoegger, M.J., Fischer, A.J., McMenimen, J.D., Ostedgaard, L.S., Tucker, A.J., Awadalla, M.A., Moninger, T.O., Michalski, A.S., Hoffman, E.A., Zabner, J.*, et al.* (2014). Impaired mucus detachment disrupts mucociliary transport in a piglet model of cystic fibrosis. Science *345*, 818-822.

Hogg, J.C. (1997). The pathology of asthma. APMIS *105*, 735-745.

Hogg, J.C., and Timens, W. (2009). The pathology of chronic obstructive pulmonary disease. Annu Rev Pathol *4*, 435-459.

Houtmeyers, E., Gosselink, R., Gayan-Ramirez, G., and Decramer, M. (1999). Effects of drugs on mucus clearance. Eur Respir J *14*, 452-467.

Hubeau, C., Le Naour, R., Abely, M., Hinnrasky, J., Guenounou, M., Gaillard, D., and Puchelle, E. (2004). Dysregulation of IL-2 and IL-8 production in circulating T lymphocytes from young cystic fibrosis patients. Clin Exp Immunol *135*, 528-534.

Hubeau, C., Lorenzato, M., Couetil, J.P., Hubert, D., Dusser, D., Puchelle, E., and Gaillard, D. (2001). Quantitative analysis of inflammatory cells infiltrating the cystic fibrosis airway mucosa. Clin Exp Immunol *124*, 69-76.

Innes, A.L., Woodruff, P.G., Ferrando, R.E., Donnelly, S., Dolganov, G.M., Lazarus, S.C., and Fahy, J.V. (2006). Epithelial mucin stores are increased in the large airways of smokers with airflow obstruction. Chest *130*, 1102-1108.

Irvin, C.G., and Bates, J.H. (2003). Measuring the lung function in the mouse: the challenge of size. Respir Res *4*, 4.

Jiang, Q., and Engelhardt, J.F. (1998). Cellular heterogeneity of CFTR expression and function in the lung: implications for gene therapy of cystic fibrosis. Eur J Hum Genet *6*, 12-31.

Jin, J., Liu, X., and Sun, Y. (2014). The prevalence of increased serum IgE and Aspergillus sensitization in patients with COPD and their association with symptoms and lung function. Respir Res *15*, 130.

John-Schuster, G., Hager, K., Conlon, T.M., Irmler, M., Beckers, J., Eickelberg, O., and Yildirim, A.O. (2014). Cigarette smoke-induced iBALT mediates macrophage activation in a B cell-dependent manner in COPD. Am J Physiol Lung Cell Mol Physiol *307*, L692-706.

Jovanovic, D.V., Martel-Pelletier, J., Di Battista, J.A., Mineau, F., Jolicoeur, F.C., Benderdour, M., and Pelletier, J.P. (2000). Stimulation of 92-kd gelatinase (matrix metalloproteinase 9) production by interleukin-17 in human monocyte/macrophages: a possible role in rheumatoid arthritis. Arthritis Rheum *43*, 1134-1144.

Justice, J.P., Crosby, J., Borchers, M.T., Tomkinson, A., Lee, J.J., and Lee, N.A. (2002). CD4(+) T cell-dependent airway mucus production occurs in response to IL-5 expression in lung. Am J Physiol Lung Cell Mol Physiol *282*, L1066-1074.

Kerem, B., Rommens, J.M., Buchanan, J.A., Markiewicz, D., Cox, T.K., Chakravarti, A., Buchwald, M., and Tsui, L.C. (1989). Identification of the cystic fibrosis gene: genetic analysis. Science *245*, 1073-1080.

Knowles, M., Gatzy, J., and Boucher, R. (1981). Increased bioelectric potential difference across respiratory epithelia in cystic fibrosis. N Engl J Med *305*, 1489-1495.

Knowles, M.R., and Boucher, R.C. (2002). Mucus clearance as a primary innate defense mechanism for mammalian airways. J Clin Invest *109*, 571-577.

Knutsen, A.P., and Slavin, R.G. (2011). Allergic bronchopulmonary aspergillosis in asthma and cystic fibrosis. Clin Dev Immunol *2011*, 843763.

Kohler, D., App, E., Schmitz-Schumann, M., Wurtemberger, G., and Matthys, H. (1986). Inhalation of amiloride improves the mucociliary and the cough clearance in patients with cystic fibroses. Eur J Respir Dis Suppl *146*, 319-326.

Kotloff, R.M., Little, J., and Elias, J.A. (1990). Human alveolar macrophage and blood monocyte interleukin-6 production. Am J Respir Cell Mol Biol *3*, 497-505.

Kuperman, D.A., Huang, X., Koth, L.L., Chang, G.H., Dolganov, G.M., Zhu, Z., Elias, J.A., Sheppard, D., and Erle, D.J. (2002). Direct effects of interleukin-13 on epithelial cells cause airway hyperreactivity and mucus overproduction in asthma. Nat Med *8*, 885-889.

Kurimoto, E., Miyahara, N., Kanehiro, A., Waseda, K., Taniguchi, A., Ikeda, G., Koga, H., Nishimori, H., Tanimoto, Y., Kataoka, M.*, et al.* (2013). IL-17A is essential to the development of elastase-induced pulmonary inflammation and emphysema in mice. Respir Res *14*, 5.

Kurowska-Stolarska, M., Stolarski, B., Kewin, P., Murphy, G., Corrigan, C.J., Ying, S., Pitman, N., Mirchandani, A., Rana, B., van Rooijen, N.*, et al.* (2009). IL-33 amplifies the polarization of alternatively activated macrophages that contribute to airway inflammation. J Immunol *183*, 6469-6477.

Kuyper, L.M., Pare, P.D., Hogg, J.C., Lambert, R.K., Ionescu, D., Woods, R., and Bai, T.R. (2003). Characterization of airway plugging in fatal asthma. Am J Med *115*, 6-11.

Lachmann, B., Robertson, B., and Vogel, J. (1980). In vivo lung lavage as an experimental model of the respiratory distress syndrome. Acta Anaesthesiol Scand *24*, 231-236.

Lambrecht, B.N., and Hammad, H. (2012). The airway epithelium in asthma. Nat Med *18*, 684-692.

Lambrecht, B.N., and Hammad, H. (2015). The immunology of asthma. Nat Immunol *16*, 45-56.

Lammertyn, E.J., Vandermeulen, E., Bellon, H., Everaerts, S., Verleden, S.E., Van Den Eynde, K., Bracke, K.R., Brusselle, G.G., Goeminne, P.C., Verbeken, E.K.*, et al.* (2017). End-stage cystic fibrosis lung disease is characterised by a diverse inflammatory pattern: an immunohistochemical analysis. Respir Res *18*, 10.

Laniado-Laborin, R. (2009). Smoking and chronic obstructive pulmonary disease (COPD). Parallel epidemics of the 21 century. Int J Environ Res Public Health *6*, 209-224.

Lauzon-Joset, J.F., Marsolais, D., Langlois, A., and Bissonnette, E.Y. (2014). Dysregulation of alveolar macrophages unleashes dendritic cell-mediated mechanisms of allergic airway inflammation. Mucosal Immunol *7*, 155-164.

Laval, J., Ralhan, A., and Hartl, D. (2016). Neutrophils in cystic fibrosis. Biol Chem *397*, 485-496.

Lewis, C.C., Aronow, B., Hutton, J., Santeliz, J., Dienger, K., Herman, N., Finkelman, F.D., and Wills-Karp, M. (2009). Unique and overlapping gene expression patterns driven by IL-4 and IL-13 in the mouse lung. J Allergy Clin Immunol *123*, 795-804 e798.

Li, L., Lee, H.H., Bell, J.J., Gregg, R.K., Ellis, J.S., Gessner, A., and Zaghouani, H. (2004). IL-4 utilizes an alternative receptor to drive apoptosis of Th1 cells and skews neonatal immunity toward Th2. Immunity *20*, 429-440.

Linden, A., and Adachi, M. (2002). Neutrophilic airway inflammation and IL-17. Allergy *57*, 769-775.

Livraghi-Butrico, A., Grubb, B.R., Wilkinson, K.J., Volmer, A.S., Burns, K.A., Evans, C.M., O'Neal, W.K., and Boucher, R.C. (2017). Contribution of mucus concentration and secreted mucins Muc5ac and Muc5b to the pathogenesis of muco-obstructive lung disease. Mucosal Immunol *10*, 395-407.

Livraghi, A., Grubb, B.R., Hudson, E.J., Wilkinson, K.J., Sheehan, J.K., Mall, M.A., O'Neal, W.K., Boucher, R.C., and Randell, S.H. (2009). Airway and lung pathology due to mucosal surface dehydration in {beta}-epithelial Na+ channel-overexpressing mice: role of TNF-{alpha} and IL-4R{alpha} signaling, influence of neonatal development, and limited efficacy of glucocorticoid treatment. J Immunol *182*, 4357-4367.

Livraghi, A., and Randell, S.H. (2007). Cystic fibrosis and other respiratory diseases of impaired mucus clearance. Toxicol Pathol *35*, 116-129.

Louten, J., Rankin, A.L., Li, Y., Murphy, E.E., Beaumont, M., Moon, C., Bourne, P., McClanahan, T.K., Pflanz, S., and de Waal Malefyt, R. (2011). Endogenous IL-33 enhances Th2 cytokine production and T-cell responses during allergic airway inflammation. Int Immunol *23*, 307-315.

MacNee, W. (2005). Pathogenesis of chronic obstructive pulmonary disease. Proc Am Thorac Soc *2*, 258-266; discussion 290-251.

Mall, M., Bleich, M., Greger, R., Schreiber, R., and Kunzelmann, K. (1998). The amiloride-inhibitable Na+ conductance is reduced by the cystic fibrosis transmembrane conductance regulator in normal but not in cystic fibrosis airways. J Clin Invest *102*, 15-21.

Mall, M., Grubb, B.R., Harkema, J.R., O'Neal, W.K., and Boucher, R.C. (2004). Increased airway epithelial Na+ absorption produces cystic fibrosis-like lung disease in mice. Nat Med *10*, 487-493.

Mall, M.A., Harkema, J.R., Trojanek, J.B., Treis, D., Livraghi, A., Schubert, S., Zhou, Z., Kreda, S.M., Tilley, S.L., Hudson, E.J.*, et al.* (2008). Development of chronic bronchitis and emphysema in beta-epithelial Na+ channel-overexpressing mice. Am J Respir Crit Care Med *177*, 730-742.

Mall, M.A., and Hartl, D. (2014). CFTR: cystic fibrosis and beyond. Eur Respir J *44*, 1042-1054.

Mannino, D.M., and Buist, A.S. (2007). Global burden of COPD: risk factors, prevalence, and future trends. Lancet *370*, 765-773.

Marini, M., Vittori, E., Hollemborg, J., and Mattoli, S. (1992). Expression of the potent inflammatory cytokines, granulocyte-macrophage-colony-stimulating factor and interleukin-6 and interleukin-8, in bronchial epithelial cells of patients with asthma. J Allergy Clin Immunol *89*, 1001-1009.

Matsui, H., Davis, C.W., Tarran, R., and Boucher, R.C. (2000). Osmotic water permeabilities of cultured, well-differentiated normal and cystic fibrosis airway epithelia. J Clin Invest *105*, 1419-1427.

Matsui, H., Grubb, B.R., Tarran, R., Randell, S.H., Gatzy, J.T., Davis, C.W., and Boucher, R.C. (1998). Evidence for periciliary liquid layer depletion, not abnormal ion composition, in the pathogenesis of cystic fibrosis airways disease. Cell *95*, 1005-1015.

Messer, J.W., Peters, G.A., and Bennett, W.A. (1960). Causes of death and pathologic findings in 304 cases of bronchial asthma. Dis Chest *38*, 616-624.

Messina, M.S., O'Riordan, T.G., and Smaldone, G.C. (1991). Changes in mucociliary clearance during acute exacerbations of asthma. Am Rev Respir Dis *143*, 993-997.

Miossec, P., and Kolls, J.K. (2012). Targeting IL-17 and TH17 cells in chronic inflammation. Nat Rev Drug Discov *11*, 763-776.

Mombaerts, P., Iacomini, J., Johnson, R.S., Herrup, K., Tonegawa, S., and Papaioannou, V.E. (1992). RAG-1-deficient mice have no mature B and T lymphocytes. Cell *68*, 869-877.

Mott, L.S., Park, J., Murray, C.P., Gangell, C.L., de Klerk, N.H., Robinson, P.J., Robertson, C.F., Ranganathan, S.C., Sly, P.D., Stick, S.M., and Arest, C.F. (2012). Progression of early structural lung disease in young children with cystic fibrosis assessed using CT. Thorax *67*, 509-516.

Muir, R., Osbourn, M., Dubois, A.V., Doran, E., Small, D.M., Monahan, A., O'Kane, C.M., McAllister, K., Fitzgerald, D.C., Kissenpfennig, A.*, et al.* (2016). Innate Lymphoid Cells Are the Predominant Source of IL-17A during the Early Pathogenesis of Acute Respiratory Distress Syndrome. Am J Respir Crit Care Med *193*, 407-416.

Mukaida, N. (2003). Pathophysiological roles of interleukin-8/CXCL8 in pulmonary diseases. Am J Physiol Lung Cell Mol Physiol *284*, L566-577.

Neill, D.R., Wong, S.H., Bellosi, A., Flynn, R.J., Daly, M., Langford, T.K., Bucks, C., Kane, C.M., Fallon, P.G., Pannell, R.*, et al.* (2010). Nuocytes represent a new innate effector leukocyte that mediates type-2 immunity. Nature *464*, 1367-1370.

Papotto, P.H., Ribot, J.C., and Silva-Santos, B. (2017). IL-17+ gammadelta T cells as kick-starters of inflammation. Nat Immunol *18*, 604-611.

Pavia, D., Bateman, J.R., Sheahan, N.F., Agnew, J.E., and Clarke, S.W. (1985). Tracheobronchial mucociliary clearance in asthma: impairment during remission. Thorax *40*, 171-175.

Pfaffl, M.W. (2001). A new mathematical model for relative quantification in real-time RT-PCR. Nucleic Acids Res *29*, e45.

Plantinga, M., Guilliams, M., Vanheerswynghels, M., Deswarte, K., Branco-Madeira, F., Toussaint, W., Vanhoutte, L., Neyt, K., Killeen, N., Malissen, B.*, et al.* (2013). Conventional and monocyte-derived CD11b(+) dendritic cells initiate and maintain T helper 2 cell-mediated immunity to house dust mite allergen. Immunity *38*, 322-335.

Pope, S.M., Brandt, E.B., Mishra, A., Hogan, S.P., Zimmermann, N., Matthaei, K.I., Foster, P.S., and Rothenberg, M.E. (2001). IL-13 induces eosinophil recruitment into the lung by an IL-5- and eotaxin-dependent mechanism. J Allergy Clin Immunol *108*, 594-601.

Postma, D.S., and Rabe, K.F. (2015). The Asthma-COPD Overlap Syndrome. N Engl J Med *373*, 1241-1249.

Prause, O., Bozinovski, S., Anderson, G.P., and Linden, A. (2004). Increased matrix metalloproteinase-9 concentration and activity after stimulation with interleukin-17 in mouse airways. Thorax *59*, 313-317.

Prescott, S.L., Macaubas, C., Holt, B.J., Smallacombe, T.B., Loh, R., Sly, P.D., and Holt, P.G. (1998). Transplacental priming of the human immune system to environmental allergens: universal skewing of initial T cell responses toward the Th2 cytokine profile. J Immunol *160*, 4730-4737.

Raju, S.V., Lin, V.Y., Liu, L., McNicholas, C.M., Karki, S., Sloane, P.A., Tang, L., Jackson, P.L., Wang, W., Wilson, L.*, et al.* (2017). The Cystic Fibrosis Transmembrane Conductance Regulator Potentiator Ivacaftor Augments Mucociliary Clearance Abrogating Cystic Fibrosis Transmembrane Conductance Regulator Inhibition by Cigarette Smoke. Am J Respir Cell Mol Biol *56*, 99-108.

Ramsey, B.W. (1996). Management of pulmonary disease in patients with cystic fibrosis. N Engl J Med *335*, 179-188.

Ramsey, B.W., Davies, J., McElvaney, N.G., Tullis, E., Bell, S.C., Drevinek, P., Griese, M., McKone, E.F., Wainwright, C.E., Konstan, M.W.*, et al.* (2011). A CFTR potentiator in patients with cystic fibrosis and the G551D mutation. N Engl J Med *365*, 1663-1672.

Ratner, D., and Mueller, C. (2012). Immune responses in cystic fibrosis: are they intrinsically defective? Am J Respir Cell Mol Biol *46*, 715-722.

Riordan, J.R., Rommens, J.M., Kerem, B., Alon, N., Rozmahel, R., Grzelczak, Z., Zielenski, J., Lok, S., Plavsic, N., Chou, J.L., and et al. (1989). Identification of the cystic fibrosis gene: cloning and characterization of complementary DNA. Science *245*, 1066-1073.

Robinson, D.S., Hamid, Q., Ying, S., Tsicopoulos, A., Barkans, J., Bentley, A.M., Corrigan, C., Durham, S.R., and Kay, A.B. (1992). Predominant TH2-like bronchoalveolar T-lymphocyte population in atopic asthma. N Engl J Med *326*, 298-304.

Rommens, J.M., Iannuzzi, M.C., Kerem, B., Drumm, M.L., Melmer, G., Dean, M., Rozmahel, R., Cole, J.L., Kennedy, D., Hidaka, N., and et al. (1989). Identification of the cystic fibrosis gene: chromosome walking and jumping. Science *245*, 1059-1065.

Rosenfeld, M., Gibson, R.L., McNamara, S., Emerson, J., Burns, J.L., Castile, R., Hiatt, P., McCoy, K., Wilson, C.B., Inglis, A.*, et al.* (2001). Early pulmonary infection, inflammation, and clinical outcomes in infants with cystic fibrosis. Pediatr Pulmonol *32*, 356-366.

Saetta, M., Shiner, R.J., Angus, G.E., Kim, W.D., Wang, N.S., King, M., Ghezzo, H., and Cosio, M.G. (1985). Destructive index: a measurement of lung parenchymal destruction in smokers. Am Rev Respir Dis *131*, 764-769.

Saglani, S., Mathie, S.A., Gregory, L.G., Bell, M.J., Bush, A., and Lloyd, C.M. (2009). Pathophysiological features of asthma develop in parallel in house dust mite-exposed neonatal mice. Am J Respir Cell Mol Biol *41*, 281-289.

Sauer, K.A., Scholtes, P., Karwot, R., and Finotto, S. (2006). Isolation of CD4+ T cells from murine lungs: a method to analyze ongoing immune responses in the lung. Nat Protoc *1*, 2870-2875.

Scott, D.W., Walker, M.P., Sesma, J., Wu, B., Stuhlmiller, T.J., Sabater, J.R., Abraham, W.M., Crowder, T.M., Christensen, D.J., and Tarran, R. (2017). SPX-101 is a Novel ENaC-targeted Therapeutic for Cystic Fibrosis that Restores Mucus Transport. Am J Respir Crit Care Med.

Sennhauser, F.H., Braun-Fahrlander, C., and Wildhaber, J.H. (2005). The burden of asthma in children: a European perspective. Paediatr Respir Rev *6*, 2-7.

Shalaby, K.H., Gold, L.G., Schuessler, T.F., Martin, J.G., and Robichaud, A. (2010). Combined forced oscillation and forced expiration measurements in mice for the assessment of airway hyperresponsiveness. Respir Res *11*, 82.

Shore, S.A., Abraham, J.H., Schwartzman, I.N., Murthy, G.G., and Laporte, J.D. (2000). Ventilatory responses to ozone are reduced in immature rats. J Appl Physiol (1985) *88*, 2023-2030.

Smith, J.J., and Welsh, M.J. (1992). cAMP stimulates bicarbonate secretion across normal, but not cystic fibrosis airway epithelia. J Clin Invest *89*, 1148-1153.

Solovjov, D.A., Pluskota, E., and Plow, E.F. (2005). Distinct roles for the alpha and beta subunits in the functions of integrin alphaMbeta2. J Biol Chem *280*, 1336-1345.

Soroosh, P., Doherty, T.A., Duan, W., Mehta, A.K., Choi, H., Adams, Y.F., Mikulski, Z., Khorram, N., Rosenthal, P., Broide, D.H., and Croft, M. (2013). Lung-resident tissue macrophages generate Foxp3+ regulatory T cells and promote airway tolerance. J Exp Med *210*, 775-788.

Spits, H., Artis, D., Colonna, M., Diefenbach, A., Di Santo, J.P., Eberl, G., Koyasu, S., Locksley, R.M., McKenzie, A.N., Mebius, R.E.*, et al.* (2013). Innate lymphoid cells--a proposal for uniform nomenclature. Nat Rev Immunol *13*, 145-149.

Steer, C.A., Martinez-Gonzalez, I., Ghaedi, M., Allinger, P., Matha, L., and Takei, F. (2017). Group 2 innate lymphoid cell activation in the neonatal lung drives type 2 immunity and allergen sensitization. J Allergy Clin Immunol.

Sutherland, E.R., and Martin, R.J. (2003). Airway inflammation in chronic obstructive pulmonary disease: comparisons with asthma. J Allergy Clin Immunol *112*, 819-827; quiz 828.

Swedin, L., Saarne, T., Rehnberg, M., Glader, P., Niedzielska, M., Johansson, G., Hazon, P., and Catley, M.C. (2017). Patient stratification and the unmet need in asthma. Pharmacol Ther *169*, 13-34.

Tan, H.L., Regamey, N., Brown, S., Bush, A., Lloyd, C.M., and Davies, J.C. (2011). The Th17 pathway in cystic fibrosis lung disease. Am J Respir Crit Care Med *184*, 252-258.

Tiringer, K., Treis, A., Fucik, P., Gona, M., Gruber, S., Renner, S., Dehlink, E., Nachbaur, E., Horak, F., Jaksch, P.*, et al.* (2013). A Th17- and Th2-skewed cytokine profile in cystic fibrosis lungs represents a potential risk factor for Pseudomonas aeruginosa infection. Am J Respir Crit Care Med *187*, 621-629.

Trojanek, J.B., Cobos-Correa, A., Diemer, S., Kormann, M., Schubert, S.C., Zhou-Suckow, Z., Agrawal, R., Duerr, J., Wagner, C.J., Schatterny, J.*, et al.* (2014). Airway mucus obstruction triggers macrophage activation and matrix metalloproteinase 12-dependent emphysema. Am J Respir Cell Mol Biol *51*, 709-720.

van der Strate, B.W., Postma, D.S., Brandsma, C.A., Melgert, B.N., Luinge, M.A., Geerlings, M., Hylkema, M.N., van den Berg, A., Timens, W., and Kerstjens, H.A. (2006). Cigarette smoke-induced emphysema: A role for the B cell? Am J Respir Crit Care Med *173*, 751-758.

Van Goor, F., Hadida, S., Grootenhuis, P.D., Burton, B., Stack, J.H., Straley, K.S., Decker, C.J., Miller, M., McCartney, J., Olson, E.R.*, et al.* (2011). Correction of the F508del-CFTR protein processing defect in vitro by the investigational drug VX-809. Proc Natl Acad Sci U S A *108*, 18843-18848.

van Rijt, L.S., Jung, S., Kleinjan, A., Vos, N., Willart, M., Duez, C., Hoogsteden, H.C., and Lambrecht, B.N. (2005). In vivo depletion of lung CD11c+ dendritic cells during allergen challenge abrogates the characteristic features of asthma. J Exp Med *201*, 981-991.

Voss, M., Wolf, L., Kamyschnikow, A., Wonnenberg, B., Honecker, A., Herr, C., Lepper, P.M., Wegmann, M., Menger, M.D., Bals, R., and Beisswenger, C. (2015). Il-17A contributes to maintenance of pulmonary homeostasis in a murine model of cigarette smoke-induced emphysema. Am J Physiol Lung Cell Mol Physiol *309*, L188-195.

Wanner, A., Salathe, M., and O'Riordan, T.G. (1996). Mucociliary clearance in the airways. Am J Respir Crit Care Med *154*, 1868-1902.

Weibel, E.R. (1963). Principles and methods for the morphometric study of the lung and other organs. Lab Invest *12*, 131-155.

Welsh, M.J., Ramsey, B.W., Accurso, F., Scriver, C.R., Beaudet, A.L., Sly, W.S., and Valle, D. (2001). The Metabolic & Molecular Bases of Inherited Disease, 8th edn (New York: McGraw-Hill).

Welsh, M.J., and Smith, A.E. (1993). Molecular mechanisms of CFTR chloride channel dysfunction in cystic fibrosis. Cell *73*, 1251-1254.

Wielputz, M.O., Eichinger, M., Zhou, Z., Leotta, K., Hirtz, S., Bartling, S.H., Semmler, W., Kauczor, H.U., Puderbach, M., and Mall, M.A. (2011). In vivo monitoring of cystic fibrosis-like lung disease in mice by volumetric computed tomography. Eur Respir J *38*, 1060-1070.

Yuan, S., Hollinger, M., Lachowicz-Scroggins, M.E., Kerr, S.C., Dunican, E.M., Daniel, B.M., Ghosh, S., Erzurum, S.C., Willard, B., Hazen, S.L.*, et al.* (2015). Oxidation increases mucin polymer cross-links to stiffen airway mucus gels. Sci Transl Med *7*, 276ra227.

Zhou-Suckow, Z., Duerr, J., Hagner, M., Agrawal, R., and Mall, M.A. (2017). Airway mucus, inflammation and remodeling: emerging links in the pathogenesis of chronic lung diseases. Cell Tissue Res *367*, 537-550.

Zhou, Z., Treis, D., Schubert, S.C., Harm, M., Schatterny, J., Hirtz, S., Duerr, J., Boucher, R.C., and Mall, M.A. (2008). Preventive but not late amiloride therapy reduces morbidity and mortality of lung disease in betaENaC-overexpressing mice. Am J Respir Crit Care Med *178*, 1245-1256.

Zhu, Z., Homer, R.J., Wang, Z., Chen, Q., Geba, G.P., Wang, J., Zhang, Y., and Elias, J.A. (1999). Pulmonary expression of interleukin-13 causes inflammation, mucus hypersecretion, subepithelial fibrosis, physiologic abnormalities, and eotaxin production. J Clin Invest *103*, 779-788.

Publications from PhD studies

Original articles:

Fritzsching, B.*, Hagner, M.*, Dai, L.*, Christochowitz, S., Agrawal, R., van Bodegom, C., Schmidt, S., Schatterny, J., Hirtz, S., Brown, R., et al. (2017). Impaired mucus clearance exacerbates allergen-induced type 2 airway inflammation in juvenile mice. J Allergy Clin Immunol 140, 190-203 e195. (*These authors contributed equally to this work)

Review articles:

Zhou-Suckow, Z., Duerr, J., Hagner, M., Agrawal, R., and Mall, M.A. (2017). Airway mucus, inflammation and remodeling: emerging links in the pathogenesis of chronic lung diseases. Cell Tissue Res *367*, 537-550.

Published abstracts:

Hagner, M., Schmidt, S., Maier, E., Lampe, M., Mall, M.A., Fritzsching, B. (2015). Airway surface dehydration impairs pulmonary allergen clearance. Allergo J Int 24, 41.

Hagner, M., Schmidt, S., Maier, E., Lampe, M., Mall, M.A., Fritzsching, B. (2015). Pulmonary allergen clearance is impaired by airway surface dehydration. Pneumologie 69, A28.

Hagner M., Fritzsching, B., Dai, L., Van Bodegom, C., Christochowitz, S., Schmidt, S., Schatterny, J., Hirtz, S., Duerr, J., Zhou-Suckow, Z., Mall, M.A., (2016) Impaired mucus clearance promotes *Aspergillus fumigatus*-induced type 2 airway inflammation in cystic fibrosis-like lung disease in mice. J Cyst Fibros 15, S6.

Hagner M., Fritzsching, B., Dai, L., Van Bodegom, C., Christochowitz, S., Duerr, J., Zhou-Suckow, Z., Mall, M.A., (2016). Impaired mucus clearance exacerbates *Aspergillus fumigatus*-induced type 2 airway inflammation in juvenile mice with cystic fibrosis-like lung disease. Pediatr Pulmonol 51, S229.

Hagner M., Schmidt S., Christochowitz S., Mall, M.A., (2017) Lack of T cells reduces structural lung damage in mice with cystic fibrosis-like lung disease. J Cyst Fibros 16, S118.

Oral presentations:

Impaired mucus clearance promotes *Aspergillus fumigatus*-induced type 2 airway inflammation in cystic fibrosis-like lung disease in mice. 39th European Cystic Fibrosis Conference, Basel, 8th-11th June 2016.

Acknowledgements

I want to thank,

Prof. Dr. Marcus Mall for giving me the opportunity to work on this highly interesting project under his supervision; for his expertise, his critical thinking about the results, the productive meetings that gave me new ideas for my project, and most of all for being an excellent doctoral thesis supervisor.

Prof. Dr. Benedikt Fritzsching for his initial supervision and his project input.

Prof. Dr. Ana Martin-Villalba and Prof. Dr. Knut Schäkel for their interest in my work and their helpful suggestions during the TAC meetings.

Dr. Zhe Zhou-Suckow, Dr. Julia Dürr, and Dr. Raman Agrawal for their help with the busy revision and their expertise in the lab.

Sandra Christochowitz, for her help at the start of my PhD project, not getting tired of my sometimes stupid jokes, and for being around as a “lab buddy” for more than 4 years.

Dr. Ryan Brown and Dr. Michelle Paulsen for productive discussions and the proofreading of my PhD thesis.

Claudius Wagner, for the short breaks during exhausting work days that were filled with inspiring scientific philosophy and helpful advices.

Simone Schmidt, Jolanthe Schatterny, Angela Frank, Heike Scheuermann, and Stephanie Hirtz for their training in methods and their experimental help.

All lab members of the Department of Translational Pulmonology for having a nice working atmosphere, motivating lunch discussions and funny happy hours.

Hanna, for being there in busy times.

Especially, my parents Ingrid and Walter Hagner, for their support during my studies and my life; my sister Michaela and her family for always putting a smile on my face.